MINIMIZATION OF PERTURBATIVE EFFECTS ON A HIGH ECCENTRICITY, HIGHLY INCLINED 24-HOUR SATELLITE ORBIT

Allen L. Thede

Air Force Institute of Technology
Wright-Patterson Air Force Base, Ohio

June 1973

Unclassified

Security Classification

AD-769964

DOCUMENT CONTROL DATA - R & D

(Security classification of title, body of abstract and indexing annotation must be entered when the overall report is classified)

1. ORIGINATING ACTIVITY *(Corporate author)*

Air Force Institute of Technology (AFIT-EN)
Wright-Patterson AFB, Ohio 45433

2a. REPORT SECURITY CLASSIFICATION

Unclassified

2b. GROUP

3. REPORT TITLE

Minimization of Perturbative Effects on a High Eccentricity, Highly Inclined 24-Hour Satellite Orbit

4. DESCRIPTIVE NOTES *(Type of report and inclusive dates)*

5. AUTHOR(S) *(First name, middle initial, last name)*

Allen L. Thede
Captain USAF

6. REPORT DATE	7a. TOTAL NO. OF PAGES	7b. NO. OF REFS
June 1973	96	13

8a. CONTRACT OR GRANT NO.	9a. ORIGINATOR'S REPORT NUMBER(S)
b. PROJECT NO.	GA/MC/73-7
c.	9b. OTHER REPORT NO(S) *(Any other numbers that may be assigned this report)*
d.	

10. DISTRIBUTION STATEMENT

Approved for public release; distribution unlimited.

11. SUPPLEMENTARY NOTES

Approved for public release; IAW AFR 190-17

JERRY C. HIX, Captain, USAF
Director of Information

12. SPONSORING MILITARY ACTIVITY

Foreign Technology Division,
Wright-Patterson Air Force Base, Ohio

13. ABSTRACT

A study was performed to analyse and minimize the effects of the perturbative forces on a 24-hour satellite orbit having an eccentricity of 0.6 and an inclination of 60° by selection of an optimum launch date. The computer model used includes the perturbations due to the oblate earth as described by the zonal, tesseral and sectorial harmonic series through 6th order, the solar and lunar third-body forces, and the solar radiation pressure on a vehicle whose area-to-mass ratio is 10 ft^2/slug. The orbit was computed for one year following launch with orbital parameter variations presented as functions of the launch date during 1970. The results of the study indicate that the total required impulse is significantly dependent on the launch date and oscillatory behavior of the orbital parameters due to the lunar-cycle. The largest component of the total impulse, due to the plane change to correct the nodal line and inclination, amounted to approximately 66 percent of the total yearly magnitude. The minimum total yearly impulse of 405 m/sec was required when daily o ital corrections were made following a 30 May 1970 launch. When the orbit was corrected at 14-day intervals, in phase with the lunar-cycle, two local minimums were found to be 355 m/sec for a 15 June 1970 launch or 360 m/sec for a 26 March 1970 launch.

DD FORM 1 NOV 68 1473

Unclassified
Security Classification

14. KEY WORDS	LINK A		LINK B		LINK C	
	ROLE	WT	ROLE	WT	ROLE	WT
24-Hour Satellite Orbit						
Orbital Perturbations						
Orbital Parameter Variation						
Optimum Launch Date						
Oblate Earth Perturbation						
Lunar Third-Body Perturbation						
Solar Third-Body Perturbation						
Solar Radiation Pressure Perturbation						
Station Keeping Impulse						

MINIMIZATION OF PERTURBATIVE EFFECTS ON A HIGH ECCENTRICITY, HIGHLY INCLINED 24-HOUR SATELLITE ORBIT

THESIS

Presented to the Faculty of the School of Engineering
of the Air Force Institute of Technology

Air University

in Partial Fulfillment of the
Requirements for the Degree of

Master of Science

by

Allen L. Thede, B.S.M.E
Capt USAF

Graduate Astronautics

June 1973

Approved for public release; distribution unlimited.

Preface

This report is the result of a study of the effects of perturbative forces on a specific high eccentricity, high inclination 24-hour satellite. In particular, I have attempted to determine the optimum launch date in an arbitrary time frame of one year on the basis of minimum corrective impulse required to maintain the nominal orbital parameters. The work was inspired by and in some respects parallels the work done by Arnold Ricci (Ref 11) in which a method of making a choice of orbital parameters to minimize the perturbative effect on the ground track was investigated. It is hoped that this study will provide a measure of value to the future student of perturbative analysis.

I would like to acknowledge the special help and guidance provided by Prof. Peter Bielkowicz who introduced me to the fascinating study of astrodynamics in general and suggested this area of special study. Finally, I wish to express my deepest appreciation to my wife and family for their patience and encouragement during the course of this study.

Allen L. Thede

Contents

List of Figures

List of Tables

List of Symbols

a	Semi-major axis of orbital ellipse (R_e)
a_o	nominal semi-major axis (R_e)
a.u.	astronomical unit (1.4959965×10^8 km = 23454.967 R_e)
A	1) point of apogee 2) area of vehicle presented to solar radiation (ft^2)
C_m	conversion factor for lunar distance from semi-diameter (3.8775087 R_e/arc min)
C_{nk}	earth geopotential harmonic coefficients
e	eccentricity of orbital ellipse
e_o	nominal eccentricity
E	eccentric anomaly of orbital ellipse (deg)
E_o	eccentric anomaly at reference orbital point (deg)
f	series expansion of the parameter q in Encke's method
f_1	function of perturbative acceleration $w^2 \vec{r}$ (R_e)
f_s	fraction of solar area presented to the vehicle
h	angular momentum of vehicle in orbit (R_e^2/hr)
H	highest point above reference equatorial plane
i	inclination of orbital ellipse (deg)
i_o	nominal inclination (deg)
$\hat{I},\hat{J},\hat{K}$	unit vectors in the geocentric equatorial system XYZ
J_n	earth geopotential zonal harmonic coefficients
K_e	earth gravitational parameter ($3.98604 \times 10^5 km^3/sec^2$ = 19.9095 R_e/hr^2)
K_m	lunar gravitational parameter (4.88180×10^3 km^3/sec^2 = 0.244090 R_e/hr^2)
K_s	solar gravitational parameter (1.32715×10^{11} km^3/sec^2 = 6.6289×10^6 R_e/hr^2)
L	lowest point below reference equatorial plane

m	mass of vehicle in orbit (slug)
p	semi-latus rectum of orbital ellipse (R_e)
P	point of perigee
P_0	solar constant (4.7×10^{-5} dynes/cm^2 = 9.8163×10^{-8} lb/ft^2)
$P_n^k(x)$	Legendre polynomial functions of the variable x
$\hat{P},\hat{Q},\hat{W}$	unit vectors in the perifocal coordinate system
q	parameter in Encke's method
r	radial distance from center of earth to vehicle (R_e)
r_a	radial distance of vehicle at apogee (R_e)
r_p	radial distance of vehicle at perigee (R_e)
$\ddot{r}$	two-body acceleration (R_e/hr^2)
$\ddot{r}'$	perturbative acceleration (R_e/hr^2)
R_e	earth radii (6378.165 km)
s	lunar semi-diameter
s'	reference lunar semi-diameter (15.543 arc min at 384400 km)
S_{nk}	earth geopotential harmonic coefficients
t	time in orbit from reference point
t_o	time of perigee passage (hrs)
T_o	time of vehicle injection into orbit (days)
TP	period of revolution (hrs)
u	argument of latitude at epoch (deg)
v	total orbital velocity of vehicle (R_e/hr)
v_a	velocity of vehicle at apogee (R_e/hr)
v_p	velocity of vehicle at perigee (R_e/hr)
w	time interval between equally spaced points (hrs)
x,y,z	position components in XYZ system (R_e)
$\dot{x},\dot{y},\dot{z}$	velocity components in XYZ system (R_e)

$\ddot{x},\ddot{y},\ddot{z}$	acceleration components in XYZ system (R_e/hr^2)
x_m,y_m,z_m	distance components of r_m between earth and moon (R_e)
x_s,y_s,z_s	distance components of r_s between earth and sun (R_e)
XYZ	geocentric equatorial coordinate system
α	right ascension, angle measured eastward from $\hat{I}$ (deg)
α_m	apparent right ascension of the moon (deg)
δ	declination, angle measued northward from celestial equator (deg)
δ_m	apparent declination of moon (deg)
δ_i^n	n^{th} order differences in numerical integration (R_e)
$\delta x,\delta y,\delta z$	perturbative position components (R_e)
$\delta\dot{x},\delta\dot{y},\delta\dot{z}$	perturbative velocity components (R_e/hr)
$\delta\ddot{x},\delta\ddot{y},\delta\ddot{z}$	perturbative acceleration components (R_e/hr^2)
Δv_n	impulse normal to orbital plane toward earth (m/sec)
Δv_{ta}	impulse tangential to orbit made at apogee (m/sec)
Δv_{tp}	impulse tangential to orbit made at perigee (m/sec)
Δv_w	impulse orthogonal to orbit and pointing northward (m/sec)
θ_{gi}	Greenwich sidereal time at vehicle injection (hr)
θ_{go}	Greenwich sidereal time at 0^h 1 Jan 1970 ($6^h\ 40^m\ 55.338^s$)
λ_E	longitude measured eastward from Greenwich to the vehicle (deg)
μ	mean motion (rad/hr)
ν	true anomaly measured in direction of motion from perigee (deg)
ρ_x,ρ_y,ρ_z	position components of reference orbit in XYZ system (R_e)
$\dot{\rho}_x,\dot{\rho}_y,\dot{\rho}_z$	velocity components of reference orbit in XYZ system (R_e)
$\ddot{\rho}_x,\ddot{\rho}_y,\ddot{\rho}_z$	acceleration components of reference orbit in XYZ system (R_e)
Σ^1,Σ^2	first and second sum in numerical integration
τ	normalized time unit
ϕ	geographic latitude (deg)

Φ	earth potential function (R_e^2/hr^2)
ω	argument of perigee, angle from ascending node to perigee (deg)
ω_o	nominal argument of perigee (deg)
ω_e	angular velocity of the earth about its axis (rad/hr)
Ω	longitude of ascending node, angle measured eastward from $\hat{I}$ to where the vehicle crosses the equatorial plane in a northerly direction (deg)
Ω_o	nominal longitude of ascending node (deg)
$\frac{\partial}{\partial x}$	partial differential operator
∇	gradient operator
$\left\{ \right\}$	column vector representation

Abstract

A study was performed to analyse and minimize the effects of the perturbative forces on a 24-hour satellite orbit having an eccentricity of 0.0 and an inclination of 60° by selection of an optimum launch date. The computer model used includes the perturbations due to the oblate earth as described by the zonal, tesseral and sectorial harmonic series through 6th order, the solar and lunar third-body forces, and the solar radiation pressure on a vehicle whose area-to-mass ratio is 10 ft^2/slug. The orbit was computed for one year following launch with orbital parameter variations presented as functions of the launch date during 1970. The results of the study indicate that the total required impulse is significantly dependent on the launch date and oscillatory behavior of the orbital parameters due to the lunar-cyle. The largest component of the total impulse, due to the plane change to correct the nodal line and inclination, amounted to approximately 66 percent of the total yearly magnitude. The minimum total yearly impulse of 405 m/sec was required when daily orbital corrections were made following a 30 May 1970 launch. When the orbit was corrected at 14-day intervals, in phase with the lunar-cycle, two local minimums were found to be 355 m/sec for a 15 June 1970 launch or 360 m/sec for a 26 March 1970 launch.

MINIMIZATION OF PERTURBATIVE EFFECTS ON A HIGH ECCENTRICITY, HIGHLY INCLINED 24-HOUR SATELLITE ORBIT

I. Introduction

Synchronous (24-Hour) satellites are potentially very useful in communication relay networks, weather and oceanographic data collection and ecological surveys. Satellites with appropriate orbital parameters can provide a myriad of ground tracks or earth traces which are characterized by figure-8 patterns (Ref 5). These patterns can provide optimized data collection or retrieval for opposite hemispheres based on the relative times spent in various parts of the ground track. The potential application of these qualities to various reconnaissance missions is also apparent.

Satellites in orbits with large inclinations with respect to the equatorial plane and having large eccentricities are subject to significant perturbations due to the oblate earth and lunar and solar attractive forces. These perturbations will act, in the long term, to cause the ground track to drift significantly from the nominal positions. In order to optimize the orbital station keeping of the satellite, consideration must be given to the choice of the optimum launch date.

Equatorial circular-synchronous satellite orbits have been investigated extensively in the available literature. These represent the classically considered "synchronous" satellites which remain generally over a single point on the earth surface. Highly eccentric orbits ($e > 0.8$) with orbital inclinations of approximately 30° have been

analysed by the National Aeronautics and Space Administration (NASA) to fulfill experimenter requirements of solar aspect angle and position relative to the ecliptic plane (Ref 12). Ricci has studied the effects of general perturbations on 24-Hour satellites in order to determine how the injection parameters could be modified to minimize the perturbations in the ground track (Ref 11).

This study is concerned with the detailed analysis of a specific orbit having an eccentricity of 0.6 and an inclination of 60°. The period of revolution is equal to the sidereal time of the earth rotation about its axis. The other specific orbital parameters were chosen to provide a small loop at the maximum southern latitude, over the Indian Ocean. This orbit does not correspond to any known orbit at the present time.

The purpose of the analysis is to determine the optimum launch date during the arbitrary calendar year 1970. The optimum date will be chosen on the basis of minimum corrective impulse to provide nominal station keeping for a period of one year. The computer model used in the analysis applies the Encke technique of integration and was written to be used on the CDC 6600 computer at the Wright-Patterson AFB Computer Science Center.

The oblate earth has been modeled by using the J_2 through J_6 terms of the zonal harmonics and includes the tesseral and sectorial harmonics through the 6^{th} order terms. The effects of the lunar and solar third-body attractive forces as well as the radiation pressure due to solar photons have been included in the model. The vehicle is assumed to be a spherically symmetric perfectly absorptive body with an area-to-mass

ratio of 10 ft^2/slug. The perturbative forces due to atmospheric drag on the vehicle and the third-body attractions of the planets have been neglected since their magnitudes are insignificant compared to the other sources considered.

Several other basic assumptions have been made during the course of this study. It is assumed that the gravitational field of the earth is accurately modeled by the harmonic series used. It is assumed that the satellite has been injected at perigee of the initial orbit from some available launch facility. The study does not include analysis of the injection phase. It is assumed that the satellite attitude control system operation does not significantly perturb the orbit.

The analysis and study results are presented in the chapters which follow. The general analysis approach is discussed in Chapter II with detailed formulations developed and presented in the appended sections. The results of the study phases are presented largely in graphical form in Chapter III. The final chapter provides a summary of conclusions and makes recommendations for further study.

II. Analysis Approach

This chapter of the study presents the methodology used during the analysis beginning with a definition of the general approach. The second section is devoted to the discussion of integral parts of the computer model used. The aspects of choosing initial conditions for the various launch dates are discussed in the third section. Finally, the last section presents the technique used to determine the impulse necessary to provide station keeping.

General Discussion

The approach to the analysis of the orbit consisted of three specific phases. The first phase involved the study of daily variations in the orbital parameters. The variations were calculated as functions of each of the perturbation sources for a typical orbital revolution and for the total perturbative force. The second phase included the calculation of the orbit for a full year following injection at perigee on the launch date. Successive launch dates were chosen throughout the calendar year of 1970. The final phase provided for the selection of an optimum launch date by calculation of the impulse required for station keeping given various launch dates.

The specific orbit which was chosen for analysis has the following orbital parameters:

$$a = 6.610725\ R_e$$
$$e = 0.6$$
$$i = 60^\circ$$
$$\omega = 135^\circ$$
$$\Omega = 0^\circ \quad (\text{for } 0^h \text{ 1 Jan 1970 launch time})$$
$$TP = 23^h\ 56^m\ 4.09054^s$$

The choice of the longitude of ascending node Ω for launch dates other than T_o = 1 Jan 1970 are discussed in the third section of this chapter on page 15, with the initial launch conditions illustrated in Fig. 7. Most of the orbital calculations in the analysis were performed in the geocentric equatorial frame of reference system XYZ, defined by the unit vectors $\hat{I}$, $\hat{J}$ and $\hat{K}$. The perifocal system of coordinates PQW was used to facilitate calculations in the orbital plane. The geometry of these frames of reference is shown in Fig. 1.

Computer Model

Reference Orbit. The reference orbit was calculated according to the development in Appendix B. The orbital parameters used for the first reference orbit are the nominal values given previously. The first step in the calculation is to determine the values of the eccentric anomaly E by solution of the Kepler equation

$$mw = \frac{TP}{2\pi}(E - e \sin E) \tag{1}$$

where m is an integer step and w is the desired time interval between equally spaced data points around the orbit. An interval of w = 0.1 hr was used in this analysis.

The position and velocity components of the reference orbit were then calculated by using the general vector equations

$$\bar{r} = r \cos\nu \, \hat{P} + r \sin\nu \, \hat{Q} \tag{2}$$

$$\bar{v} = \sqrt{\frac{K_e}{p}}\left[-\sin\nu \, \hat{P} + (e + \cos\nu)\, \hat{Q}\right] \tag{3}$$

These equations are transferred from the perifocal reference system PQW to the equatorial coordinate system XYZ in Appendix B.

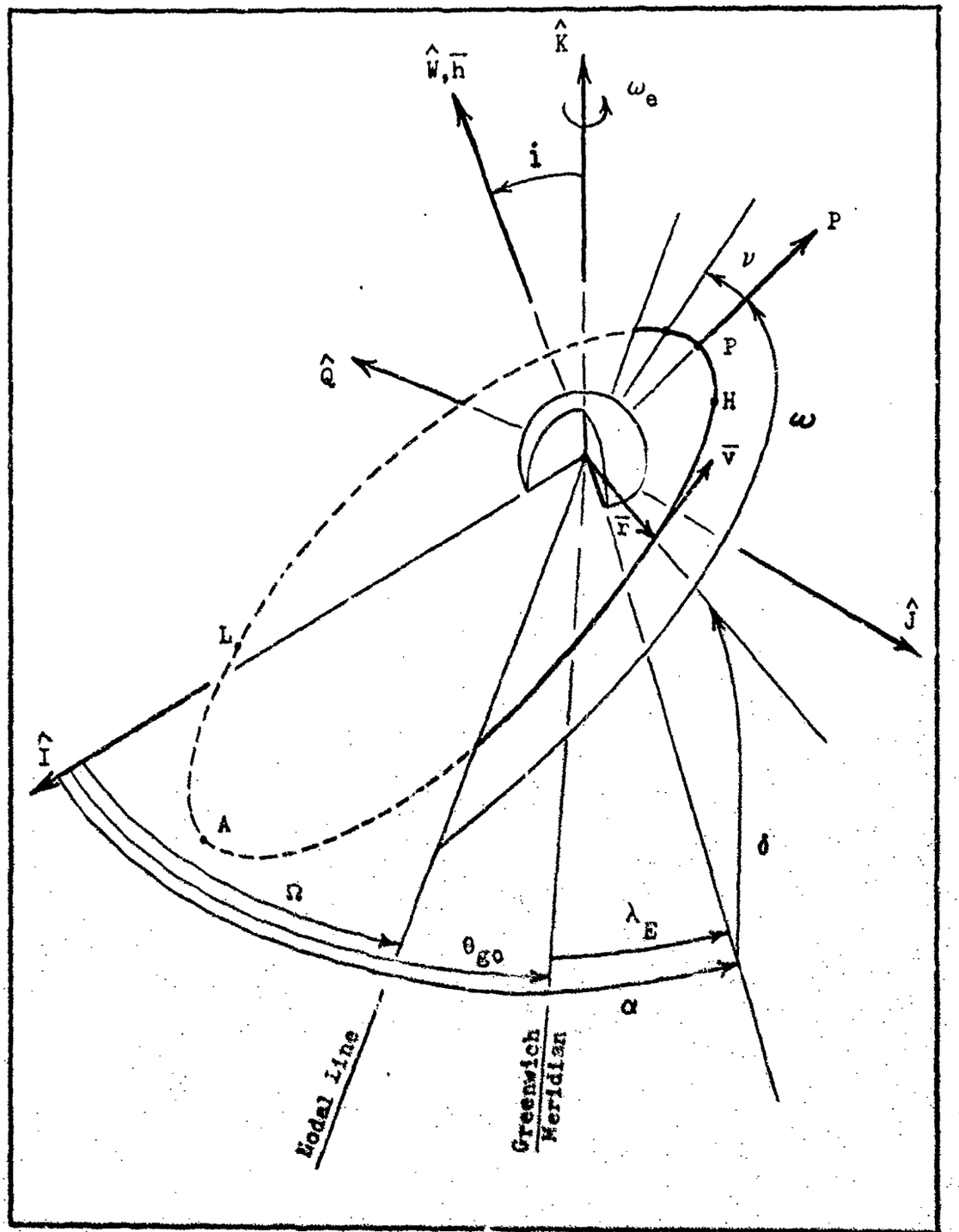

Figure 1. Orbital Geometry

Perturbations.

1) Oblate Earth. The components of the perturbative accelerations due to the oblate earth were calculated using the form of the gravitational potential expressed as

$$\phi = \frac{K_e}{r}\left[1 + \sum_{n=2}^{6}\left[\sum_{k=0}^{n}\left(\frac{P_n^k(\sin\delta)}{r^n}\right)\left[C_{nk}\cos(k\lambda_E) + S_{nk}\sin(k\lambda_E)\right]\right]\right] \quad (4)$$

A 6^{th} order series is used to assure sufficient accuracy while not being unwieldy in computer calculations. The gradient of Φ can be decomposed, as in Appendix A, to yield the zonal, tesseral and sectorial harmonic functions which describe the perturbative contributions to the gravitational acceleration of a body in earth space. These functions are given by Eqs (22) through (24) in Appendix A, and illustrated in Figs. 2 through 4 for the first orbit following injection at perigee at 0^h 1 Jan 1970.

It can be seen that the zonal contributions are the most significant with peak perturbations near perigee being on the order of 10^{-4} R_e/hr^2. The second most significant components are those of the sectorial harmonics which describe the equatorial ellipticity. Peak sectorial contributions are on the order of 10^{-5} R_e/hr^2. The tesseral harmonics, which further describe the nature of the geoid, have peaks on the order of 10^{-7} R_e/hr^2. The tesseral harmonics contribute very little to the variation of orbital parameters, as will be shown.

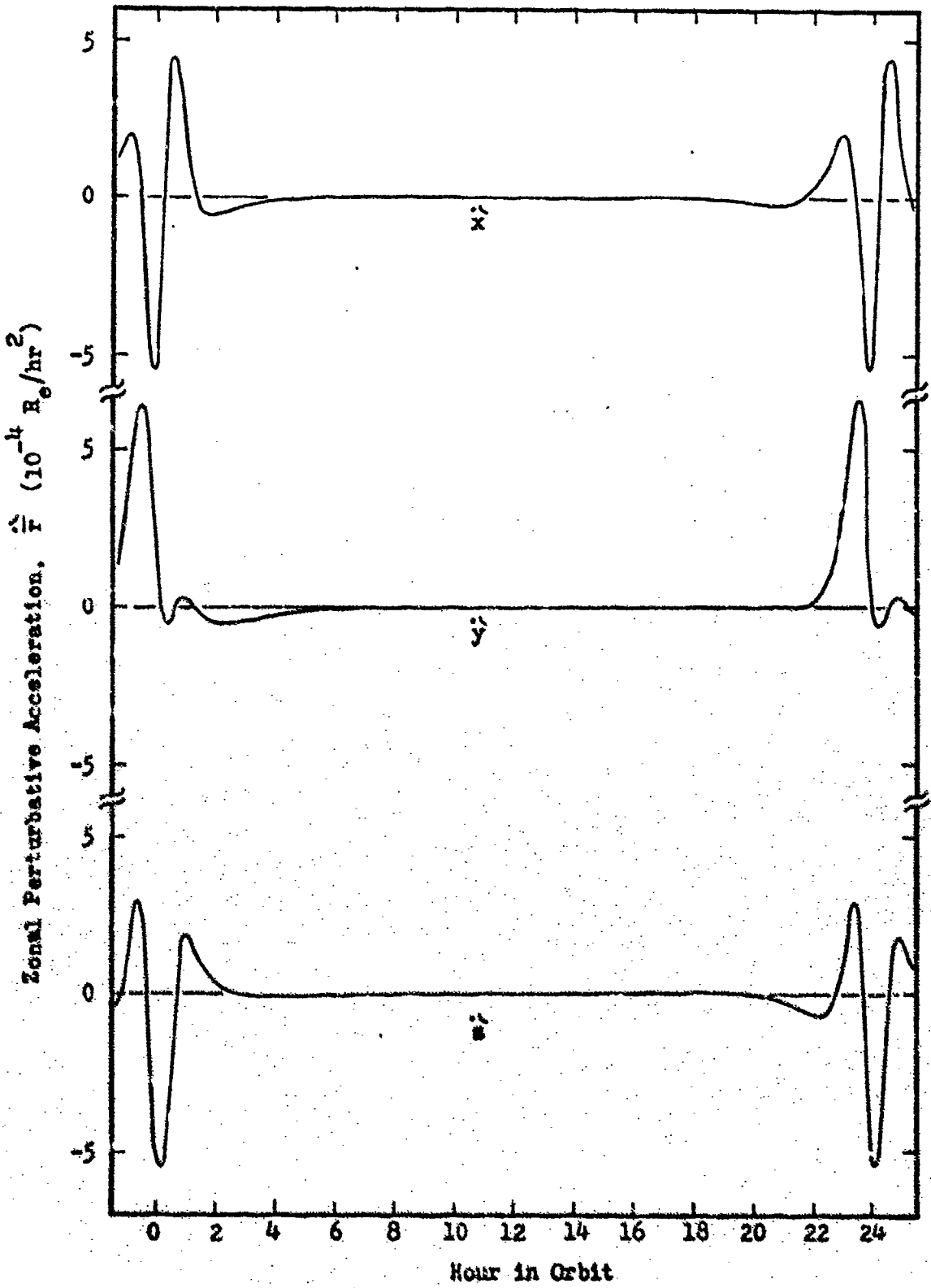

Figure 2. Zonal Perturbative Acceleration Components

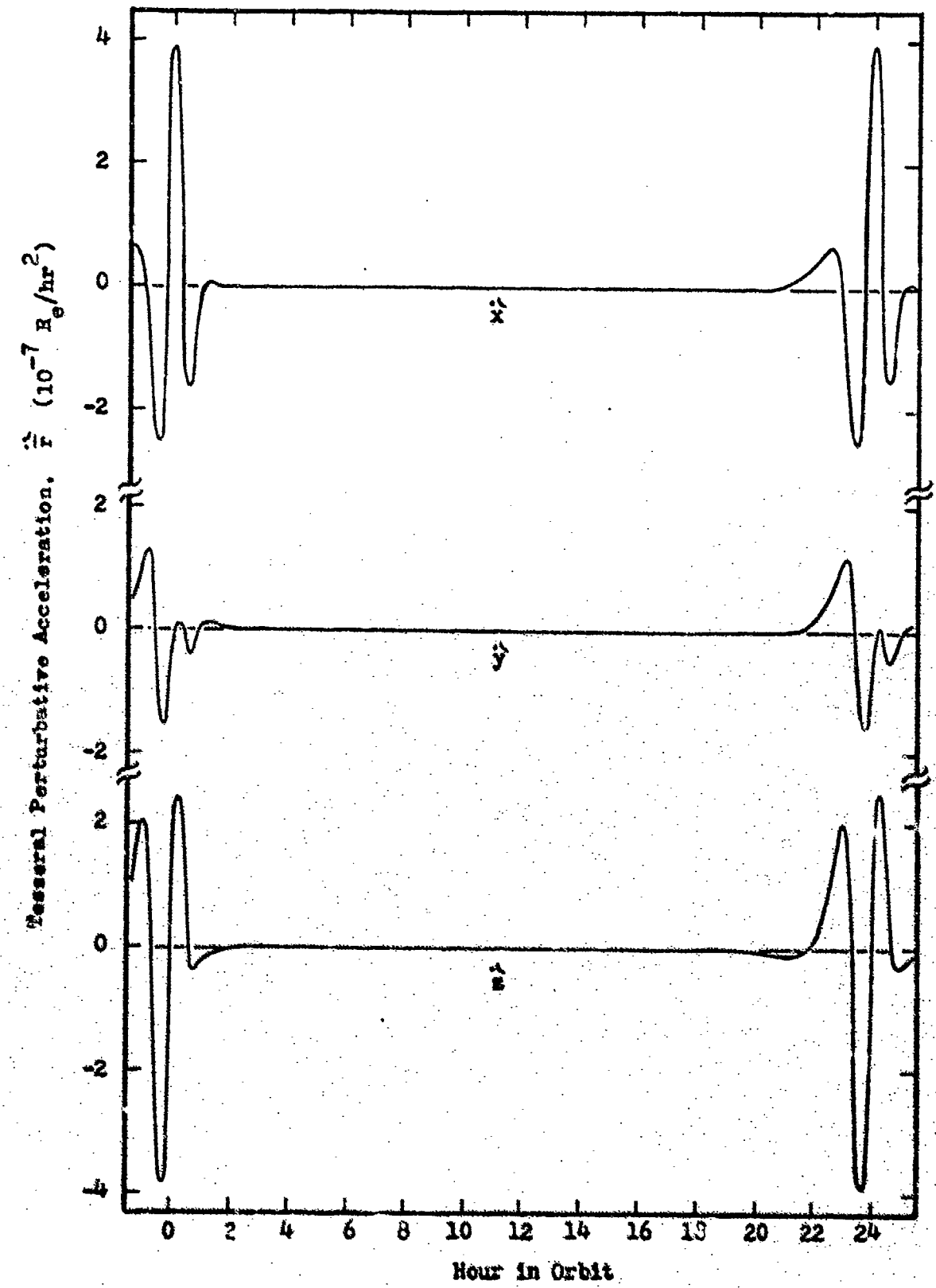

Figure 3. Tesseral Perturbative Acceleration Components

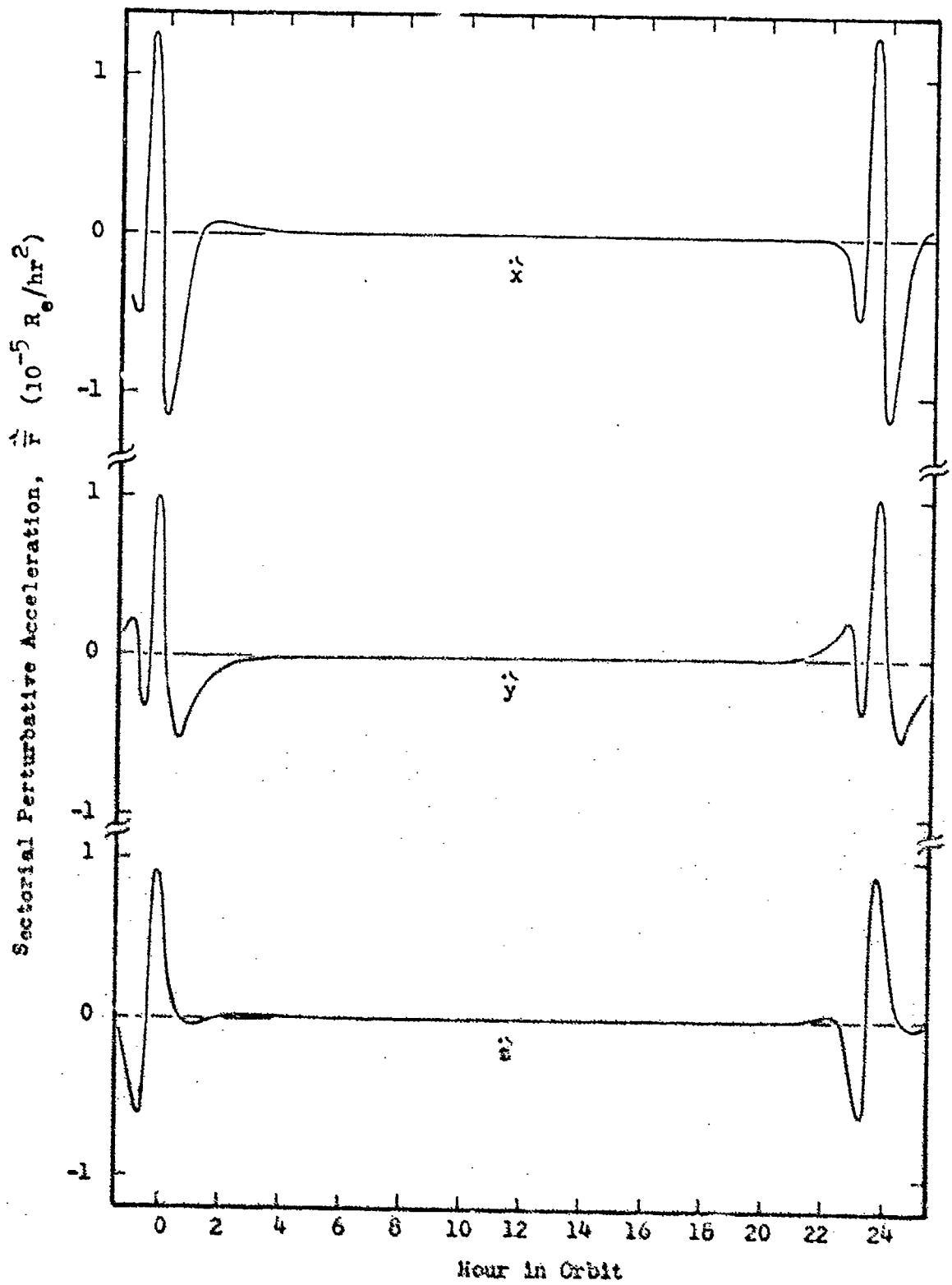

Figure 4. Sectorial Perturbative Acceleration Components

2) Third-Body Attraction. The contributions to the perturbative accelerations due to third-body attractive forces of the moon and sun, in the geocentric equatorial system, were calculated by the general form of Eqs (69) and (70) given in Appendix A;

$$\ddot{\vec{r}}_j = \begin{Bmatrix} \ddot{x} \\ \ddot{y} \\ \ddot{z} \end{Bmatrix} = -K_j \left[\frac{1}{r_{pj}^3} \begin{Bmatrix} x - x_j \\ y - y_j \\ z - z_j \end{Bmatrix} + \frac{1}{r_j^3} \begin{Bmatrix} x \\ y \\ z \end{Bmatrix} \right] \qquad (5)$$

The contributions for the orbit beginning at 0^h 1 Jan 1970 due to the lunar and solar attractions are shown in Figs. 5 and 6 respectively.

Although the maximum accelerations are on the order of 10^{-5} and 10^{-6} R_e/hr^2, they are present for longer periods of time during the orbit. Their duration causes perturbative displacements in the orbit which exceed the effects of the sectorial harmonics and approach those due to even the zonal harmonics.

3) Solar Radiation Pressure. Finally, the contribution due to the solar radiation is calculated by the equation

$$\ddot{\vec{r}}_{rad} = f_s P_0 \frac{A}{m} \frac{1}{r_{ps}^3} \begin{Bmatrix} x - x_s \\ y - y_s \\ z - z_s \end{Bmatrix} \qquad (6)$$

Although the contributions due to this perturbative source are not shown they are on the order of 10^{-7} R_e/hr^2 for an area-to-mass ratio $\frac{A}{m}$ = 10 $ft^2/slug$. Since, in the heliocentric system, the satellite is at a relatively constant distance from the sun, the perturbative acceleration is also nearly constant. The x, y, and z-components for the 0^h 1 Jan 1970 orbit are approximately -1.15×10^{-7}, 5.67×10^{-7} and 2.45×10^{-7} R_e/hr^2 respectively.

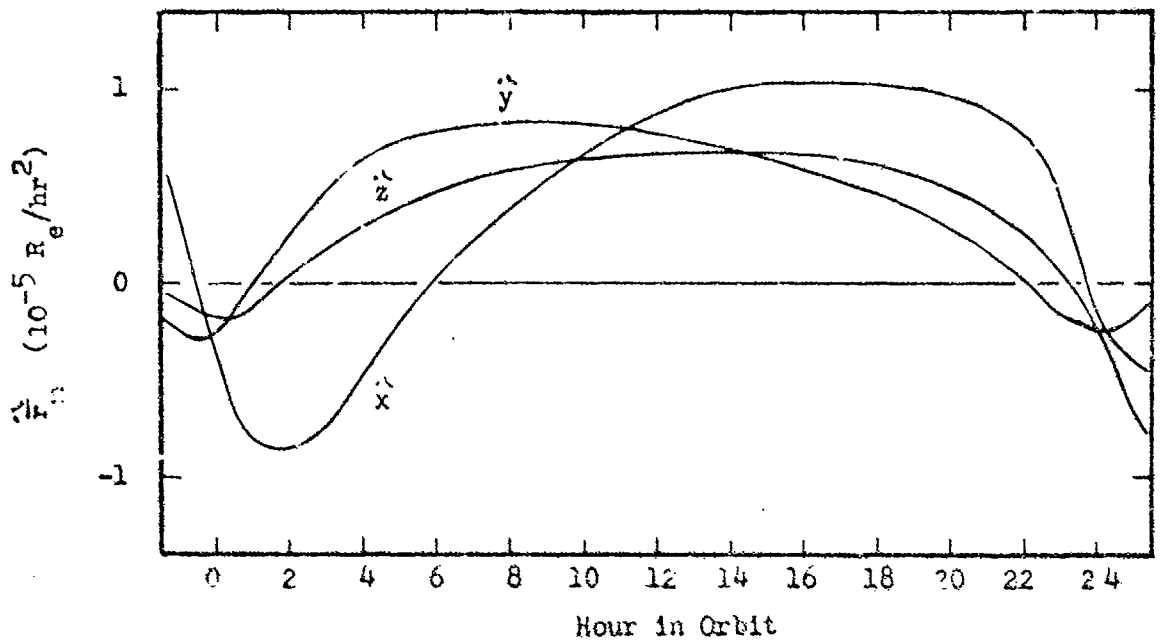

Figure 5. Lunar Third-Body Perturbative Acceleratic Components

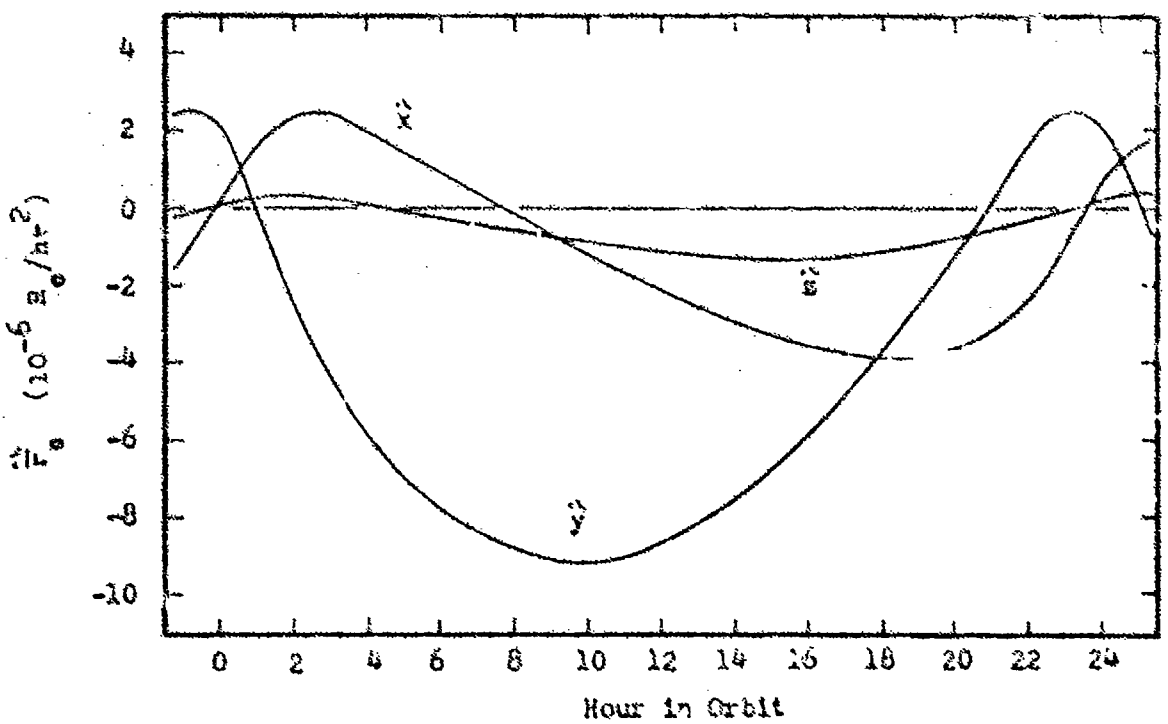

Figure 6. Solar Third-Body Perturbative Acceleration Components

The value of 10 ft^2/slug is considered to be a maximum value for $\frac{A}{m}$ for most typical satellites. In fact, this value is higher than envisioned for many vehicles designed with large solar arrays necessary for some ion-propulsion applications. The factor f_s can be considered to be identically equal to unity for this $\frac{A}{m}$ when the vehicle is in the sunlit portion of the orbit, and equal to zero when it enters the shadowed areas behind the earth.

4) Neglected Perturbations. The most significant perturbation which has been neglected in this analysis is that due to the atmospheric drag on the vehicle, particularly at perigee. It can be shown, however, that its contribution is negligible compared to those already discussed. The total decelerative perturbation along the path of the orbit is given by the general relation

$$\ddot{r}_{drag} \simeq \frac{1}{2} C_D \frac{A}{m} \rho v^2 \qquad (7)$$

The greatest drag force occurs at perigee where the nominal velocity v is 6.149 km/sec = 20,175 ft/sec and the altitude is 10488 km = 34.408×10^6 ft. The density ρ at this altitude is certainly no greater than 10^{-19} slug/ft^3 (Ref 7:200). Considering the case of $\frac{A}{m}$ = 10 ft^2/slug and assuming that the drag coefficient maximum is C_D = 2, the deceleration $\ddot{r}$ is no greater than 2.52×10^{-10} R_e/hr^2. This value is at least three orders of magnitude less than the tesseral component which is the smallest contribution considered in the analysis.

In general, a less significant perturbation results from the third-body attraction of near-by planets, specifically the larger ones. The approximate values of these perturbative accelerations can be obtained

by using a simplified form of Eq (5) given as

$$\ddot{\bar{r}}_{pl} \simeq -K_{pl} \frac{r_{max}}{r_{pl}^3} \tag{8}$$

where $K_{pl} = M_{pl}K_e$ is the gravitational parameter of the planet of mass M_{pl}. The maximum value of the perturbative force will be reached for a maximum radial distance of the vehicle from the earth r_{max} and a minimum distance between the vehicle and the perturbing planet, r_{pl}. Assuming the planets, including earth, are in the equatorial plane, the minimum value of r_{pl} is at closest approach, or approximately the difference between the semi-major axes of the orbits of the earth and planet about the sun.

The maximum third-body perturbation due to the nearest planets based on closest possible approach are tabulated in Table I below. The planetary masses, semi-major axes and the minimum approach distances are also provided. The perturbations are based on a maximum vehicle distance of $r_{max} = 10.577\ R_e$.

Table I. Third-Body Perturbations of Selected Planets

Planet	Mass (M_e)	Semi-major Axis (a.u.)	r_{pl} (a.u.)	$\ddot{r}_{max}$ (R_e/hr^2)
Venus	0.81485	0.723332	0.276668	627.94×10^{-12}
Mars	0.10770	1.523691	0.523691	12.24×10^{-12}
Jupiter	317.890	5.202694	4.202694	69.89×10^{-12}
Saturn	95.1200	9.538836	8.538836	2.49×10^{-12}

Launch Date Variation

In order to maintain the same relative conditions of solar aspect for the satellite with respect to the desired earth trace, it is necessary to adjust the longitude of ascending node for each launch date. The adjustment is based on the launch (injection at perigee) at 0^h on the date of interest. Since the value at 0^h 1 Jan 1970 is $\Omega_o = 0°$, the value for any other time of launch, as shown in Fig. 7, is

$$\Omega_i = \theta_{gi} - \theta_{go} \tag{9}$$

where θ_{go} is the Greenwich sidereal time at 0^h 1 Jan 1970, which is $6^h\ 40^m\ 55.338^s = 100.25°$, and θ_{gi} is the Greenwich sidereal time at 0^h on the launch date (Ref 1:10). The dates shown in Fig. 7 represent launch dates for initial orbital positions shown in the heliocentric equatorial system X'Y'Z' .

The longitude and latitude of the vehicle with respect to the earth is given by the relations

$$\lambda_E = \alpha - \theta_{gi} - \omega_e (t - t_o) \tag{10}$$

$$\phi = \sin^{-1}\left(\frac{z}{r}\right) \tag{11}$$

where $\alpha = \tan^{-1}\left(\frac{y}{x}\right)$ is the right ascension of the vehicle and $(t-t_o)$ is the time from perigee. Given the nominal orbital parameters, Eqs (10) and (11) can be used to generate the ground track or earth trace as shown in Fig. 8. The points along the ground track in Fig. 8 represent intervals of one hour, which demonstrates the utility of an orbit of this type for collection of data in the general area of the small loop. Approximately one third of the total orbital time is spent in the general area of this loop.

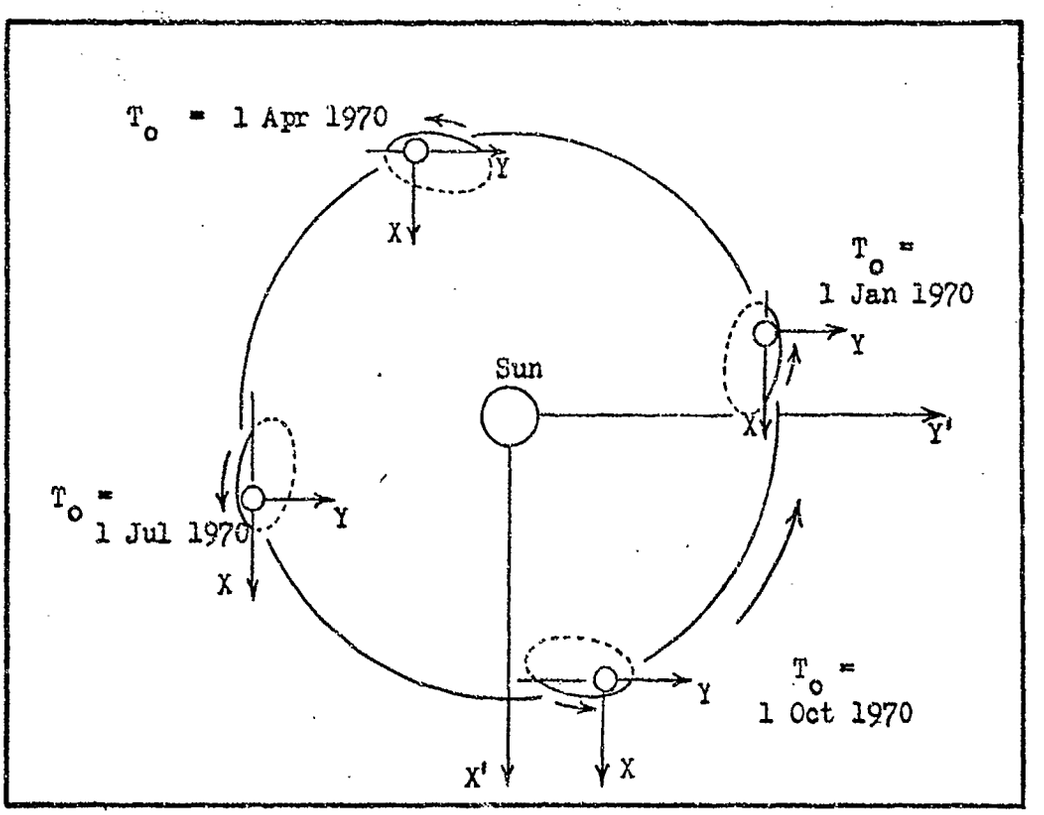

Figure 7. Orbital Geometry in Heliocentric Coordinate System

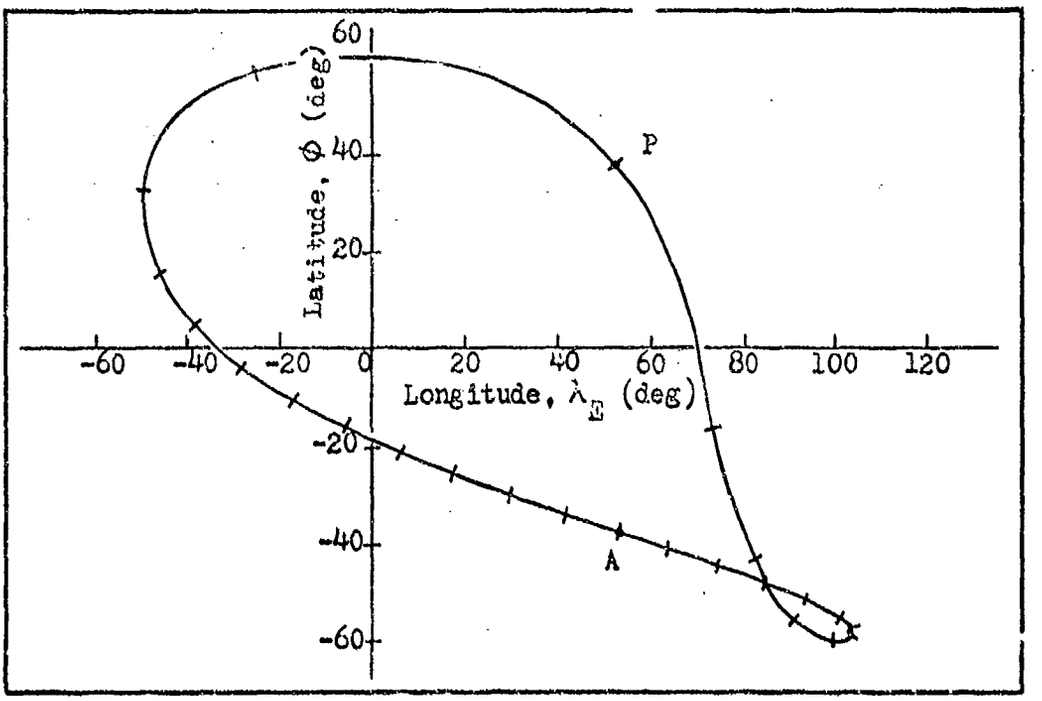

Figure 8. Nominal Ground Track

Following the orbital calculations for each of the selected launch dates using the variable longitude of ascending node, the perturbed ground track can be calculated using Eqs (10) and (11). The value of θ_{gi}, however, must be determined specifically for the time of perigee passage for the orbit of interest.

Orbital Correction

Following the necessary analysis of orbital parameter variation as a function of launch date, a series of orbital integrations were performed to determine the optimum launch date. Detailed analysis was made only for the selected general area in order to minimize the computer time required. The method used to correct the orbit is discussed in more detail in Appendix B although basically it involved making four impulsive thrusts during each orbit being corrected.

The first correction was an orthogonal impulse made near the lowest point L in the orbit below the equatorial plane to correct the values of inclination and longitude of ascending node. This correction is

$$\Delta v_w = \frac{\Delta i \; v_L}{\cos (\nu_L - \nu_\Omega)} = \frac{\Delta\Omega \, v_L \sin i_L}{\sin (\nu_L - \nu_\Omega)} \tag{12}$$

where $$\nu_L - \nu_\Omega = \tan^{-1}\left(\frac{\Delta\Omega}{\Delta i} \sin i_L\right)$$

The second impulse was made at apogee to correct the apsidal line or argument of perigee. It was made normal to the velocity vector, toward the center of attraction and has a magnitude given by

$$\Delta v_n = \frac{\Delta\omega \; a_A e_A v_A}{2 a_A e_A + r_A \cos (\nu_A - \nu_o)} \tag{13}$$

The third impulse was also made at apogee but in a direction which is tangential to the orbit. This correction provides a partial correction of the eccentricity and semi-major axis and is based on restoring the perigee distance to the nominal value. This impulse is given by

$$\Delta v_{ta} = \frac{\Delta a_A K_e}{2 a_A^2 v_A} \tag{14}$$

The final tangential impulse was given at perigee to fully restore the nominal eccentricity and semi-major axis and is given by

$$\Delta v_{tp} = \frac{\Delta e_p v'_p}{3 (e'_p + \cos \nu_p)} \tag{15}$$

where the primed values are those just prior to the impulse being made.

The choice of the optimum launch date finally depends on the criteria of total impulse necessary for orbital correction. Although the ultimate design of the thruster assembly to perform the correction is beyond the scope of this study, an understanding of the basic requirements is of interest. Due to the oscillatory nature of the parameter changes, the impulse required for daily correction will be somewhat higher than if the correction were made periodically as a function of the lunar cycle. The final choice of the corrective technique depends on the accuracy which is required for station keeping.

III. Results

The results of the various phases of this study are discussed in this chapter with the aid of graphical presentations of the data acquired. The effects of the perturbations on the orbital parameters during a typical orbit are discussed in the first section. The longer term effects of these perturbative sources are presented in the second section as functions of the date in orbit and launch date. Finally, the optimum launch date is selected on the basis of minimum corrective impulse being required to maintain nominal orbital parameters.

Hourly Variation of Orbital Parameters

The effects of the various mechanisms of perturbation on the orbital parameters are shown for the first orbit after injection at 0^h 1 Jan 1970 in Figs. 9 through 13. The individual curves for the various components of perturbation are explicitly the effect due to those components alone, while the total effect is due to the sum of the accelerations considered together. It can be seen, however, that an accurate approximation can be determined by summing the effects due to each individual contribution. If a component such as solar radiation pressure or tesseral harmonic is not shown, there is a negligible change in the nominal value of the parameter considered.

Figure 9 illustrates the effect of the various perturbations on the semi-major axis during this typical orbit. Note that the most significant effect is caused by the zonal harmonics. The sharp spikes occurring near perigee will also be seen in the variation of other orbital parameters. As discussed by Shute (Ref 12:15), the effects of these spikes will be averaged out following perigee passage. The variations in the semi-major

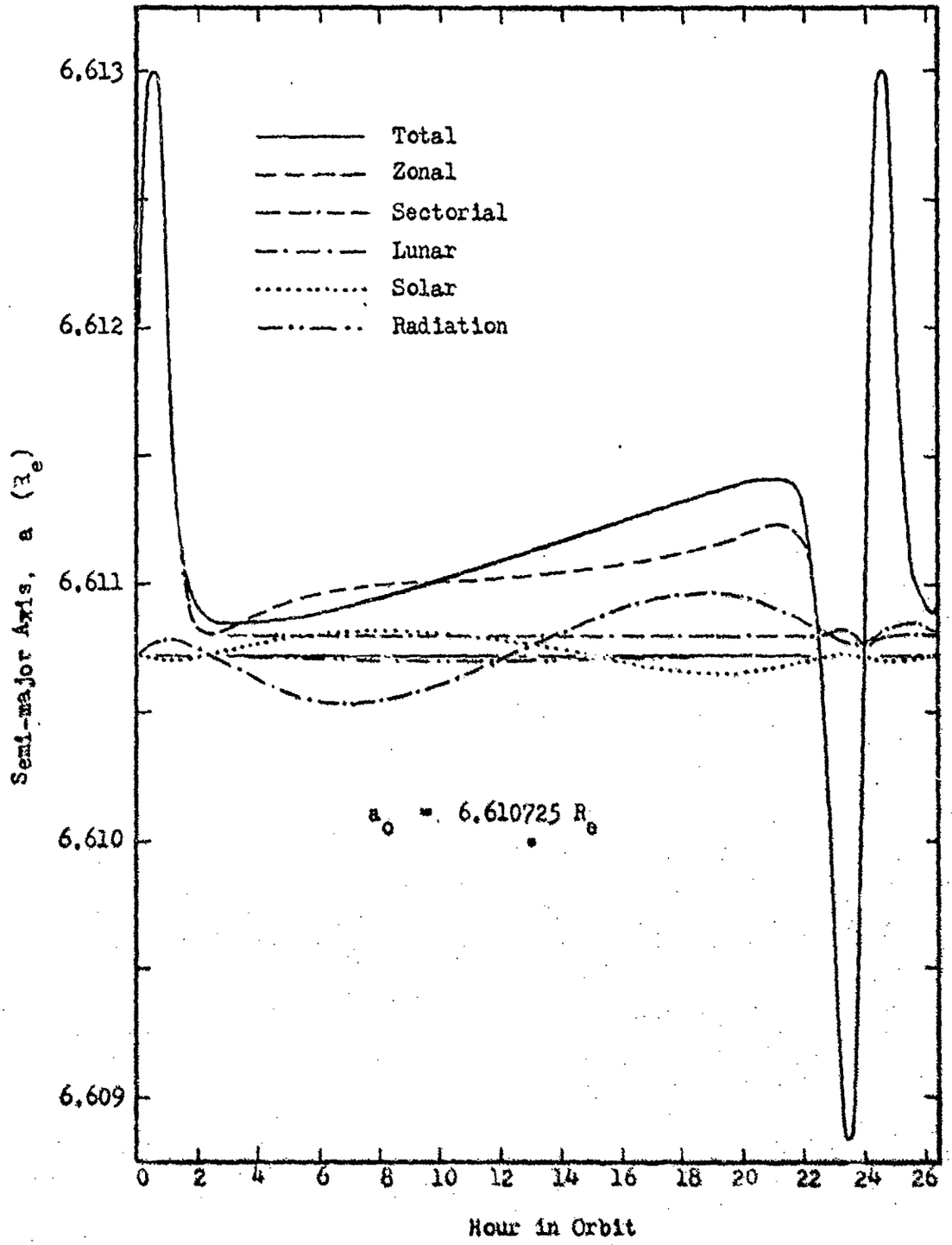

Figure 9. Variation of Semi-major Axis with Hour in Orbit

axis due to the zonal harmonics will then be of the same order of magnitude as compared to the other contributions at the perigee point. The effects of the earth oblateness will remain essentially as shown for any orbit given any launch date, since the orbit is constant relative to the surface of the earth. This will also be true for the other orbital parameters discussed.

The next most significant contributions which cause variation in the semi-major axis are the lunar and solar third-body attractions. Unlike the oblateness effects, these variations will depend on the positions of the moon and the sun with respect to the earth. The variations shown in Fig. 9 are therefore only typical in magnitude. The variations due to solar radiation pressure, with $\frac{A}{m} = 10$ $ft^2/slug$, and the tesseral harmonics (not shown) are seen to be minimal in comparison with the other contributions.

The variation of the eccentricity is illustrated in Fig. 10 where it is noted that the lunar attraction is the most significant perturbation source. The solar attraction offsets this effect somewhat for this typical orbit, as do the zonal harmonics. The effects due to the tesseral and sectorial harmonics and the solar radiation pressure are significant compared to those due to the sources shown.

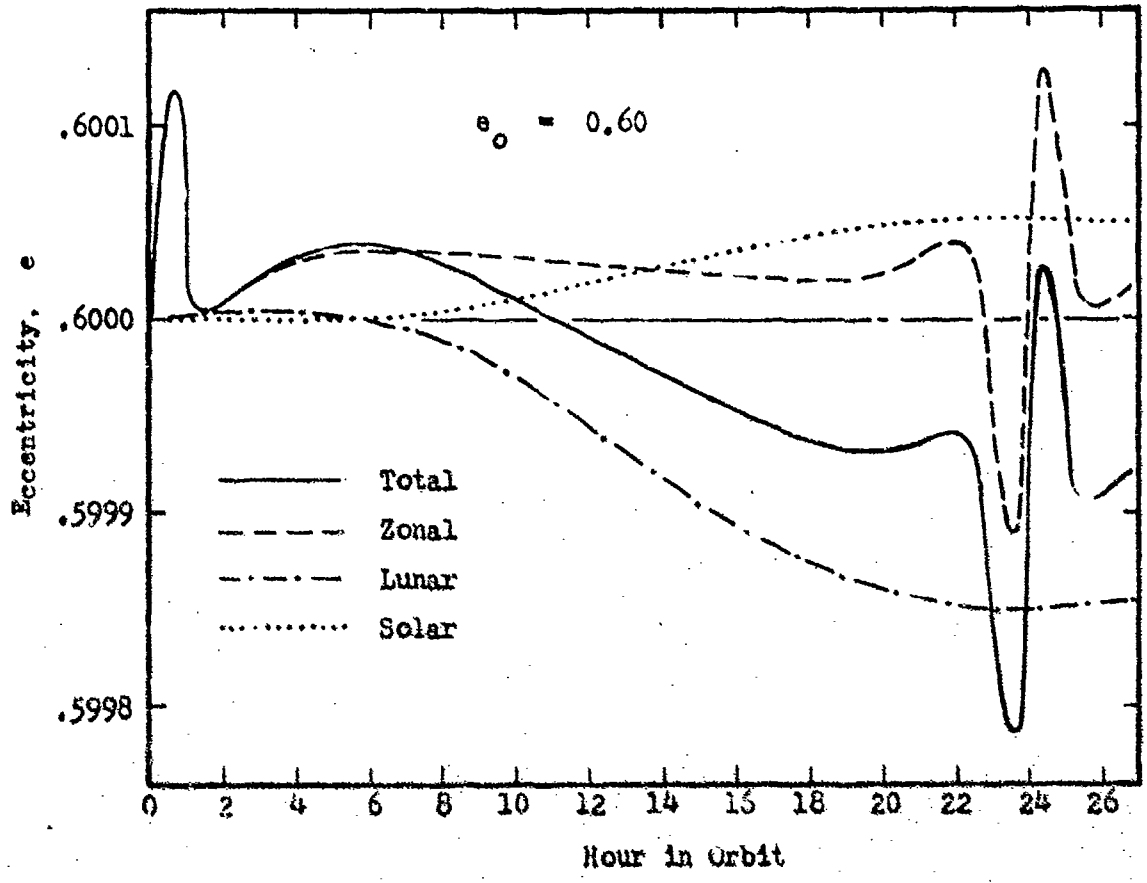

Figure 10. Variation of Eccentricity with Hour in Orbit

The inclination is also affected most significantly by the lunar, solar and zonal contributions as shown in Fig. 11. The sectorial harmonics and solar radiation pressure cause less significant variation although cannot be neglected. The solar attraction for the orbital case shown causes an increase in the inclination which is twice the increase caused by the zonal harmonics, while the lunar attraction cancels some of its effect.

The argument of perigee ω is affected most significantly by the zonal harmonics as shown in Fig. 12. The solar and lunar attractive influences tend to cancel for this particular case, but as noted earlier, will not generally.

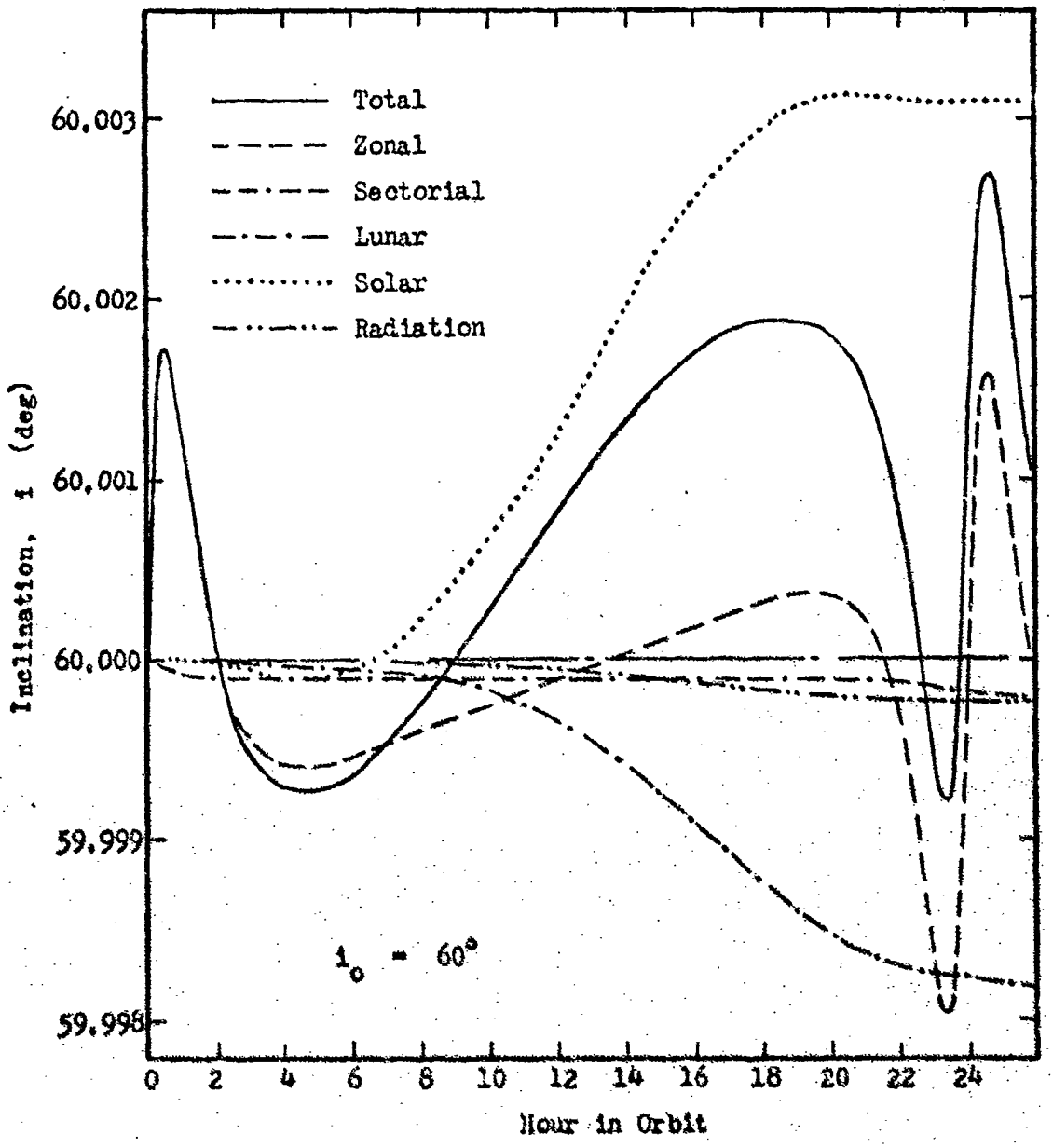

Figure 11. Variation of Inclination with Hour in Orbit

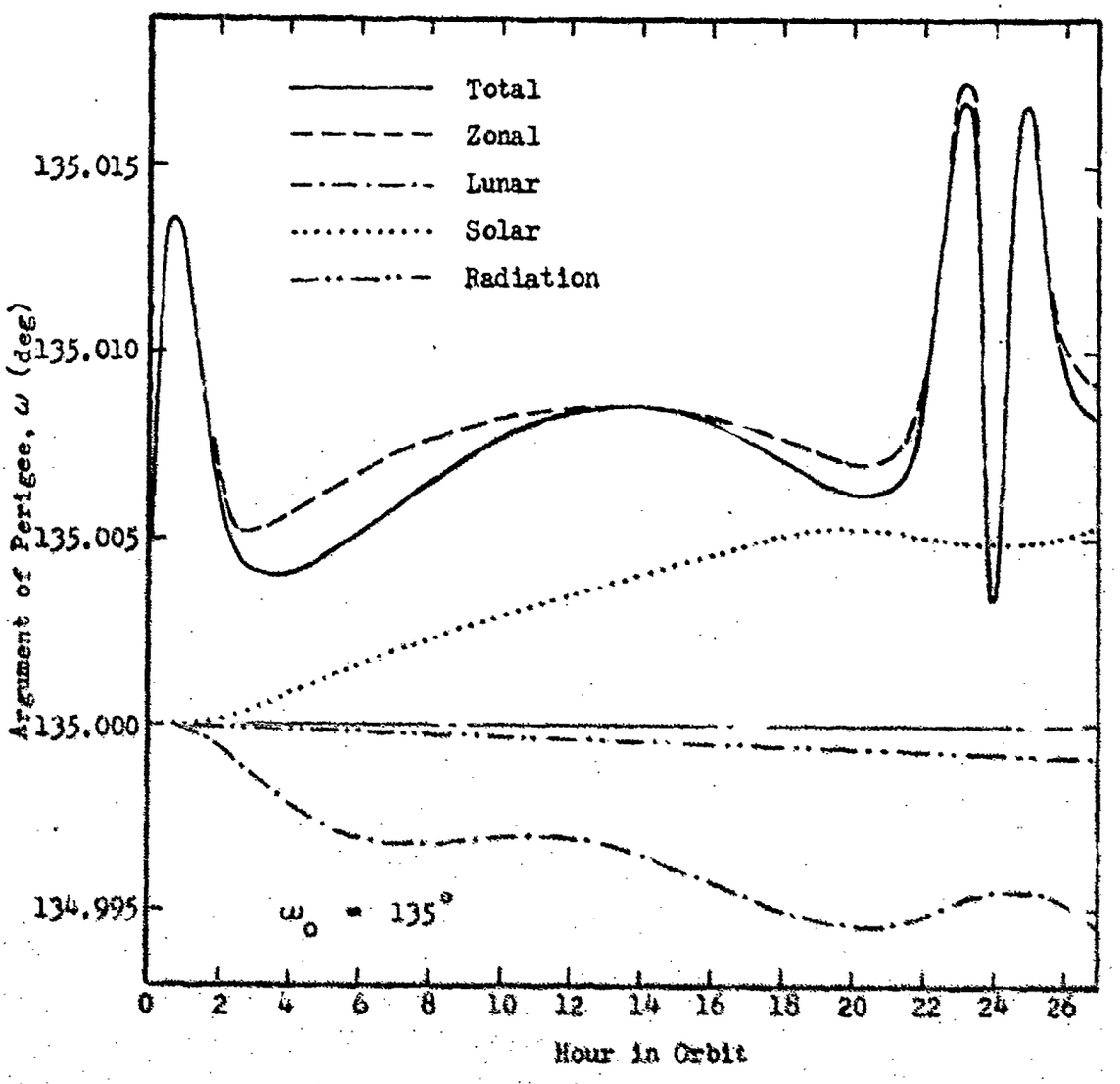

Figure 12. Variation of Argument of Perigee with Hour in Orbit

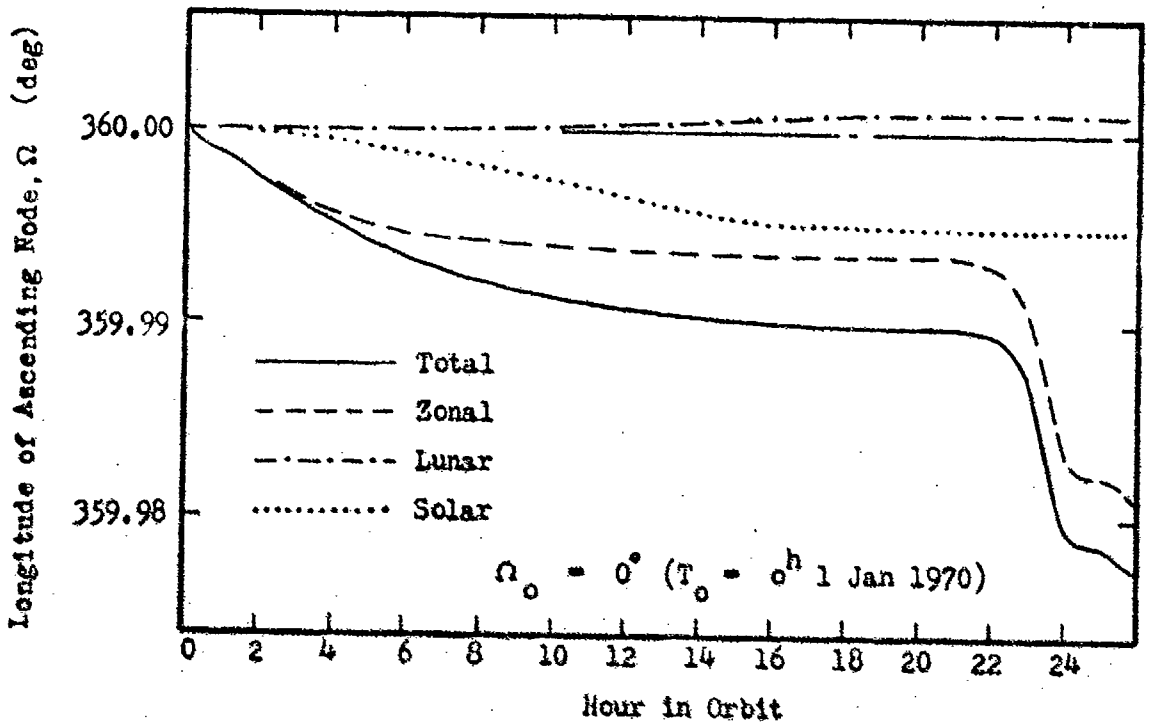

Figure 13. Variation of Longitude of Ascending Node with Hour in Orbit

Finally, Fig. 13 above illustrates the hourly change in the longitude of the ascending node for the orbit following injection at 0^h 1 Jan 1970 where Ω_o = 0°. The zonal, solar and lunar perturbations are seen to be the most effective in the variation of this parameter.

Launch Date Variation

Parameter Dependence on Date in Orbit. The orbit was calculated for a period of one year following the selected launch dates which were chosen during the period of 1 Jan 1970 through 1 Jan 1971. The results of selected orbital computations which are illustrated in Figs. 14 through 19 represent the changes of the orbital parameters as a function of the time in orbit. The separate curves shown in each figure represent different launch dates T_o (injection of vehicle into orbit at perigee). The specific launch date cases shown were selected to illustrate in

general the extremes of the parameter variation which result regardless of launch date. The individual curves are based on the value of each parameter at successive perigee points of the orbit.

The short-period oscillatory behavior evident in these figures is the effect of the lunar-cycle, while the longer period oscillations are due to the solar-cycle. These oscillations are superimposed on the general variation trend which is due to the oblateness of the earth.

Figure 14 illustrates the variation of the semi-major axis as a function of time in orbit following injection on the dates indicated. The daily orbital variation as shown for $T_o = 274$ includes the effect of the lunar cycle, while the cases for $T_o = 69$ and $T_o = 182$ illustrate the longer period variation as a result of smoothing the curves. The three cases shown represent an envelope into which most other launch cases fall. The smoothed curves were used here to avoid a cluttered representation and will not be used for other parameters.

The variation of eccentricity is shown in Fig. 15 for several launch dates. The least variation in the nominal value is obtained for a launch date of $T_o = 69$ and the maximum change is for a launch at $T_o = 182$. The general trend in decreasing the eccentricity causes the orbit to circularize in time.

Figure 16 illustrates the variation of inclination for a selected group of launch dates. The greatest variation is obtained for a launch date of $T_o = 51$, while for $T_o = 305$, the inclination oscillates about the nominal value of 60°. In general, the perturbations tend to increase the orbital inclination.

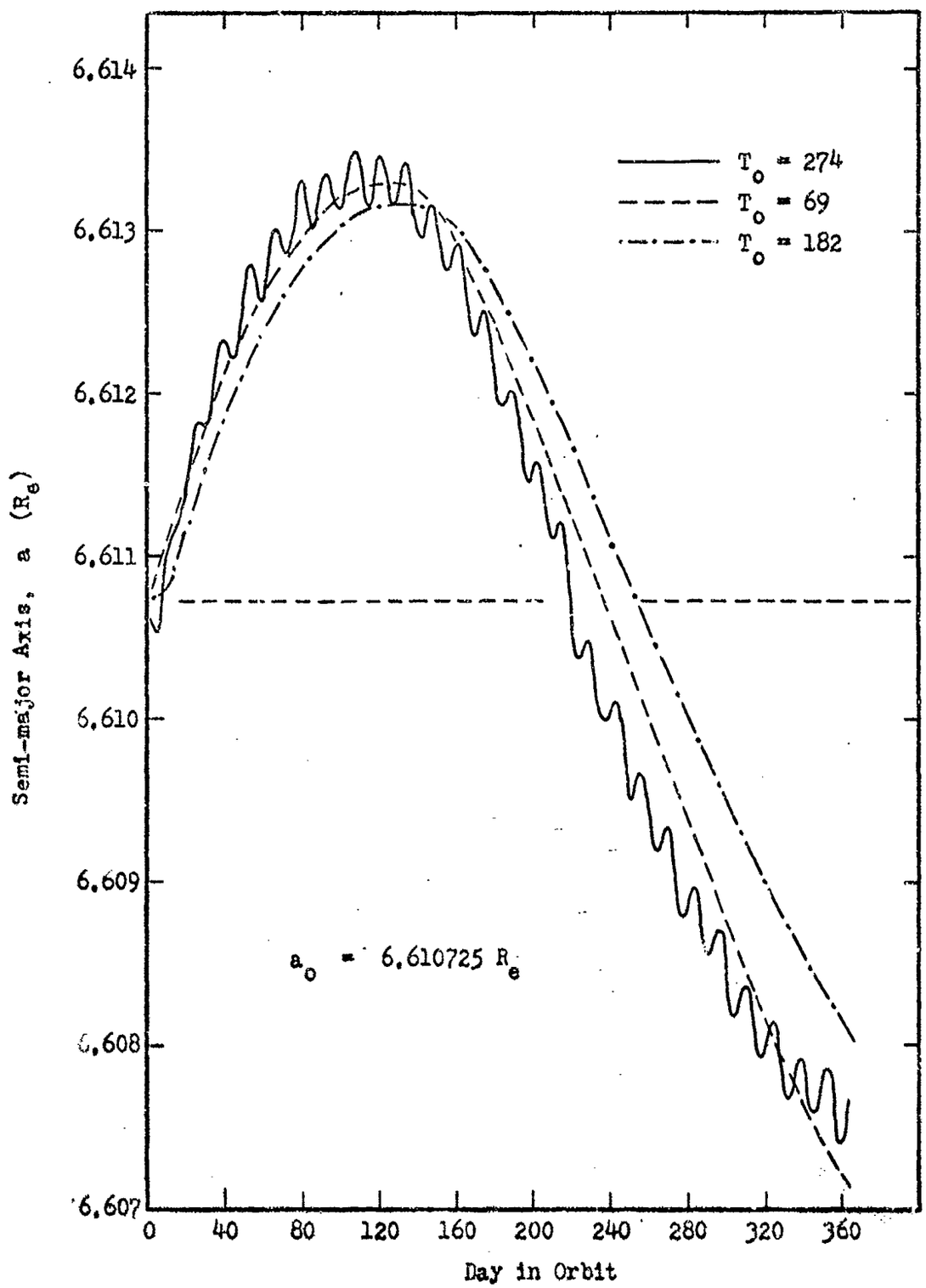

Figure 14. Variation of Semi-major Axis with Day in Orbit

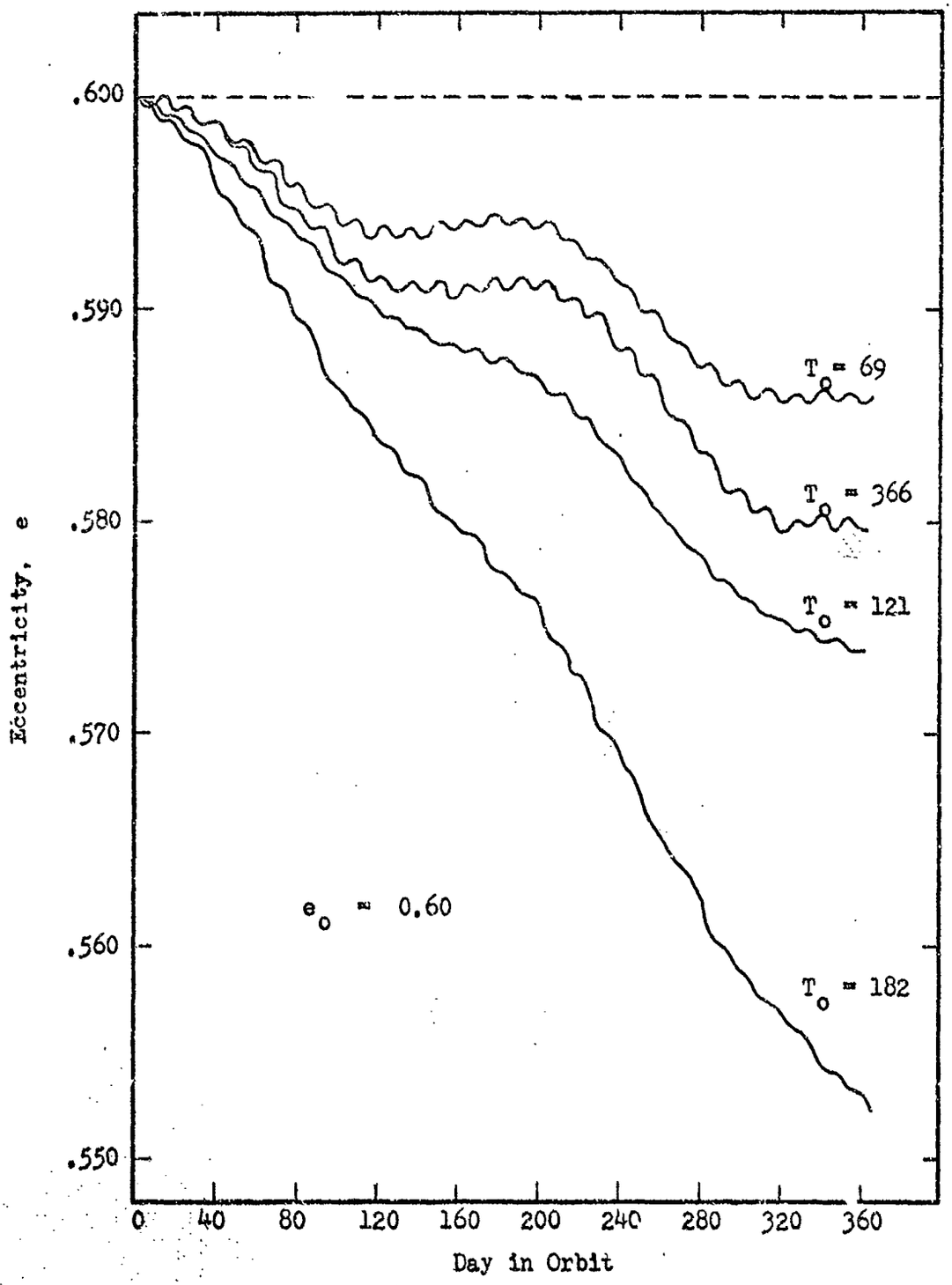

Figure 15. Variation of Eccentricity with Day in Orbit

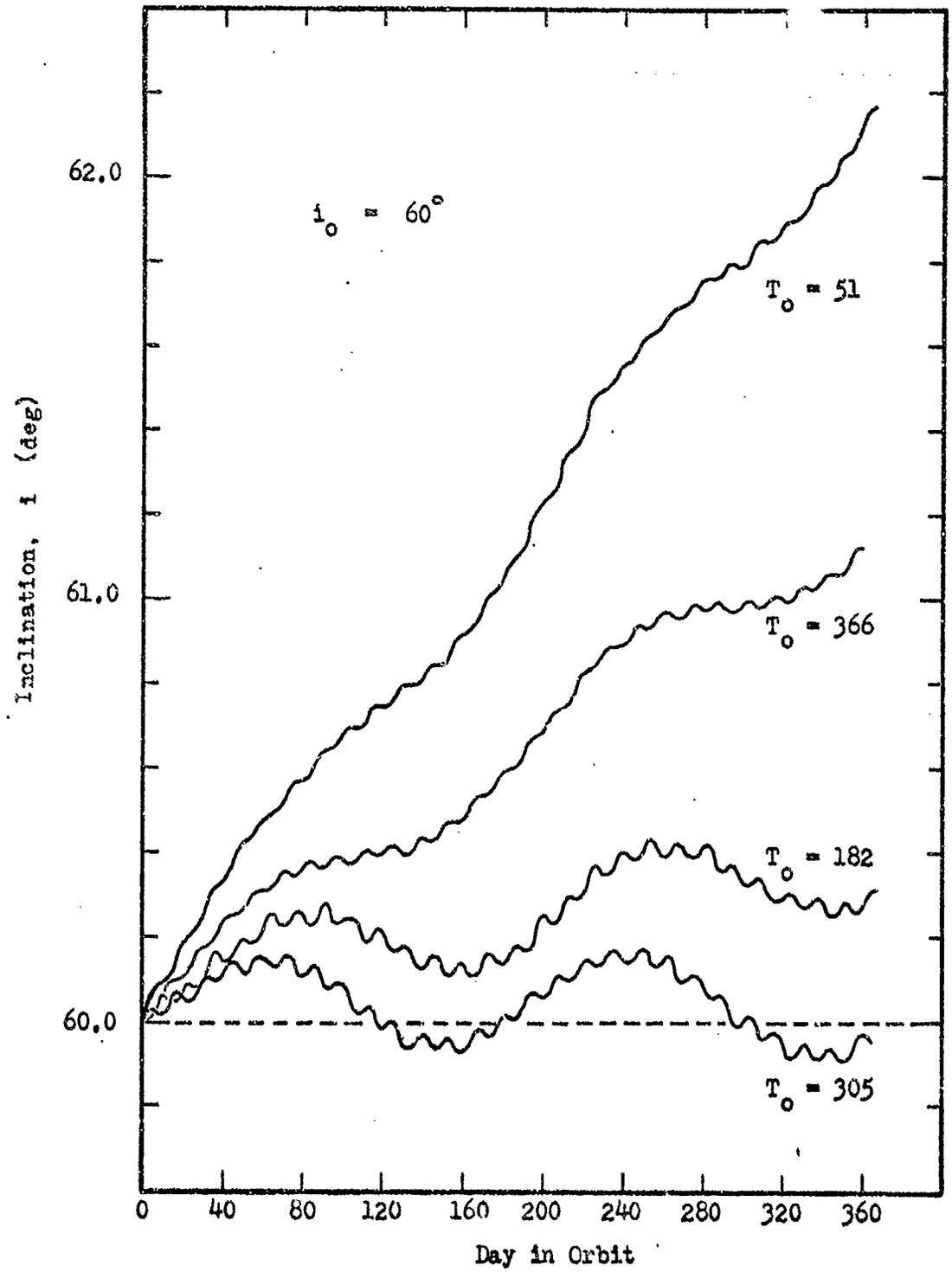

Figure 16. Variation of Inclination with Day in Orbit

The general trend of the perturbations lead to an increased value of the argument of the perigee as shown in Fig 17. The greatest decrease in ω is obtained for a launch date of T_o = 121 while the maximum increase is reached for T_o = 274. The variation of the apsidal line is most dependent on the variations in the orbital inclination and eccentricity.

Since the initial values of the longitude of ascending node Ω varies with the launch date, Fig. 18 represents the variation of $\Delta\Omega$. In general, the trend of westward regression is noted with a minimum drift resulting for T_o = 182 and maximum drift at T_o = 51. The variation due to the lunar-cycle is absent from these curves and the solar-cycle is only vaguely apparent.

The variation of the perigee distance r_p is shown in Fig. 19 and illustrates the close dependence on the variations in the eccentricity as shown in Fig. 15. Note that the minimum change in r_p is obtained for T_o = 69 while the maximum variation is reached at T_o 182.

Parameter Dependence on Launch Date. In order to more clearly determine the effect of the launch date choice on the variation of the orbital parameters, the data has been presented as a function of launch date in Figs. 20 through 24. The separate curves in each figure represent the variations after 90, 180, 270 and 360 days in orbit. These plots clearly indicate the launch dates which will provide the minimum changes in given orbital parameters. These characteristics in themselves, however, cannot be directly used in selecting the optimum launch date as will be shown in the following section.

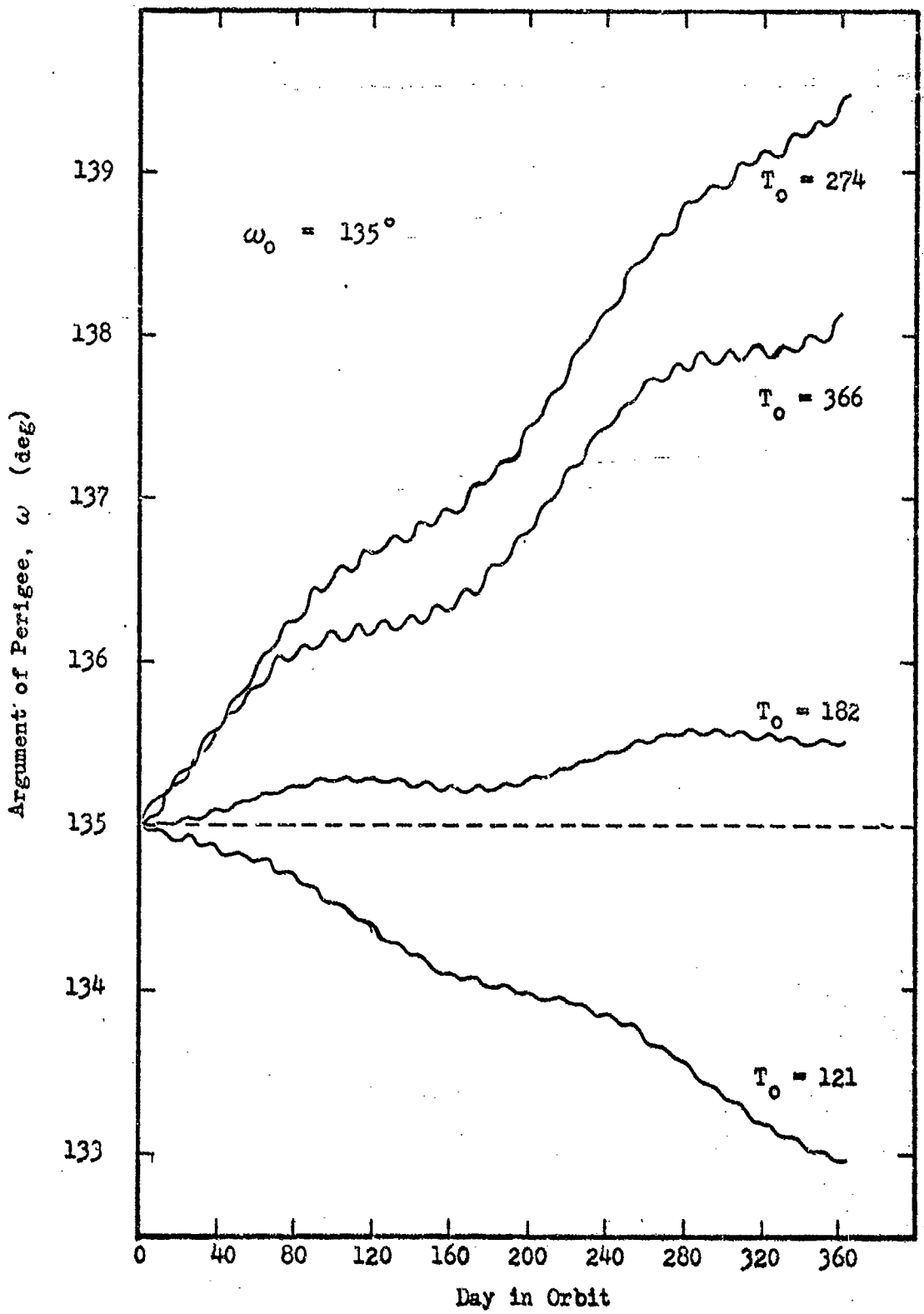

Figure 17. Variation of Argument of Perigee with Day in Orbit

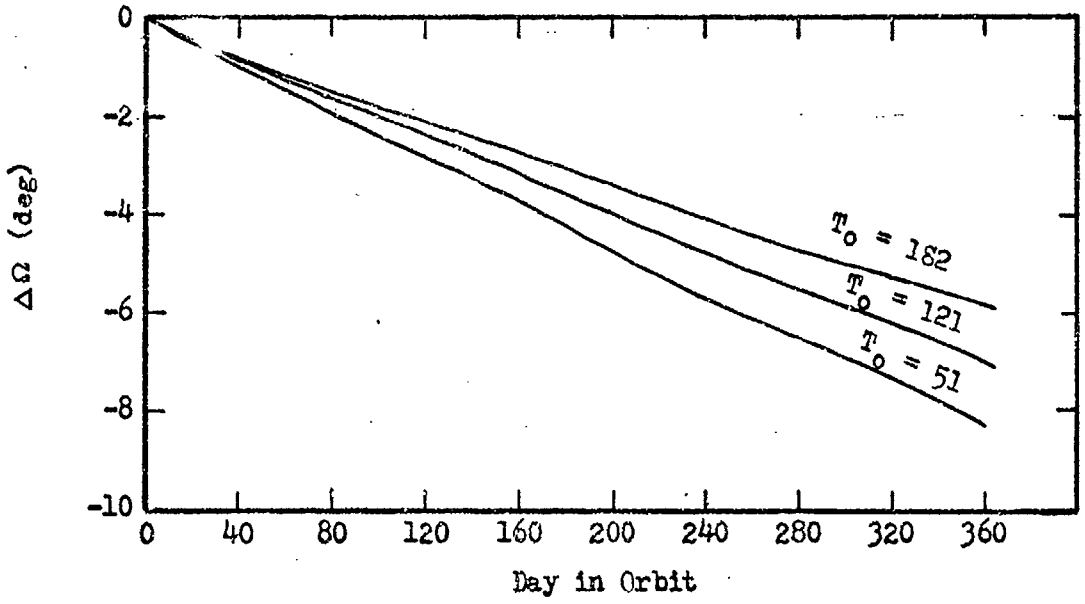

Figure 18. Variation of Longitude of Ascending Node with Day in Orbit

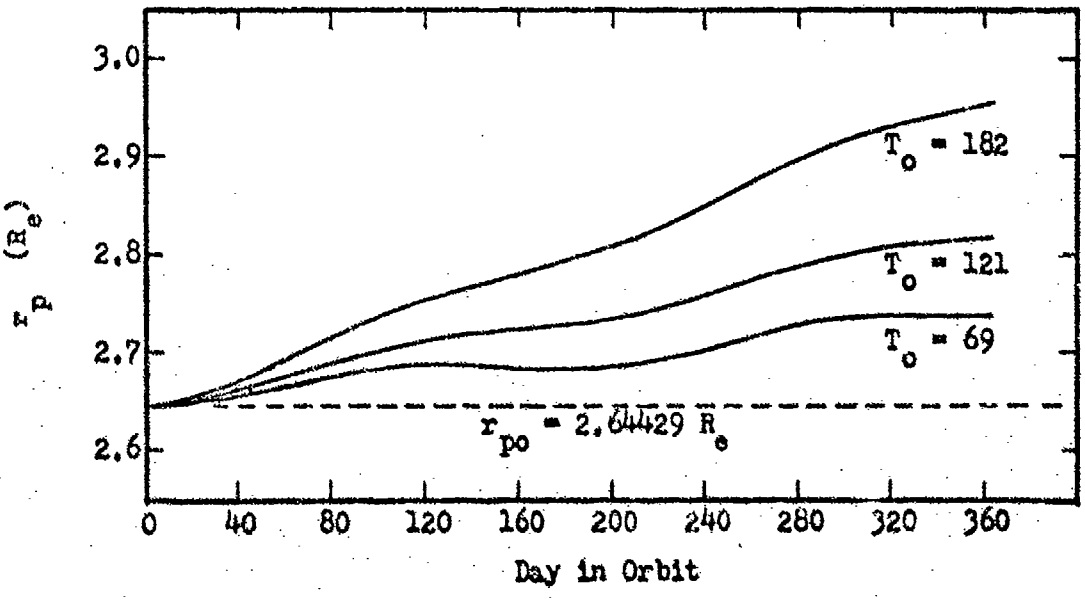

Figure 19. Variation of Radius of Perigee with Day in Orbit

Since the semi-major axis varies in a very small envelope regardless of the launch date, its variation as a function of launch date is not shown in this section. Figure 20 represents the variation of eccentricity as a function of launch date which clearly indicates a maximum rate of change at a launch date of $T_o = 182$. There are two launch dates which provide minimum changes and are at $T_o = 60$ and $T_o = 300$. The minimum changes represent a decrease in the eccentricity by 2.42 percent while the maximum decrease represents a 7.85 percent change.

The variation of the inclination is shown in Fig. 21 which illustrates that there are two launch dates which provide minimum changes during the year in orbit while there are also two dates which provide maximum changes. The maximum at $T_o = 60$ represents an increase in the inclination by 3.5 percent , while the maximum at $T_o = 222$ is an increase of only 0.83 percent. The minimum at $T_o = 165$ is only a 0.45 percent increase while that at T_o represents a negligible change by oscillating about the nominal value of 60°.

The variation in the argument of perigee shown in Fig. 22 indicates two possible launch dates which provide essentially no change; $T_o = 70$ and $T_o = 175$. A maximum increase by 3.3 percent is found for $T_o = 280$ while the maximum decrease of 1.48 percent is reached at $T_o = 125$.

Figure 23 illustrates the variation in the longitude of the ascending node. The greatest magnitude is a 2.3 percent decrease at $T_o = 50$ (percentage based on a nominal value of 360°). The minimum change is a 1.61 percent decrease at $T_o = 176$.

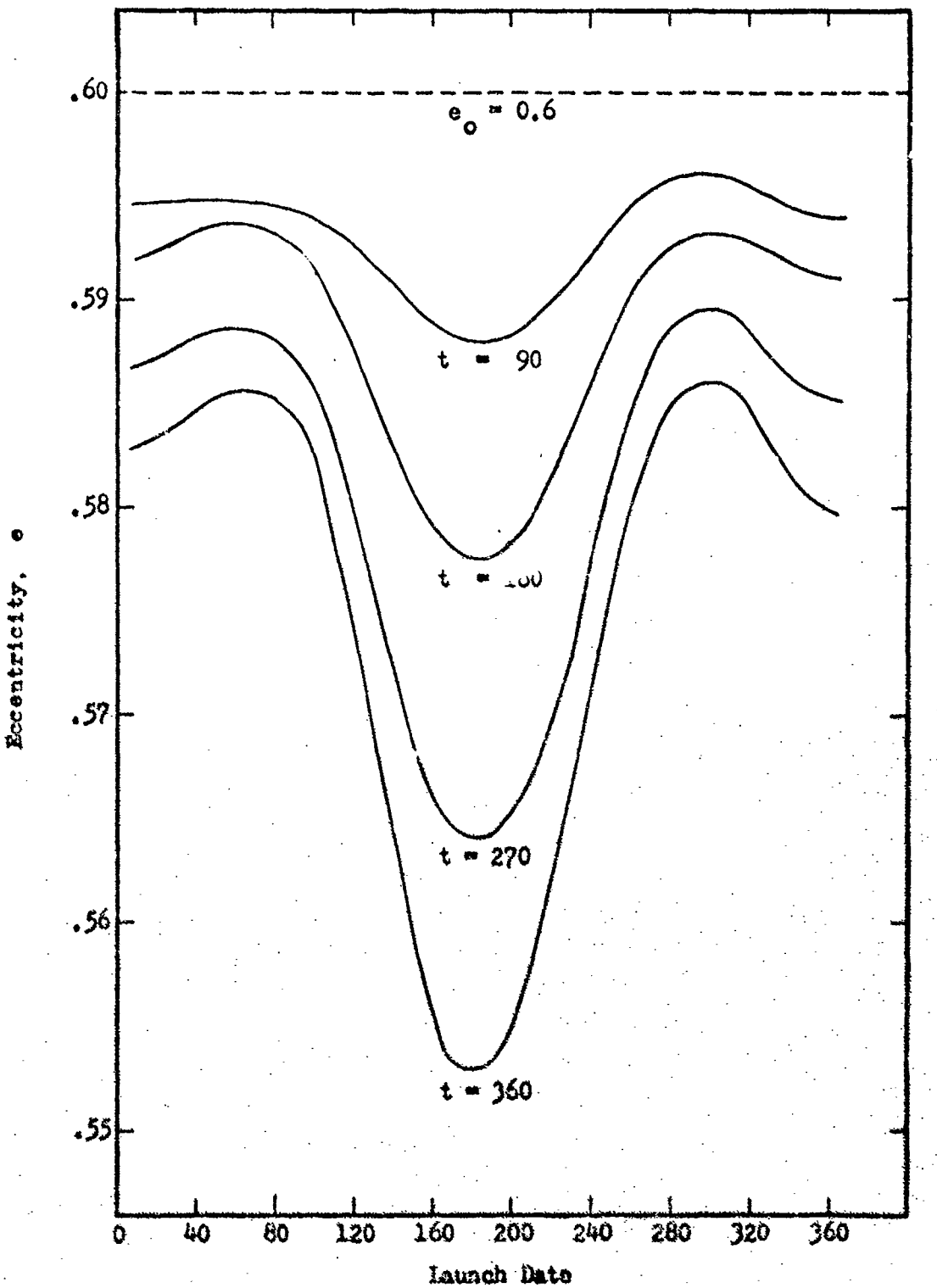

Figure 20. Variation of Eccentricity with Launch Date

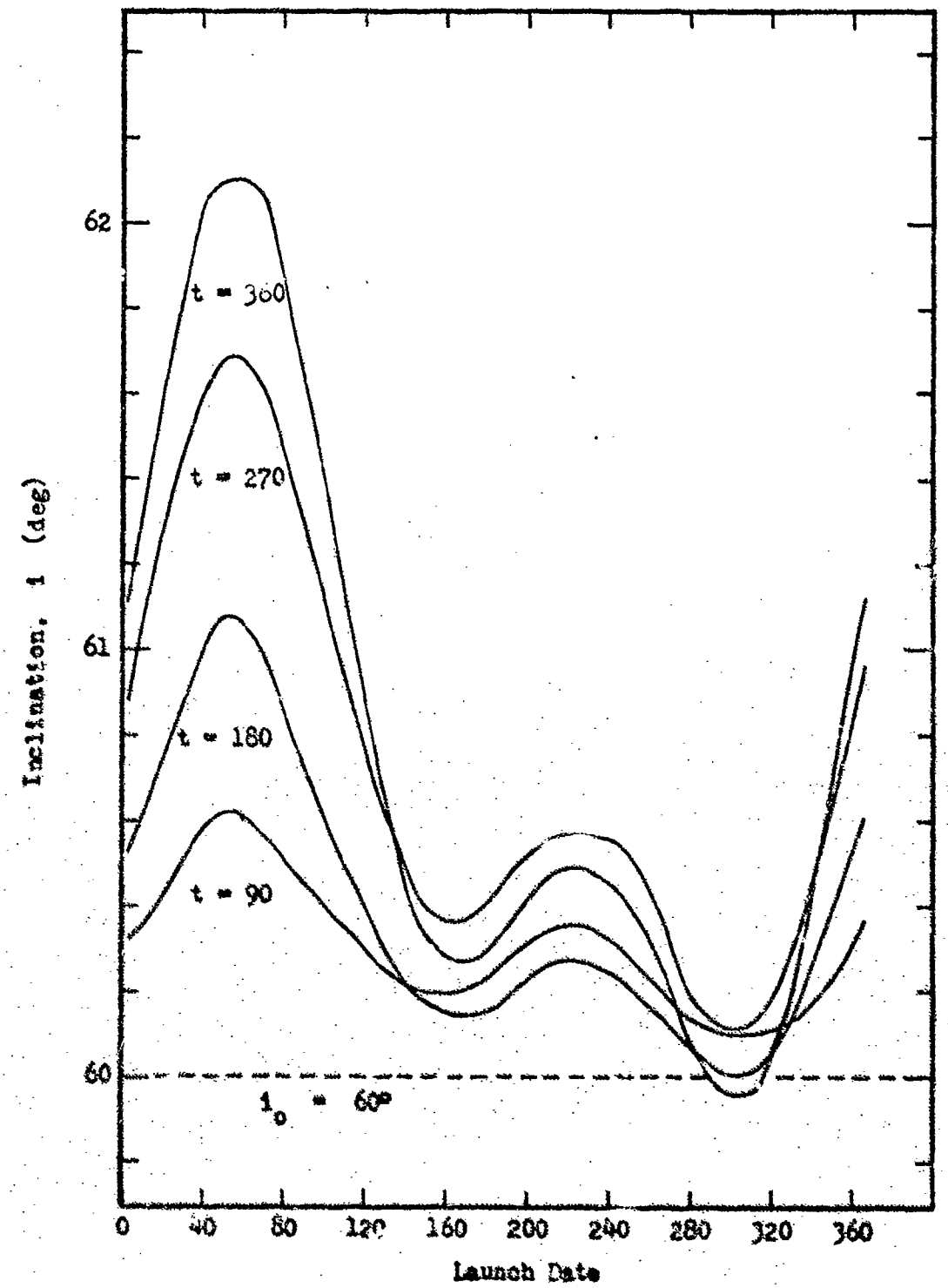

Figure 21. Variation of Inclination with Launch Date

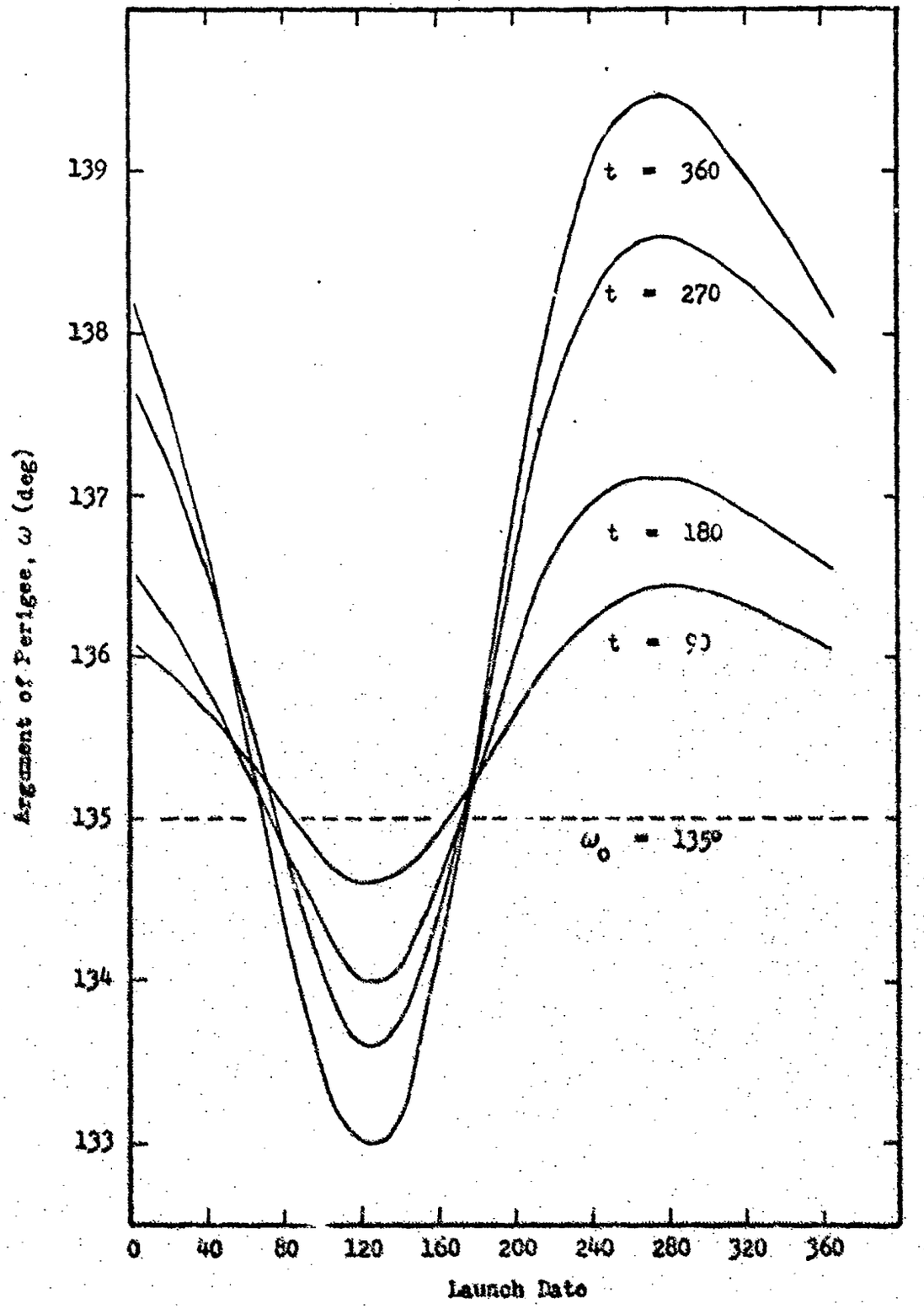

Figure 22. Variation of Argument of Perigee with Launch Date

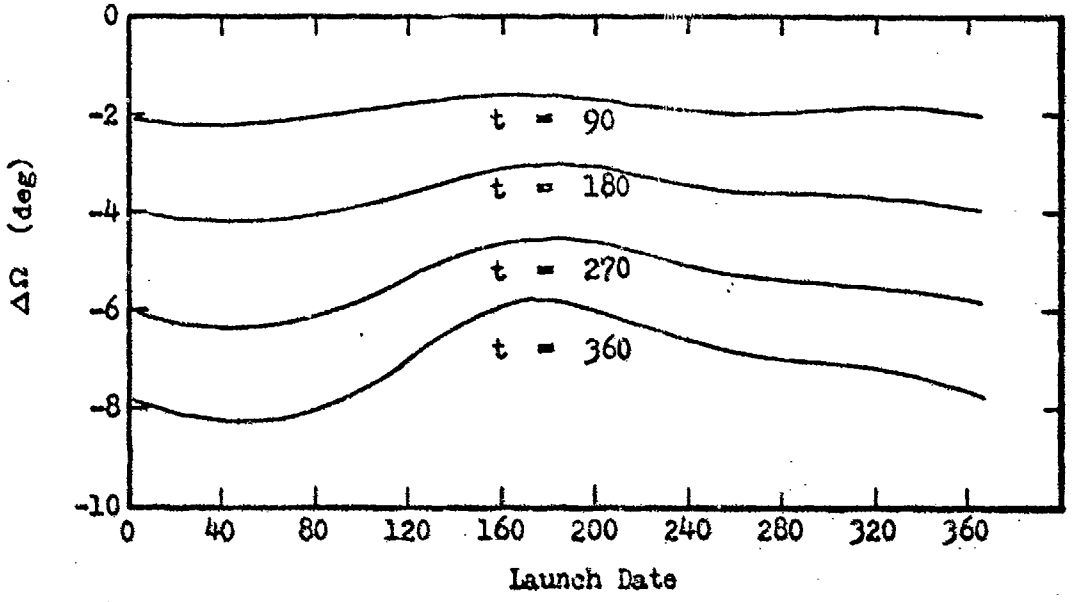

Figure 23. Variation of Longitude of Ascending Node with Launch Date

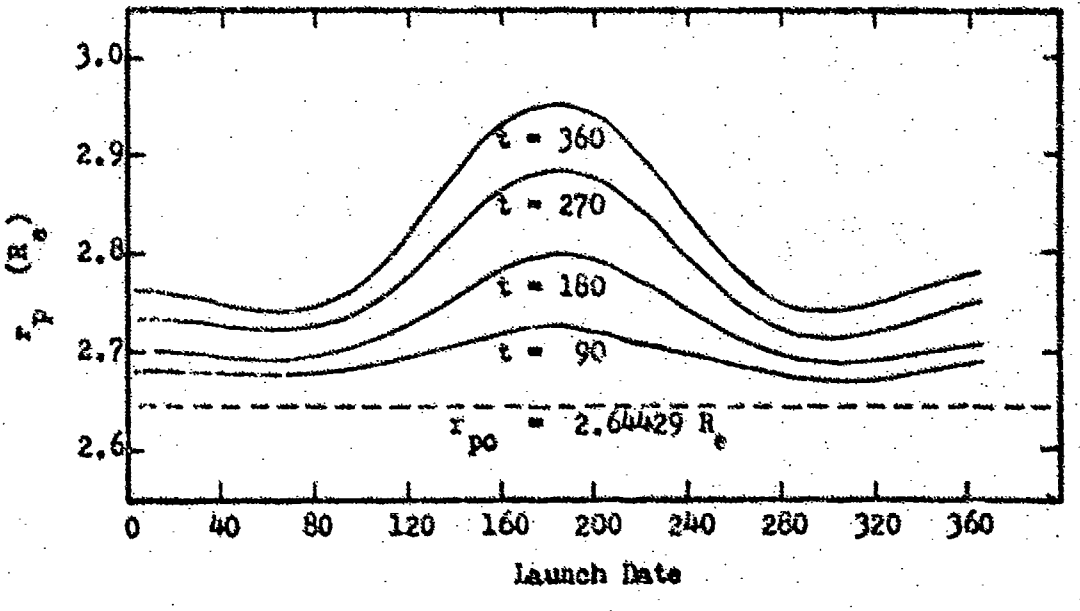

Figure 24. Variation of Radius of Perigee with Launch Date

Finally, the variation in the perigee distance is shown in Fig. 24. The maximum increase by 11.55 percent at $T_o = 182$ represents a very significant change. The minimum changes at $T_o = 70$ and $T_o = 300$ represent 3.62 percent increases in the nominal value of r_p.

Earth Trace Variation. The effect of the orbital parameter changes on the earth trace after one year in orbit is shown in Fig. 25. The two cases shown were selected to illustrate two extreme examples of drift. The trace for $T_o = 121$ represents the maximum westward drift of the small loop in the southern hemisphere, while the case for $T_o = 274$ represents the maximum eastward drift.

The relative size and position of the small loop can be roughly determined by referring to Fig. 26, which illustrates the longitudes of the most easterly point and crossover point as functions of the launch dates. Figure 27 illustrates the latitudes of the most easterly and crossover points in a similar manner.

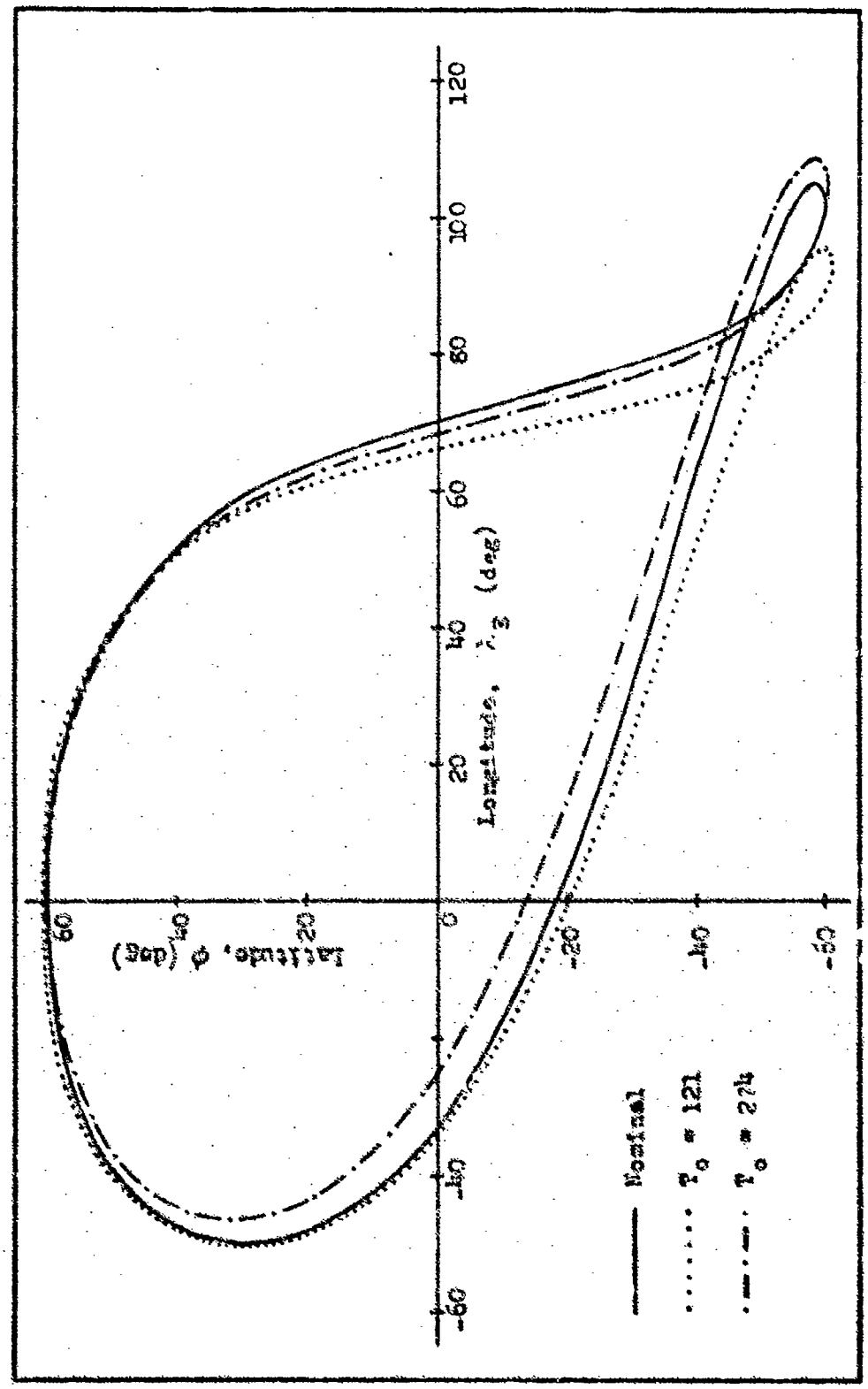

Figure 25. Comparison of Earth Traces of Perturbed and Nominal Orbits After One Year

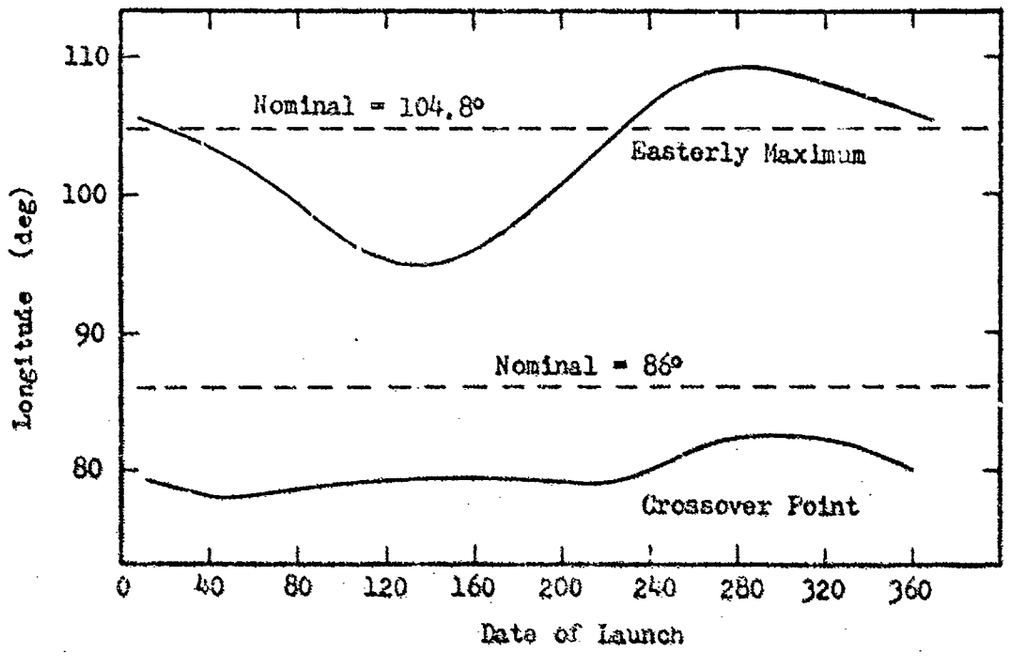

Figure 26. Longitudes of Small Loop as Function of Launch Date After One Year

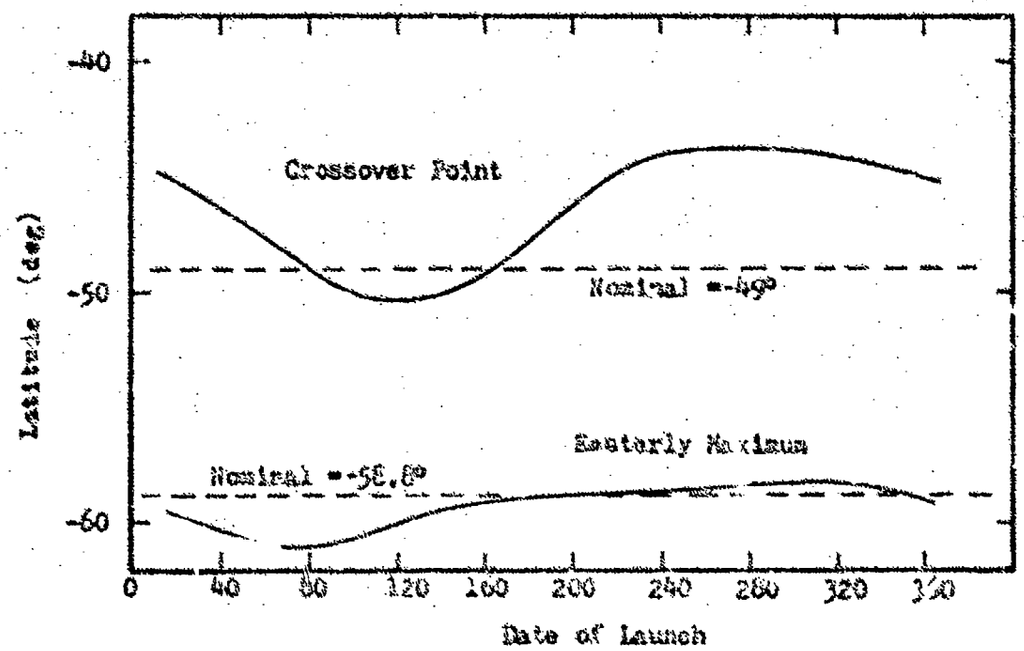

Figure 27. Latitudes of Small Loop as Function of Launch Date After One Year

Orbital Correction

The total impulse required for daily correction has been compared with total impulse required for correction every 14 orbits. Figure 28 illustrates the magnitudes of impulses required for the two options studied. As indicated in the figure, the area of interest is the range of launch dates providing for minimum corrective impulse. Except where short-term oscillations result in continually increasing (or decreasing) orbital parameters, the daily corrective impulses are greater in magnitude than those made periodically.

The largest component of the total corrective impulse required is due to the orthogonal impulse Δv_W required to correct the line of nodes and inclination. The magnitude of Δv_W is most heavily dependent on the change required in the longitude of ascending node rather than the inclination. The minimum value for this impulsive component is obtained at T_o = 170 with 268 m/sec and 244 m/sec being required for the daily and the 14-day interval corrections respectively. These values are nearly 66 percent of the total impulse required for correction after a year in orbit.

The second most significant contribution to the total yearly impulse is generally due to the normal impulse necessary to correct the argument of perigee or apsidal line. The minimum value of Δv_n for daily correction is at 50 m/sec at T_o = 165. If corrections are made at 14-day intervals, however, two local minimums are found. The minimum at T_o = 165 is only 20 m/sec while the one at T_o = 30 is 40 m/sec. The normal impulse approaches the magnitude of the orthogonal impulse for a launch date of T_o = 274 when it reaches a maximum value of approximately 200 m/sec.

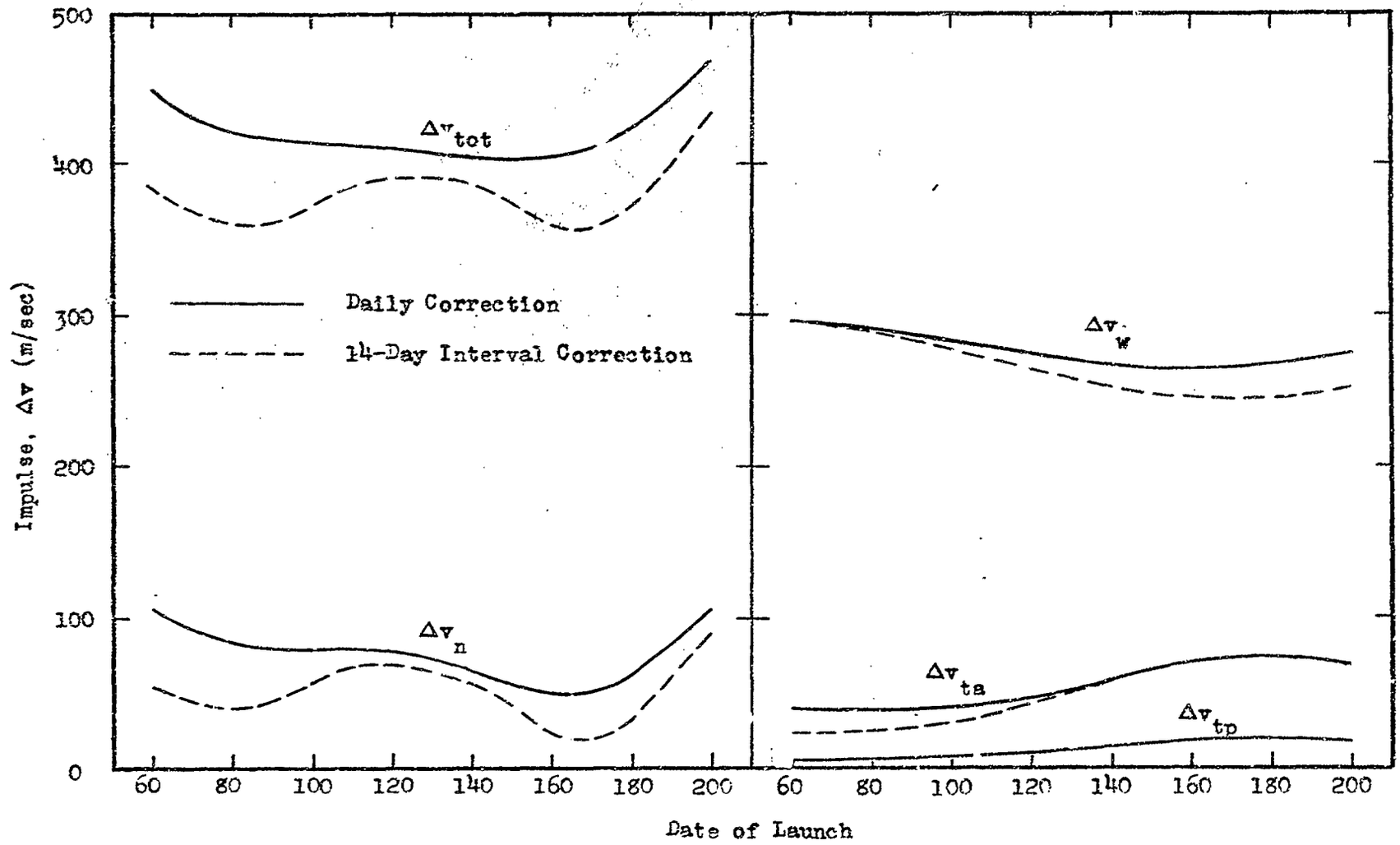

Figure 28. Components of Corrective Impulse Required to Maintain Nominal Orbital Parameters

As is expected, the shape of the curve depicting Δv_n is dependent primarily on the absolute magnitude of the variation of the argument of perigee.

The tangential impulses Δv_{ta} and Δv_{tp} are generally the smallest components of the total yearly correction and are primarily dependent on the magnitude of the variation in the eccentricity. The impulse made at apogee is necessarily largest of the two since it depends inversely on the orbital velocity. The apogee impulses are four to five times larger than those made at perigee and are directed in the opposite direction relative to vehicle motion. The minimum values for the tangential impulses are obtained for $T_o = 60$. The magnitudes of Δv_{ta} for daily and 14-day interval corrections are 40 m/sec and 25 m/sec respectively. The minimum value of Δv_{tp} is 6 m/sec for either technique of correction.

The minimum total impulse required to maintain the nominal orbit using daily corrections is obtained for a launch date of $T_o = 150$ and has a magnitude of 405 m/sec. The required impulse is less than 410 m/sec for a range of launch dates from $T_o = 130$ to $T_o = 165$. Two local minimums are obtained if corrections are applied at 14-day intervals. These points are reached for $T_o = 85$ and $T_o = 166$ and indicate minimum required impulses of 360 m/sec and 355 m/sec respectively. The technique of using 14-day intervals for corrections provides reductions in the total impulse of 14.3 percent and 13.4 percent for $T_o = 85$ and $T_o = 166$ respectively as compared to those for daily corrections.

The foregoing analysis of the minimum impulse required to maintain the nominal orbit should be contrasted with that required if the worst date were chosen for launch during the calendar year of 1970. The total

impulse required for a launch on T_o = 300 would be approximately 558 m/sec if the orbit were corrected on a daily basis. The impulse would be nearly this value if corrected at 14-day intervals since the orbital parameters change rapidly and the lunar oscillations are not as effective. This value is 49.4 percent higher than for the daily corrected optimum case and 55.9 percent greater than the 14-day interval case.

IV. Conclusions and Recommendations

Analysis of the perturbative effects on the orbit that was studied, for the sources considered, has prompted some general observations. Although the zonal harmonics cause the most significant oblate earth contribution to the perturbed orbit, the sectorial harmonics cannot generally be neglected in the long term. The lunar and solar third-body perturbations are second only to the zonal harmonics. The radiation pressure for the area-to-mass ratio of 10 ft^2/slug is generally more significant than the sectorial harmonics. The tesseral harmonics could probably be neglected for this type of study.

The study has resulted in the determination of optimum launch dates to minimize the total station keeping impulse required for one year in orbit. The optimum dates, however, were found to depend on the specific technique of impulse application, or more correctly the timing of the application. If, for example, the orbit were corrected daily, using instantaneous impulses, the magnitude of the minimum value was found to be only 72.5 percent of the maximum value necessary in the worst case for launch. However, if the corrections were applied at 14-day intervals, based on the lunar-cycle, the minimum value is only 63.5 percent of the maximum value. These results should play a very important role in the ultimate design of the thruster assembly and impulse programming control system aboard the satellite.

The results of this study indicate that further study should be applied to the optimization of the magnitude of the corrective impulse necessary by 1) variation of the orbital parameters about their nominal values and 2) by determining the nature of an optimum impulse

program timing for the thruster. Study could also be extended to a similar analysis of orbits which have periods of revolution which are integral fractions of the sidereal rotational period of earth about its axis.

Bibliography

1. The American Ephemeris and Nautical Almanac for the Year 1970. Nautical Almanac Office, United States Naval Observatory. Washington: U.S. Government Printing Office, 1968.

2. Baker, Robert M. L., Jr. Astrodynamics: Application and Advanced Topics. New York: Academic Press, 1967.

3. Baker, Robert M. L., Jr. and M. W. Makemson. An Introduction to Astrodynamics (2nd Edition). New York: Academic Press, 1967.

4. Bate, Roger R., et al. Fundamentals of Astrodynamics. New York: Dover Publications, Inc., 1971.

5. B. kowicz, Peter. "Ground Tacks of Earth-Period (24-Hr) Satellites". AIAA Journal, 4:2190-2195 (December 1966).

6. Ehricke, Krafft A. Principles of Guided Missile Design, Space Flight. Vol. I: Environment and Celestial Mechanics, edited by Grayson Merrill. Princeton, New Jersey: D. Van Nostrand Company, Inc., 1960.

7. Ehricke, Krafft A. Principles of Guided Missile Design, Space Flight. Vol. II: Dynamics, edited by Grayson Merrill. Princeton, New Jersey: D. Van Nostrand Company, Inc., 1962.

8. Escobal, Pedro Ramon. Methods of Astrodynamics. New York: John Wiley & Sons, Inc., 1968.

9. Gaposchkin, E. M. and K. Lambeck. 1969 Smithsonian Standard Earth (II). SAO Special Report No. 315. Cambridge, Massachusetts: Smithsonian Institution, Astrophysical Observatory, May 18, 1970.

10. Kotter, R. L. and S. P. Prawel, Jr. Modern Methods of Engineering Computation. New York: McGraw-Hill Book Company, 1969.

11. Ricci, Arnold A. 24 Hour Satellite. GA/AE/68-4, Unpublished Thesis. Wright-Patterson Air Force Base, Ohio: Air Force Institute of Technology, June 1968.

12. Shute, Barbara E. Prelaunch Analysis of High Eccentricity Orbits. NASA Technical Note D-2530, Washington: National Aeronautics and Space Administration, December 1964.

13. Wolaver, Lynn E. Modern Techniques in Astrodynamics - An Introduction. ARL 70-0278. Wright-Patterson Air Force Base, Ohio: Aerospace Research Laboratories, December 1970.

Appendix A

Perturbation Equations

Oblate Earth. The most general expression which is used to describe the gravitational potential of the oblate earth is given by Baker (Ref 3: 174) as

$$\phi = \frac{K_e}{r}\left\{1 + \sum_{n=2}^{\infty}\left[\sum_{k=0}^{n}\left(\frac{P_n^k(\sin\delta)}{r^n}\right)\left[C_{nk}\cos(k\lambda_E) + S_{nk}\sin(k\lambda_E)\right]\right]\right\} \quad (4)$$

The Legendre polynomials $P_n^k(\sin\delta)$ and the harmonic coefficients C_{nk} and S_{nk} are developed and tabulated at the end of this section. The east longitude of the vehicle is given by

$$\lambda_E = \alpha - \theta_{go} - \omega_e(t - t_o) \quad (10)$$

The harmonic function given above can be separated into four parts and given by $\phi = \phi_1 + \phi_2 + \phi_3 + \phi_4$ where the two-body term is

$$\phi_1 = \frac{K_e}{r} \quad (16)$$

The remaining terms are the zonal harmonics,

$$\phi_2 = \frac{K_e}{r}\sum_{n=2}^{\infty} J_n \frac{P_n^o(\sin\delta)}{r^n} \quad (17)$$

where J_n are the zonal harmonic coefficients tabulated later; the tesseral harmonics,

$$\phi_3 = \frac{K_e}{r} \left\{ \sum_{n=2}^{\infty} \left[\sum_{k=1}^{n-1} \left(\frac{P_n^k (\sin \delta)}{r^n} \right) \left[C_{nk} \cos(k\lambda_E) + S_{nk} \sin(k\lambda_E) \right] \right] \right\} \quad (18)$$

and the sectorial harmonics

$$\phi_4 = \frac{K_e}{r} \sum_{n=2}^{\infty} \frac{P_n^n (\sin \delta)}{r^n} \left[C_{nn} \cos(n\lambda_E) + S_{nn} \sin(n\lambda_E) \right]$$

$$= \frac{K_e}{r} \sum_{n=2}^{\infty} \frac{(2n)!}{2^n n!\, r^n} \left[C_{nn} \cos(n\lambda_E) + S_{nn} \sin(n\lambda_E) \right] \quad (19)$$

The contributions to gravitational acceleration of a body in earth space is given in terms of the gradient of the potential function as

$$\ddot{\vec{r}} + \ddot{\vec{r}} = \nabla\phi_1 + \nabla\phi_2 + \nabla\phi_3 + \nabla\phi_4 \quad (20)$$

where the two-body acceleration vector is given by

$$\ddot{\vec{r}} = \begin{bmatrix} \ddot{x} \\ \ddot{y} \\ \ddot{z} \end{bmatrix} = \nabla\phi_1 = -\frac{K_e}{r} \begin{bmatrix} x \\ y \\ z \end{bmatrix} \quad (21)$$

where the two-body position components must be those of the reference orbit. The perturbative contributions $\ddot{\vec{r}}$, due to the zonal, tesseral and sectorial harmonics are given by

$$\nabla\phi_2 = K_e \sum_{n=2}^{\infty} J_n \left[\frac{(n+1)}{r^{n+3}} \begin{bmatrix} x \\ y \\ z \end{bmatrix} P_n^o \left(\frac{z}{r}\right) - \frac{1}{r^{n+1}} \nabla P_n^o \left(\frac{z}{r}\right) \right] \quad (22)$$

where $(\sin \delta)$ has been replaced by its equivalent $\left(\frac{z}{r}\right)$,

$$\nabla\phi_3 = K_e \sum_{n=2}^{\infty} \left\{ \sum_{k=1}^{n-1} \left[\frac{-(n+1)}{r^{n+3}} \begin{Bmatrix} x \\ y \\ z \end{Bmatrix} P_n^k\left(\frac{z}{r}\right) + \frac{1}{r^{n+1}} \nabla P_n^k\left(\frac{z}{r}\right) \right] \left[C_{nk}\cos(k\lambda_E) + S_{nk}\sin(k\lambda_E) \right] + \frac{P_n^k\left(\frac{z}{r}\right)}{r^{n+1}} \left[-C_{nk}\sin(k\lambda_E) + S_{nk}\cos(k\lambda_E) \right] k \nabla\lambda_E \right\} \quad (23)$$

$$\nabla\phi_4 = K_e \sum_{n=2}^{\infty} \frac{(2n)!}{2^n\, n!} \left\{ \frac{-(n+1)}{r^{n+3}} \begin{Bmatrix} x \\ y \\ z \end{Bmatrix} \left[C_{nn}\cos(n\lambda_E) + S_{nn}\sin(n\lambda_E) \right] + \frac{1}{r^{n+1}} \left[-C_{nn}\sin(n\lambda_E) + S_{nn}\cos(n\lambda_E) \right] n \nabla\lambda_E \right\} \quad (24)$$

where $\nabla\lambda_E = \nabla\alpha = \nabla(\tan^{-1}\frac{y}{x})$, which gives

$$\frac{\partial\alpha}{\partial x} = \frac{-y}{x^2 + y^2}, \quad \frac{\partial\alpha}{\partial y} = \frac{x}{x^2 + y^2} \quad \text{and} \quad \frac{\partial\alpha}{\partial z} = 0 \quad (25)$$

The adopted zonal harmonic coefficients as used in the analysis are given in Table II (Ref 9:8).

Table II. Zonal Harmonic Coefficients

n	J_n
2	1082.628×10^{-6}
3	-2.538×10^{-6}
4	-1.593×10^{-6}
5	-0.230×10^{-6}
6	0.502×10^{-6}

The normalized tesseral and sectorial harmonic coefficients used in the analysis are presented in Table III (Ref 9:60), with the normalizing coefficients N_{nk} obtained from the relation

$$N_{nk} = \left[\frac{2\,(2n+1)\,(n-k)!}{(n+k)!}\right]^{1/2} \tag{26}$$

Table III. Normalized Tesseral and Sectorial Coefficients

n	k	$\bar{C}_{nk}$ ($\times 10^6$)	$\bar{S}_{nk}$ ($\times 10^6$)	N_{nk}
2	2	2.41290	-1.36410	0.64550
3	1	1.96980	0.26015	1.08010
3	2	0.89204	-0.63468	0.34157
3	3	0.68630	1.43040	0.13944
4	1	-0.52989	-0.48765	0.94868
4	2	0.33024	0.70633	0.22361
4	3	0.98943	-0.15467	0.05976
4	4	-0.07969	0.33928	0.02113
5	1	-0.05382	-0.09791	0.85635
5	2	0.61286	-0.35087	0.16183
5	3	-0.43083	-0.08666	0.03303
5	4	-0.26693	0.08301	0.00779
5	5	0.12593	-0.59910	0.00246
6	1	-0.09898	0.03765	0.78680
6	2	0.05482	-0.35175	0.12440
6	3	0.02787	0.04463	0.02073
6	4	-0.00040	-0.40388	0.00379
6	5	-0.21143	-0.52264	0.00081
6	6	0.08869	-0.07476	0.00023

The values of the conventional coefficients (C_{nk} and S_{nk}) are determined by the relations $C_{nk} = N_{nk}\,\bar{C}_{nk}$ and $S_{nk} = N_{nk}\,\bar{S}_{nk}$.

The Legendre polynomials which are required in the zonal and tesseral harmonic functions can be obtained from the Rodrigues formula

$$P_n(x) = \frac{1}{2^n\, n!} \frac{d^n (x^2 - 1)^n}{dx^n} \tag{27}$$

where $P_n(x)$ is the polynomial of order n, and $x = \sin \delta = \frac{z}{r}$. The expressions for $n = 0$ through $n = 6$ are obtained as given below.

$$P_0(x) = 1 \tag{28}$$

$$P_1(x) = x \tag{29}$$

$$P_2(x) = \tfrac{1}{2}(3x^2 - 1) \tag{30}$$

$$P_3(x) = \tfrac{1}{2}(5x^3 - 3x) \tag{31}$$

$$P_4(x) = \tfrac{1}{8}(35x^4 - 30x^2 + 3) \tag{32}$$

$$P_5(x) = \tfrac{1}{8}(63x^5 - 70x^3 + 15x) \tag{33}$$

$$P_6(x) = \tfrac{1}{16}(231x^6 - 315x^4 + 105x^2 - 5) \tag{34}$$

The associated Legendre polynomials are obtained using the relation

$$P_n^k(x) = (1 - x^2)^{k/2} \frac{d^k P_n^0(x)}{dx^n} \tag{35}$$

where $P_n^0(x) = P_n(x)$. The expressions which result are given as follows:

$$P_n^k(x) = 0 \quad , \quad n < k \tag{36}$$

$$P_1^1(x) = (1 - x^2)^{1/2} \tag{37}$$

$$P_2^1(x) = 3x\,(1 - x^2)^{1/2} \tag{38}$$

$$P_3^1(x) = \tfrac{3}{2}(5x^2 - 1)\,(1 - x^2)^{1/2} \tag{39}$$

$$P_4^1(x) = \frac{5}{2}(7x^3 - 3x)(1 - x^2)^{1/2} \tag{40}$$

$$P_5^1(x) = \frac{15}{8}(21x^4 - 14x^2 + 1)(1 - x^2)^{1/2} \tag{41}$$

$$P_6^1(x) = \frac{21}{8}(33x^5 - 30x^3 + 5x)(1 - x^2)^{1/2} \tag{42}$$

$$P_2^2(x) = 3(1 - x^2) \tag{43}$$

$$P_3^2(x) = 15x(1 - x^2) \tag{44}$$

$$P_4^2(x) = \frac{15}{2}(7x^2 - 1)(1 - x^2) \tag{45}$$

$$P_5^2(x) = \frac{105}{2}(3x^3 - x)(1 - x^2) \tag{46}$$

$$P_6^2(x) = \frac{105}{8}(33x^4 - 18x^2 + 1)(1 - x^2) \tag{47}$$

$$P_3^3(x) = 15(1 - x^2)^{3/2} \tag{48}$$

$$P_4^3(x) = 105x(1 - x^2)^{3/2} \tag{49}$$

$$P_5^3(x) = \frac{105}{2}(9x^2 - 1)(1 - x^2)^{3/2} \tag{50}$$

$$P_6^3(x) = \frac{315}{2}(11x^3 - 3x)(1 - x^2)^{3/2} \tag{51}$$

$$P_4^4(x) = 105(1 - x^2)^2 \tag{52}$$

$$P_5^4(x) = 945x(1 - x^2)^2 \tag{53}$$

$$P_6^4(x) = \frac{945}{2}(1 - x^2)^2 \tag{54}$$

$$P_5^5(x) = 945(1 - x^2)^{5/2} \tag{55}$$

$$P_6^5(x) = 10395x(1 - x^2)^{5/2} \tag{56}$$

$$P_6^6(x) = 10395(1 - x^2)^3 \tag{57}$$

The components of the gradient of the associated Legendre polynomials given generally by $\nabla P_n^k\left(\frac{r}{r}\right)$ and expressed in equatorial coordinates are determined from the following relations:

$$\frac{\partial}{\partial x} P_n^k\left(\frac{z}{r}\right) = \frac{\partial}{\partial x}\left(\frac{z}{r}\right) \frac{\partial}{\partial\left(\frac{z}{r}\right)} P_n^k\left(\frac{z}{r}\right) \tag{58}$$

$$\frac{\partial}{\partial y} P_n^k\left(\frac{z}{r}\right) = \frac{\partial}{\partial y}\left(\frac{z}{r}\right) \cdot \frac{\partial}{\partial\left(\frac{z}{r}\right)} P_n^k\left(\frac{z}{r}\right) \tag{59}$$

$$\frac{\partial}{\partial z} P_n^k\left(\frac{z}{r}\right) = \frac{\partial}{\partial z}\left(\frac{z}{r}\right) \cdot \frac{\partial}{\partial\left(\frac{z}{r}\right)} P_n^k\left(\frac{z}{r}\right) \tag{60}$$

where $$r^2 = x^2 + y^2 + z^2 \tag{61}$$

$$\frac{\partial}{\partial x}\left(\frac{z}{r}\right) = -\frac{xz}{r^3} \tag{62}$$

$$\frac{\partial}{\partial y}\left(\frac{z}{r}\right) = -\frac{yz}{r^3} \tag{63}$$

$$\frac{\partial}{\partial z}\left(\frac{z}{r}\right) = \frac{r^2 - z^2}{r^3} \tag{64}$$

$$\frac{\partial}{\partial\left(\frac{z}{r}\right)} P_n^k\left(\frac{z}{r}\right) = \frac{P_n^{k+1}\left(\frac{z}{r}\right)}{\left[1 - \left(\frac{z}{r}\right)^2\right]^{1/2}} - \frac{k\left(\frac{z}{r}\right) P_n^k\left(\frac{z}{r}\right)}{1 - \left(\frac{z}{r}\right)^2} \tag{65}$$

Substitution of Eqs (62) through (65) into Eqs (58) through (60) will give the required components of the gradient functions.

Third Body Attraction. The general equation of motion for a small mass such as an earth satellite in the presence of a main attracting body, the earth, as well as other perturbing bodies is given by

$$\ddot{\vec{r}} + \ddot{\vec{r}} = \begin{Bmatrix} \ddot{x} \\ \ddot{y} \\ \ddot{z} \end{Bmatrix} + \begin{Bmatrix} \ddot{x} \\ \ddot{y} \\ \ddot{z} \end{Bmatrix} = -\frac{K_e}{r^3}\begin{Bmatrix} x \\ y \\ z \end{Bmatrix} - \sum_j K_j \left[\frac{1}{r_j^3}\begin{Bmatrix} x \\ y \\ z \end{Bmatrix}_j + \frac{1}{r_{pj}^3}\begin{Bmatrix} x \\ y \\ z \end{Bmatrix}_{pj}\right] \tag{66}$$

where $\begin{Bmatrix} x \\ y \\ z \end{Bmatrix}_j$ = radial vector between the main and j^{th} perturbing body

$\begin{Bmatrix} x \\ y \\ z \end{Bmatrix}_{pj}$ = radial vector between the satellite and j^{th} body

and $$r_j^2 = x_j^2 + y_j^2 + z_j^2 \tag{67}$$

$$r_{pj}^2 = x_{pj}^2 + y_{pj}^2 + z_{pj}^2 = (x - x_j)^2 + (y - y_j)^2 + (z - z_j)^2 \tag{68}$$

The first term of Eq (66) again represents the simple 2-body attractive acceleration while the second represents the perturbative acceleration due to the third-bodies (Ref 4:389).

The perturbative equations for the case of lunar and solar masses can be written as

$$\ddot{\vec{r}}_m = \begin{Bmatrix} \ddot{x} \\ \ddot{y} \\ \ddot{z} \end{Bmatrix}_m = -K_m \left[\frac{1}{r_{pm}^3} \begin{Bmatrix} x - x_m \\ y - y_m \\ z - z_m \end{Bmatrix} + \frac{1}{r_m^3} \begin{Bmatrix} x \\ y \\ z \end{Bmatrix}_m \right] \tag{69}$$

$$\ddot{\vec{r}}_s = \begin{Bmatrix} \ddot{x} \\ \ddot{y} \\ \ddot{z} \end{Bmatrix}_s = -K_s \left[\frac{1}{r_{ps}^3} \begin{Bmatrix} x - x_s \\ y - y_s \\ z - z_s \end{Bmatrix} + \frac{1}{r_s^3} \begin{Bmatrix} x \\ y \\ z \end{Bmatrix}_s \right] \tag{70}$$

The radial components x_s, y_s and z_s are available directly from the ephemeris tables (Ref 1:34), although the components x_m, y_m and z_m must be calculated using the tabulated right ascension, declination and semi-diameter for the moon (Ref 1:52). These calculations can be made by using the relations

$$x_m = r_m \cos \alpha_m \tag{71}$$

$$y_m = r_m \sin \alpha_m \tag{72}$$

$$z_m = r_m \sin \delta_m \tag{73}$$

$$r_m = \frac{r_m'}{s'} s \tag{74}$$

where r_m' is the reference distance given a semi-diameter s'.

Again, the components x, y and z must represent the position in the reference orbit as shown by the vector $\bar{\rho}$ in Fig. 29 .

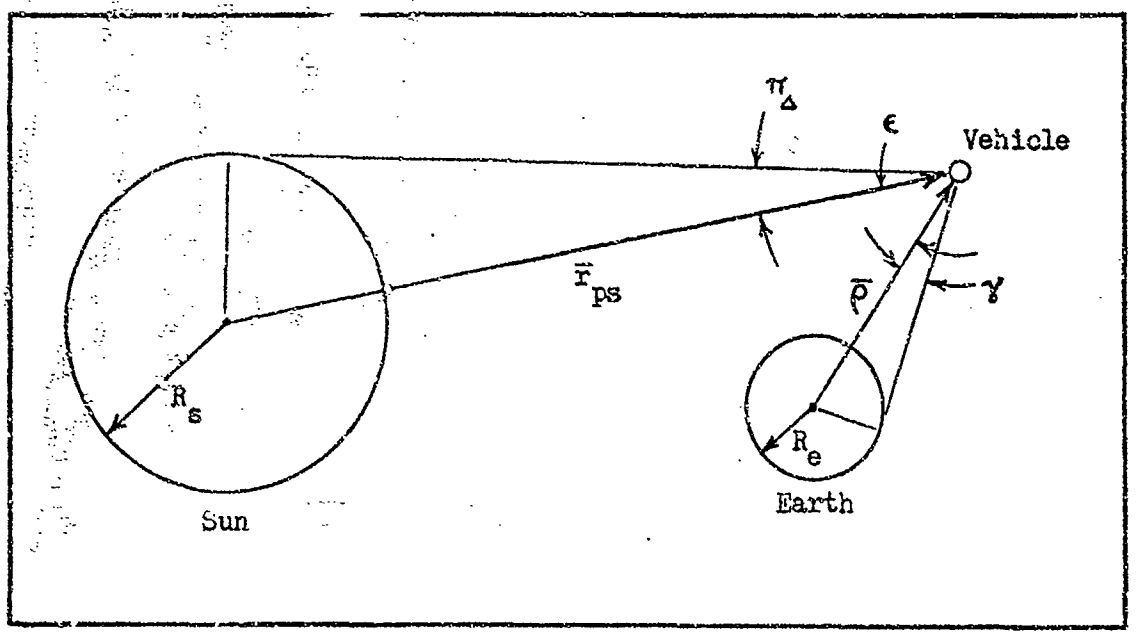

Figure 29. Third-Body Attraction and Solar Shadow Geometry

Solar Radiation Pressure. Consider a simple case of a spherically symmetric, perfectly absorptive satellite of mass m in earth orbit. The perturbative acceleration caused by the radiation pressure of solar photons impingent on the surface area A presented to the photons is

$$\ddot{\bar{r}}_{rad} = f_s P_0 \frac{A}{m} \frac{1}{r_{ps}^3} \begin{Bmatrix} x - x_s \\ y - y_s \\ z - z_s \end{Bmatrix} \tag{6}$$

where f_s is the fraction of the solar surface presented to the vehicle as the vehicle passes behind the earth and P_0 is the solar constant. Baker has indicated that for area-to-mass ratios $\frac{A}{m}$ which are less than 10 cm^2/gm the calculation need not include a variable factor f_s, that is, a point source sun may be assumed (Ref 2:186-197). In this case,

$f_s = 1$ if the vehicle is in the sunlit portion of the orbit and $f_s = 0$ if it is in the shadowed areas. Referring to Fig. 29, the factor f_s can be obtained by using the relations

$$\gamma = \sin^{-1}\left(\frac{R_e}{\rho}\right) \tag{75}$$

$$\pi_\Delta = \sin^{-1}\left(\frac{R_s}{r_{ps}}\right) = 0 \quad \text{(for point sun)} \tag{76}$$

$$\epsilon = \cos^{-1}\left(\frac{\bar{r}_{ps} \cdot \bar{\rho}}{r_{ps}\,\rho}\right) \tag{77}$$

with $f_s = 1$ if $\epsilon \geq \gamma$ or $f_s = 0$ if $\epsilon < \gamma$.

Appendix B

Orbital Equations

Position and Velocity. The position and velocity components of the vehicle in XYZ space may be determined as follows for the reference orbit defined by the orbital parameters a, e, i, ω, and Ω. The period of revolution is given by

$$TP = 2\pi\sqrt{\frac{a^3}{K_e}} \tag{78}$$

A set of values for the eccentric anomaly E at equal time intervals are first determined by solution of Kepler's equation

$$t - t_o = \frac{TP}{2\pi}\left[2k\pi + (E - e\sin E) - (E_o - e\sin E_o)\right] \tag{79}$$

where k is the number of orbits completed and E_o is the eccentric anomaly at the reference time t_o. If the values of E are to be generated at times $t = t_o + mw$ where w is the chosen interval between points and if t_o is chosen at perigee passage where $E_o = 0$, we have the following equation for integral steps (m) along the orbit

$$mw = \frac{TP}{2\pi}(E - e\sin E) \tag{1}$$

The solution of Eq (1) can be obtained by applying Newton's first-order method through iteration of the following equations:

$$f = E_i - mw\frac{2\pi}{TP} - e\sin E_i \tag{80}$$

$$f' = 1 - e\cos E_i \tag{81}$$

$$E_{i+1} = E_i - \frac{f}{f'} \tag{82}$$

The radial distance r in the orbital plane is given by

$$r = \frac{p}{1 + e \cos \nu} \tag{83}$$

where the true anomaly ν is given by the relations

$$\cos \nu = \frac{\cos E - e}{1 - e \cos E} \tag{84}$$

$$\sin \nu = \frac{a \sqrt{1 - e^2}}{r} \sin E \tag{85}$$

In terms of the perifocal coordinate system PQW, the radial and velocity vectors are given by the relations

$$\bar{r} = r \cos \nu \ \hat{P} + r \sin \nu \ \hat{Q} \tag{2}$$

$$\bar{v} = \sqrt{\frac{K_e}{p}} \left[- \sin \nu \ \hat{P} + (e + \cos \nu) \hat{Q} \right] \tag{3}$$

where $\hat{P}$ = unit vector in the direction of perigee

$\hat{Q}$ = unit vector perpendicular to P (in the direction of motion)

The unit vectors $\hat{P}$ and $\hat{Q}$ can be expressed in terms of the unit vectors $\hat{I}$, $\hat{J}$, and $\hat{K}$ in XYZ space with the use of

$$\hat{P} = (\cos\omega \cos\Omega - \sin\omega \sin\Omega \cos i) \hat{I} + (\cos\omega \sin\Omega + \sin\omega \cos\Omega \cos i) \hat{J} + \sin\omega \sin i \hat{K} \tag{86}$$

$$\hat{Q} = (-\cos\Omega \sin\omega - \sin\Omega \cos\omega \cos i) \hat{I} + (-\sin\omega \sin\Omega + \cos\omega \cos\Omega \cos i) \hat{J} + \cos\omega \sin i \hat{K} \tag{87}$$

Substitution of Eqs (86) and (87) into Eqs (2) and (3), using the relations

$$\cos u = \cos (\omega + \nu) = \cos\omega \cos\nu - \sin\omega \sin\nu \tag{88}$$

$$\sin u = \sin (\omega + \nu) = \sin\omega \cos\nu + \cos\omega \sin\nu \tag{89}$$

give the position and velocity components in the XYZ coordinate system;

$$x = r\,(\cos\Omega\cos u - \sin\Omega\sin u\cos i) \tag{90}$$

$$y = r\,(\sin\Omega\cos u + \cos\Omega\sin u\cos i) \tag{91}$$

$$z = r\sin u\sin i \tag{92}$$

$$\dot{x} = -\sin\nu\sqrt{\frac{K_e}{p}}\,(\cos\omega\cos\Omega - \sin\omega\sin\Omega\cos i) + (e+\cos\nu)\sqrt{\frac{K_e}{p}}\,(-\cos\Omega\sin\omega - \sin\Omega\cos\omega\cos i) \tag{93}$$

$$\dot{y} = -\sin\nu\sqrt{\frac{K_e}{p}}\,(\cos\omega\sin\Omega + \sin\omega\cos\Omega\cos i) + (e+\cos\nu)\sqrt{\frac{K_e}{p}}\,(-\sin\Omega\sin\omega + \cos\Omega\cos\omega\cos i) \tag{94}$$

$$\dot{z} = -\sin\nu\sqrt{\frac{K_e}{p}}\,(\sin\omega\sin i) + (e+\cos\nu)\sqrt{\frac{K_e}{p}}\,(\cos\omega\sin i) \tag{95}$$

The total orbital velocity is given by

$$v = \sqrt{K_e\left(\frac{2}{r} - \frac{1}{a}\right)} = (\dot{x}^2 + \dot{y}^2 + \dot{z}^2)^{1/2} \tag{96}$$

Osculated Orbital Elements. Given the set of position and velocity components at any point in an orbit, a set of orbital elements can be calculated. Equation (96) can be solved for the semi-major axis

$$a = \left(\frac{2}{r} - \frac{v^2}{K_e}\right)^{-1} \tag{97}$$

The components of the orbital momentum per unit mass h are

$$h_x = y\dot{z} - z\dot{y} \tag{98}$$

$$h_y = z\dot{x} - x\dot{z} \tag{99}$$

$$h_z = x\dot{y} - y\dot{x} \tag{100}$$

with

$$h^2 = h_x^2 + h_y^2 + h_z^2 \tag{101}$$

The semi-latus rectum p and eccentricity e can be determined by

$$p = \frac{h^2}{K_e} \tag{102}$$

$$e = \left(1 - \frac{p}{a}\right)^{1/2} \tag{103}$$

The eccentricity vector and its components are given as

$$\bar{e} = \frac{1}{K_e}\left(v^2 - \frac{K_e}{r}\right)\bar{r} - \frac{1}{K_e}(\bar{r}\cdot\bar{v})\,\bar{v} \tag{104}$$

$$\begin{Bmatrix} e_x \\ e_y \\ e_z \end{Bmatrix} = \frac{1}{K_e}\left(v^2 - \frac{K_e}{r}\right)\begin{Bmatrix} x \\ y \\ z \end{Bmatrix} - \frac{1}{K_e}(\bar{r}\cdot\bar{v})\begin{Bmatrix} \dot{x} \\ \dot{y} \\ \dot{z} \end{Bmatrix} \tag{105}$$

$$\bar{r}\cdot\bar{v} = x\dot{x} + y\dot{y} + z\dot{z} \tag{106}$$

The balance of the elements can now be calculated. The inclination is given by

$$i = \cos^{-1}\left(\frac{h_z}{h}\right) \tag{107}$$

The longitude of ascending node is

$$\Omega = \cos^{-1}\left(\frac{-h_y}{\sqrt{h_x^2 + h_y^2}}\right) \tag{108}$$

where if $h_x < 0$, $\Omega > 180^\circ$. The argument of perigee is

$$\omega = \cos^{-1}\left(\frac{-h_y e_x + h_x e_y}{e\sqrt{h_x^2 + h_y^2}}\right) \tag{109}$$

where if $e_z < 0$, $\omega > 180^\circ$. Finally, the true anomaly is given by

$$\nu = \cos^{-1}\left(\frac{e_x x + e_y y + e_z z}{er}\right) \tag{110}$$

where if $(\bar{r}\cdot\bar{v}) < 0$, $\nu > 180^\circ$.

Impulsive Correction of Perturbed Orbit. Very useful relations have been developed and tabulated by Ehricke (Ref 7:354) and are applied in the present section. Attention must be directed, however, to the basis of their usefulness. The impulses which are calculated using these relations are only accurate if they are much smaller than the velocity components of the vehicle. It is further assumed that the impulses are made instantaneously. The geometry of the orbital correction is shown in g. 30 .

The inclination and the longitude of the ascending node can be corrected simultaneously by making a plane change with an orthogonal impulse whose magnitude is

$$\Delta v_w = \frac{\Delta i \, v_L}{\cos (\nu_L - \nu_\Omega)} = \frac{\Delta\Omega \, v_L \sin i_L}{\sin (\nu_L - \nu_\Omega)} \qquad (12)$$

at

$$\nu_L = \nu_\Omega + \tan^{-1} \frac{\Delta\Omega}{\Delta i} \sin i_L \qquad (111)$$

where ν_Ω is the true anomaly at the ascending node and L represents the point at which the correction is made. The argument of perigee is corrected at either the apogee or perigee with a normal impulse of

$$\Delta v_n = \frac{\Delta\omega \; a_A \, e_A \, v_A}{2a_A c_A + r_A \cos (\nu_A - \nu_o)} \qquad (13)$$

where ν_o is the true anomaly at perigee and the subscript A represents values at apogee. This normal impulse will result in a negligible change in the eccentricity

$$\Delta e = - \frac{r_A \Delta v_n \sin \nu_A}{a_A \, v_A} \qquad (112)$$

since $\nu_A \simeq 180^\circ$ and $\sin \nu_A \simeq 0$.

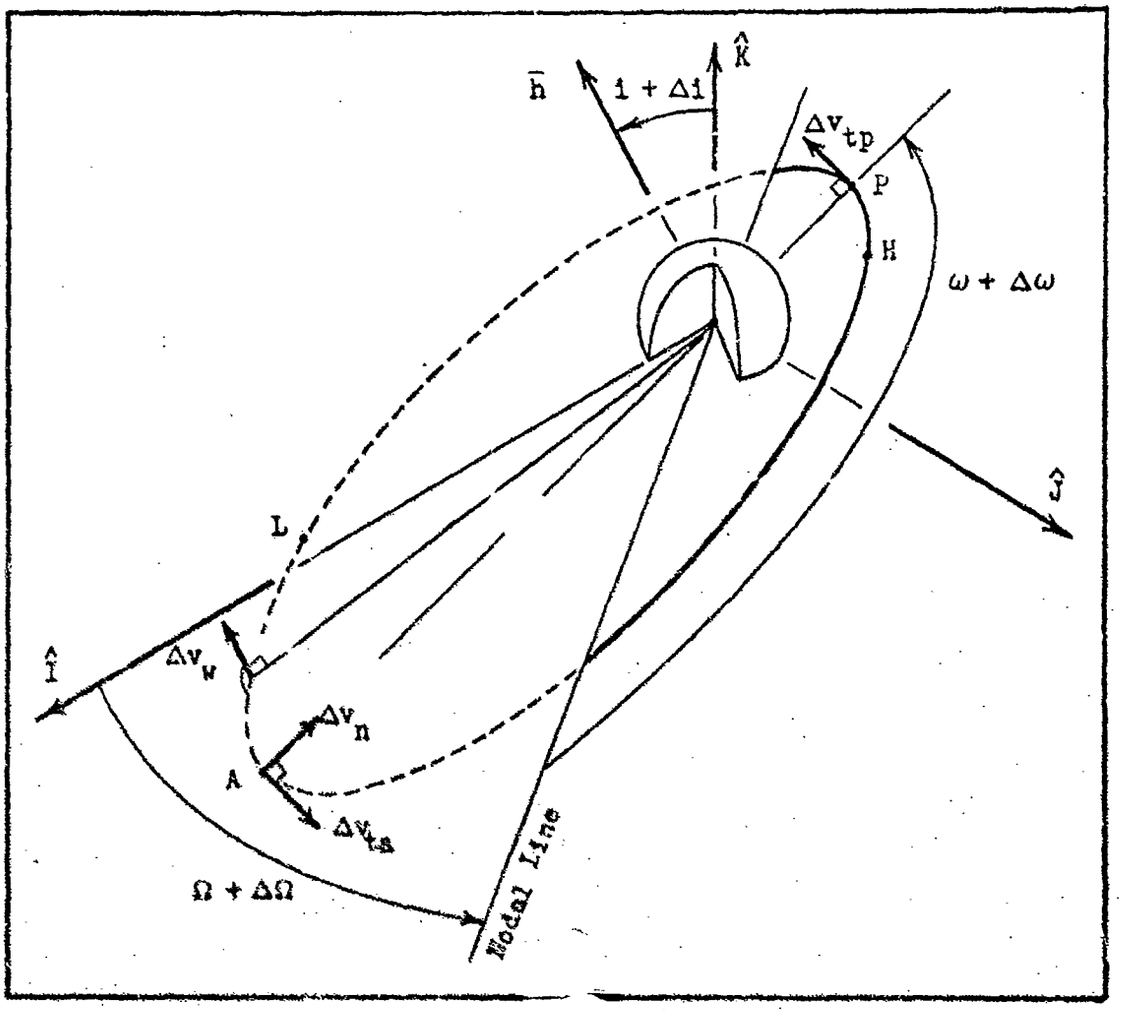

Figure 30. Geometry of Orbital Parameter Correction

The tangential impulse made at apogee is determined by the value of change required to correct the perigee distance r_p, and is related to the change required in the semi-major axis as follows

$$\Delta a_A = \frac{r_{po} - r_p}{2} \tag{113}$$

The required impulse is found to be

$$\Delta v_{tA} = \frac{\Delta a_A \, K_e}{2 \, a_A^2 \, v_A} \tag{14}$$

which results in significant changes in the eccentricity and mean motion as given by

$$\Delta e_A = 2 (e_A + \cos \nu_A) \frac{\Delta v_{ta}}{v_A} \tag{114}$$

$$\Delta \mu_A = - \frac{3 v_A \Delta v_{ta}}{K_e a_A} \tag{115}$$

In addition, a negligible change results in the argument of perigee as compared to that due to the normal impulse. This change is given by

$$\Delta \omega_A = \frac{2 \sin (\nu_A - \nu_0) \Delta v_{ta}}{e_A v_A} \tag{116}$$

Upon arrival at perigee, a second tangential impulse is required to fully restore the values of the semi-major axis and eccentricity to the nominal values. The increments of change required are

$$\Delta e_p = e_o - (e_p + \Delta e_A) \tag{117}$$

$$\Delta a_p = a_o - (a_p + \Delta a_A) \tag{118}$$

The velocity at perigee, prior to the impulse, is

$$v'_p = \left| K_e \left[\frac{1}{r_{po}} - \frac{1}{(a_p + \Delta a_p)} \right] \right|^{1/2} \tag{119}$$

and the eccentricity and semi-major axis values are

$$e'_p = e_p + \Delta e_A \tag{120}$$

$$a'_p = a_p + \Delta a_A \tag{121}$$

The tangential impulse may now be calculated using the relation

$$\Delta v_{tp} = \frac{\Delta e_p v'_p}{2 (e'_p + \cos \nu_p)} = \frac{\Delta a_p K_e}{2 a'^2_p v'_p} \tag{15}$$

and will result in changes of the mean motion and argument of perigee

$$\Delta\mu_p = - \frac{3v'_p}{\sqrt{K_e\, a'_p}} \tag{122}$$

$$\Delta\omega_p = \frac{2 \sin (\nu_p - \nu_o) \Delta v_{tp}}{e'_p\, v'_p} \tag{123}$$

The change of mean motion is of no concern to the analysis since integration of the succeeding orbit will proceed from this point. The change in argument of perigee will be vanishingly small since the nominal value will have been achieved by the normal impulse at apogee.

The values of the orbital elements (essentially the nominal values) which are obtained after the corrective impulses are given by

$$a = a_p + \Delta a_A + \Delta a_p \tag{124}$$

$$e = e_p + \Delta e_A + \Delta e_p \tag{125}$$

$$i = i_p + \Delta i \tag{126}$$

$$\omega = \omega_p + \Delta\omega \tag{127}$$

$$\Omega = \Omega_p + \Delta\Omega \tag{128}$$

The time of arrival at perigee after applying the impulses is

$$t_c = t_A + \frac{1}{\left[\frac{1}{(t_p - t_A)} + \frac{\Delta M_A}{\pi}\right]} \tag{129}$$

Appendix C

Numerical Techniques

Encke's Method. One of the more refined techniques available for computation of orbital perturbations was developed by J. F. Encke. The principal advantage of using this technique is that only the perturbative accelerations need be integrated. This leads to greater accuracy while using larger integration steps as compared to the Cowell method, in which the sum of all accelerations are integrated together (Ref 8:225, 6:469).

The equations of motion for the perturbed and reference orbit shown in Fig. 31 are

$$\ddot{\bar{r}} = -\frac{K_e}{r^3}\bar{r} + \ddot{\bar{r}} \tag{130}$$

$$\ddot{\bar{\rho}} = -\frac{K_e}{\rho^3}\bar{\rho} \tag{131}$$

respectively, where $\ddot{\bar{r}}$ is the sum of all the perturbative accelerations discussed in Appendix A.

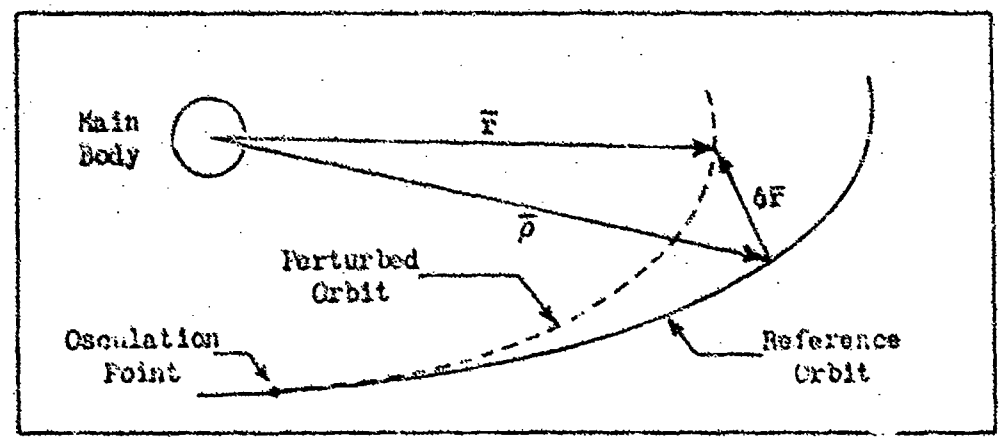

Figure 31. Geometry of Perturbed Orbit

Considering only the x-component for purposes of illustration, noting that $\delta\bar{r} = \bar{r} - \bar{\rho}$, and taking the difference between the perturbed and reference orbital equations (130) and (131), we have

$$\delta\ddot{x} = \ddot{x} - \ddot{\rho}_x = K_e\left[\frac{\rho_x}{\rho^3} - \frac{x}{r^3}\right] + \hat{x}$$

$$= K_e\left[\frac{x - \delta x}{\rho^3} - \frac{x}{r^3}\right] + \hat{x}$$

$$= \frac{K_e}{\rho^3}\left[\left(1 - \frac{\rho^3}{r^3}\right)x - \delta x\right] + \hat{x} \qquad (132)$$

Since we also have the relations

$$r^2 = x^2 + y^2 + z^2 = (\rho_x + \delta x)^2 + (\rho_y + \delta y)^2 + (\rho_z + \delta z)^2$$

$$= \rho^2 + 2\rho_x\delta x + 2\rho_y\delta y + 2\rho_z\delta z + \delta x^2 + \delta y^2 + \delta z^2 \qquad (133)$$

we can write

$$\frac{r^2}{\rho^2} = 1 + 2\left[\frac{(\rho_x + \frac{1}{2}\delta x)\delta x + (\rho_y + \frac{1}{2}\delta y)\delta y + (\rho_z + \frac{1}{2}\delta z)\delta z}{\rho^2}\right] \qquad (134)$$

Defining the quantity in the brackets as the dimensionless factor q,

$$\frac{r^2}{\rho^2} = 1 + 2q \qquad \text{and} \qquad \frac{\rho^3}{r^3} = (1 + 2q)^{-3/2} \qquad (135)$$

which can now be used to rewrite Eq (132) as

$$\delta\ddot{x} = \frac{K_e}{\rho^3}\left\{\left[1 - (1 + 2q)^{-3/2}\right]x - \delta x\right\} + \hat{x} \qquad (136)$$

Expanding the term $(1 + 2q)^{-3/2}$ in a binomial series gives the results

$$fq = 1 - (1 + 2q)^{-3/2}$$

$$= 3q - \frac{3\cdot5}{2!}q^2 + \frac{3\cdot5\cdot7}{3!}q^3 - \frac{3\cdot5\cdot7\cdot9}{4!}q^4 + \frac{3\cdot5\cdot7\cdot9\cdot11}{5!}q^5 - \cdots\cdots \quad (137)$$

$$\begin{Bmatrix}\delta\ddot{x}\\ \delta\ddot{y}\\ \delta\ddot{z}\end{Bmatrix} = \frac{K_e}{\rho^3}\left[fq\begin{Bmatrix}x\\ y\\ z\end{Bmatrix} - \begin{Bmatrix}\delta x\\ \delta y\\ \delta z\end{Bmatrix}\right] + \begin{Bmatrix}\hat{\ddot{x}}\\ \hat{\ddot{y}}\\ \hat{\ddot{z}}\end{Bmatrix} \quad (138)$$

The integration of $\delta\ddot{x}$, for example, to determine δx requires the knowledge of δx and x, and is therefore an iterative process. The first application of the numerical integration of Eq (138) can be based on $\delta x = 0$ and $x = \rho_x$ which results in

$$\delta\ddot{x} = \frac{K_e\rho_x}{\rho^3} + \hat{\ddot{x}} \quad (139)$$

and the first approximation of δx. The second iteration involves integration of Eq (138) with $x = \rho_x + \delta x$. The process of iteration is continued until insignificant changes are made in the resultant δx. The analysis in this thesis indicated that six iterations were sufficient for this purpose, using a seven-term form of Eq (137).

According to Ehricke (Ref 6:475), the subsequent iterations involve replacement of ρ_x with preceding values of x which would also imply the requirement to recalculate the values of $\hat{\ddot{x}}$ using the later values of x rather than ρ_x. The orbit was integrated using five sections, after each of which a set of osculated orbital elements were calculated. These elements, corresponding to the end point of each section, were then used to generate the next section of the reference orbit.

Method of Numerical Integration. The step integration of the perturbations was carried out by application of the Gauss-Encke method of mechanical quadrature (Ref 6:486). This technique is also called the Gauss-Jackson or Sum-Squared ($\sum^2$) method (Ref 4:418). This numerical technique requires the construction of a table of data based on equally spaced perturbative functions $f_i = w^2\,\delta\ddot{x}$ where w is the time interval between the data points, and $\delta\ddot{x}$ is the perturbative acceleration. Since the dimension of the function f_i is length, all entries in the table will be in units of length. The general construction of the table is illustrated in Table IV on the following page. Note that the entries are tabulated as a function of the normalized time unit $\tau = t_i/w$, where t_i is the time measured from some reference point (e.g., the osculation point).

Following the tabulation of the perturbative functions f_i, the first step in the generation of the data table involves the calculation of the differences δ^m_j using the following relations:

$$\delta^1_{i+\frac{1}{2}} = f_{i+1} - f_i \tag{140}$$

$$\delta^n_i = \delta^{n-1}_{i+\frac{1}{2}} - \delta^{n-1}_{i-\frac{1}{2}} \tag{141}$$

$$\delta^{n-1}_{i+\frac{1}{2}} = \delta^{n-1}_{i+1} - \delta^{n-1}_i \tag{142}$$

where $i = \ldots,-3,-2,-1,0,1,2,3,\ldots$, and $n = 2,3,4,5,\ldots$.
Assuming that the higher order differences approach a constant which is very small compared to the function f_i, the differences in the upper and lower right hand corners of the table can be approximated by using Eqs (140) through (142). The present analysis considered δ^{10}_i as constant.

Table IV. Gauss-Encke Numerical Integration Tabular Construction

τ	δx	$w\dot{\delta x}$	Σ^2	Σ^1	$f_i = w^2\ddot{\delta x}$	δ^1	δ^2	δ^3	δ^4	δ^5
-3	δx_{-3}	$w\dot{\delta x}_{-3}$	Σ^2_{-3}		f_{-3}					
				$\Sigma^1_{-5/2}$		$\delta^1_{-5/2}$				
-2	δx_{-2}	$w\dot{\delta x}_{-2}$	Σ^2_{-2}		f_{-2}		δ^2_{-2}			
				$\Sigma^1_{-3/2}$		$\delta^1_{-3/2}$		$\delta^3_{-3/2}$		
-1	δx_{-1}	$w\dot{\delta x}_{-1}$	Σ^2_{-1}		f_{-1}		δ^2_{-1}		δ^4_{-1}	
				$\Sigma^1_{-1/2}$		$\delta^1_{-1/2}$		$\delta^3_{-1/2}$		$\delta^5_{-1/2}$
0	δx_0	$w\dot{\delta x}_0$	Σ^2_0		f_0		δ^2_0		δ^4_0	
				$\Sigma^1_{1/2}$		$\delta^1_{1/2}$		$\delta^3_{1/2}$		$\delta^5_{1/2}$
1	δx_1	$w\dot{\delta x}_1$	Σ^2_1		f_1		δ^2_1		δ^4_1	
				$\Sigma^1_{3/2}$		$\delta^1_{3/2}$		$\delta^3_{3/2}$		$\delta^5_{3/2}$
2	δx_2	$w\dot{\delta x}_2$	Σ^2_2		f_2		δ^2_2		δ^4_2	
				$\Sigma^1_{5/2}$		$\delta^1_{5/2}$		$\delta^3_{5/2}$		
3	δx_3	$w\dot{\delta x}_3$	Σ^2_3		f_3		δ^2_3			
				$\Sigma^1_{7/2}$		$\delta^1_{7/2}$				
4	δx_4	$w\dot{\delta x}_4$	Σ^2_4		f_4					
				$\Sigma^1_{9/2}$						

The calculations of the sums Σ^1 and Σ^2 are not as straightforward as those of the differences. Application of central difference integration formulas gives the relations

$$w\dot{\delta x}_i = \int w^2 \ddot{\delta x}\, d\tau = (\Sigma^1_i) - \frac{1}{12}(\delta^1_i) + \frac{11}{720}(\delta^3_i) - \frac{191}{60480}(\delta^5_i) + \frac{2497}{3628800}(\delta^7_i) - \cdots \quad (143)$$

$$\delta x_i = \iint w^2 \, \delta\ddot{x} \, d\tau^2 = \Sigma_i^2 + \frac{1}{12} f_i - \frac{1}{240} \delta_i^2 + \frac{31}{60480} \delta_i^4 - \frac{289}{3628800} \delta_i^6 + \frac{317}{22809600} \delta_i^8 - \cdots\cdots \quad (144)$$

$$(\Sigma_i^1) = \frac{1}{2} \left(\Sigma_{i-\frac{1}{2}}^1 - \Sigma_{i+\frac{1}{2}}^1 \right) \quad (145)$$

$$(\delta_i^n) = \frac{1}{2} \left(\delta_{i-\frac{1}{2}}^1 - \delta_{i+\frac{1}{2}}^1 \right) \quad (146)$$

Aside from the perturbative functions f_i and the difference table which has been compiled, the values of δx_o and $w \, \delta\dot{x}_o$ at $\tau = 0$ are also known and are used to calculate $\Sigma_{\frac{1}{2}}^1$, $\Sigma_{-\frac{1}{2}}^1$ and Σ_0^2 with Eqs (143) and (144). Note, however, that since

$$\Sigma_{\frac{1}{2}}^1 - \Sigma_{-\frac{1}{2}}^1 = f_o \quad (147)$$

$$\Sigma_{\frac{1}{2}}^1 + \Sigma_{-\frac{1}{2}}^1 = 2 \Sigma_{\frac{1}{2}}^1 - f_o \quad (148)$$

we can rewrite Eqs (143), (144) and (147) to obtain the relations

$$\Sigma_{\frac{1}{2}}^1 = w \, \delta\dot{x}_o + \frac{1}{2} f_o + \frac{1}{12} (\delta_o^1) - \frac{11}{720} (\delta_o^3) + \frac{191}{60480} (\delta_o^5) - \frac{2497}{3628800} (\delta_o^7) + \cdots\cdots \quad (149)$$

$$\Sigma_{-\frac{1}{2}}^1 = \Sigma_{\frac{1}{2}}^1 - f_o \quad (150)$$

$$\Sigma_0^2 = \delta x_o - \frac{1}{12} f_o + \frac{1}{240} \delta_o^2 - \frac{31}{60480} \delta_o^4 + \frac{289}{3628800} \delta_o^6 - \frac{317}{22809600} \delta_o^8 + \cdots\cdots \quad (151)$$

Once these three key values are determined, the balance of the Σ^1 and Σ^2 columns of the table can be filled in using the following equations

$$\Sigma^1_{i+\frac{1}{2}} = \Sigma^1_{i-\frac{1}{2}} + f_i \tag{152}$$

$$\Sigma^2_i = \Sigma^2_{i-1} + \Sigma^1_{i-\frac{1}{2}} \tag{153}$$

Finally, the values of δx_i and $w\,\delta\dot{x}_i$ can be calculated using Eqs (143) and (144).

Interpolation Equation. The calculation of the perturbations due to solar and lunar attraction requires interpolation of the ephemeris data which is provided at daily intervals. Determination of the times of perigee and apogee passage is also necessary during the course of the analysis and requires the interpolation of the position and velocity components. A useful equation is the fourth-order central-difference interpolation polynomial (Ref 10:216) given by

$$\begin{aligned} y = {} & \frac{(t)(t-w)(t-2w)(t+w)}{24w^4} y_{-2} + \frac{(t)(t-w)(t-2w)(t+2w)}{-6w^4} y_{-1} \\ & + \frac{(t-w)(t-2w)(t+w)(t+2w)}{4w^4} y_0 + \frac{(t)(t-2w)(t+w)(t+2w)}{-6w^4} y_{+1} \\ & + \frac{(t)(t-w)(t+w)(t+2w)}{24w^4} y_{+2} \end{aligned} \tag{154}$$

where w is the time interval between the equally spaced data points (y_{-2} through y_{+2}) and $-2w \le t \le +2w$.

Determination of Extrema. The determination of the times of perigee and apogee passage involves the location of minimum or maximum radial distances respectively among five equally spaced points. A fourth-order polynomial (Ref 10:223) can be fitted to these five points and is generally given by

$$y = a_4 t^4 + a_3 t^3 + a_2 t^2 + a_1 t + a_0 \tag{155}$$

where the coefficients can be determined from the relations

$$a_4 = \frac{y_{-2} - 4y_{-1} + 6y_0 - 4y_{+1} + y_{+2}}{24w^4} \tag{156}$$

$$a_3 = \frac{-y_{-2} + 2y_{-1} - 2y_{+1} + y_{+2}}{12w^3} \tag{157}$$

$$a_2 = \frac{-y_{-2} + 16y_{-1} - 30y_0 + 16y_{+1} - y_{+2}}{24w^2} \tag{158}$$

$$a_1 = \frac{y_{-2} - 8y_{-1} + 8y_{+1} - y_{+2}}{12w} \tag{159}$$

$$a_0 = y_0 \tag{160}$$

The value of t for the maximum or minimum of the function y can be found by the solution of the expression

$$\frac{dy}{dt} = 0 = 4a_4 t^3 + 3a_3 t^2 + 2a_2 t + a_1 \tag{161}$$

by using Newton's method as described in Appendix B, where the function f is given by Eq (161) and

$$f' = 12a_4 t^2 + 6a_3 t + 2a_2 \tag{162}$$

Appendix D

Computer Model

General Description. The computer model written for the analysis of the problem described in this thesis consisted of the executive program PROGRAM ENCKE and appropriate subroutines which were used to make repeated calculations during specific phases. This section is devoted to a brief explanation and description of each segment of the model.

1) PROGRAM ENCKE is used to provide for the source of input of initial parameters and ephemeris data and output of desired data following the various phases of analysis. It also provides the framework for relating the calculations performed by the subroutines. The listing presented in the following section specifically represents the case which includes daily correction of the perturbed orbit. A flow diagram which provides for other cases is shown in Fig. 32.

2) SUBROUTINE POSIT calculates the position and velocity components of the reference orbit following the generation of a set of eccentric anomaly values by solution of Kepler's equation. Since the values are equally spaced at small time intervals, successive trial values of E_i are assumed to be those of the point just determined. Values for all orbital points are generated at a single call from PROGRAM ENCKE.

3) SUBROUTINE POLYLEG calculates the values of the Legendre polynomials and their gradients for each orbital point as called for individually by PROGRAM ENCKE.

4) SUBROUTINE ZONAL calculates the value of the zonal harmonic contribution to the oblate earth perturbative acceleration for each orbital point as called by PROGRAM ENCKE.

5) SUBROUTINE TESSER provides the tesseral contribution of the

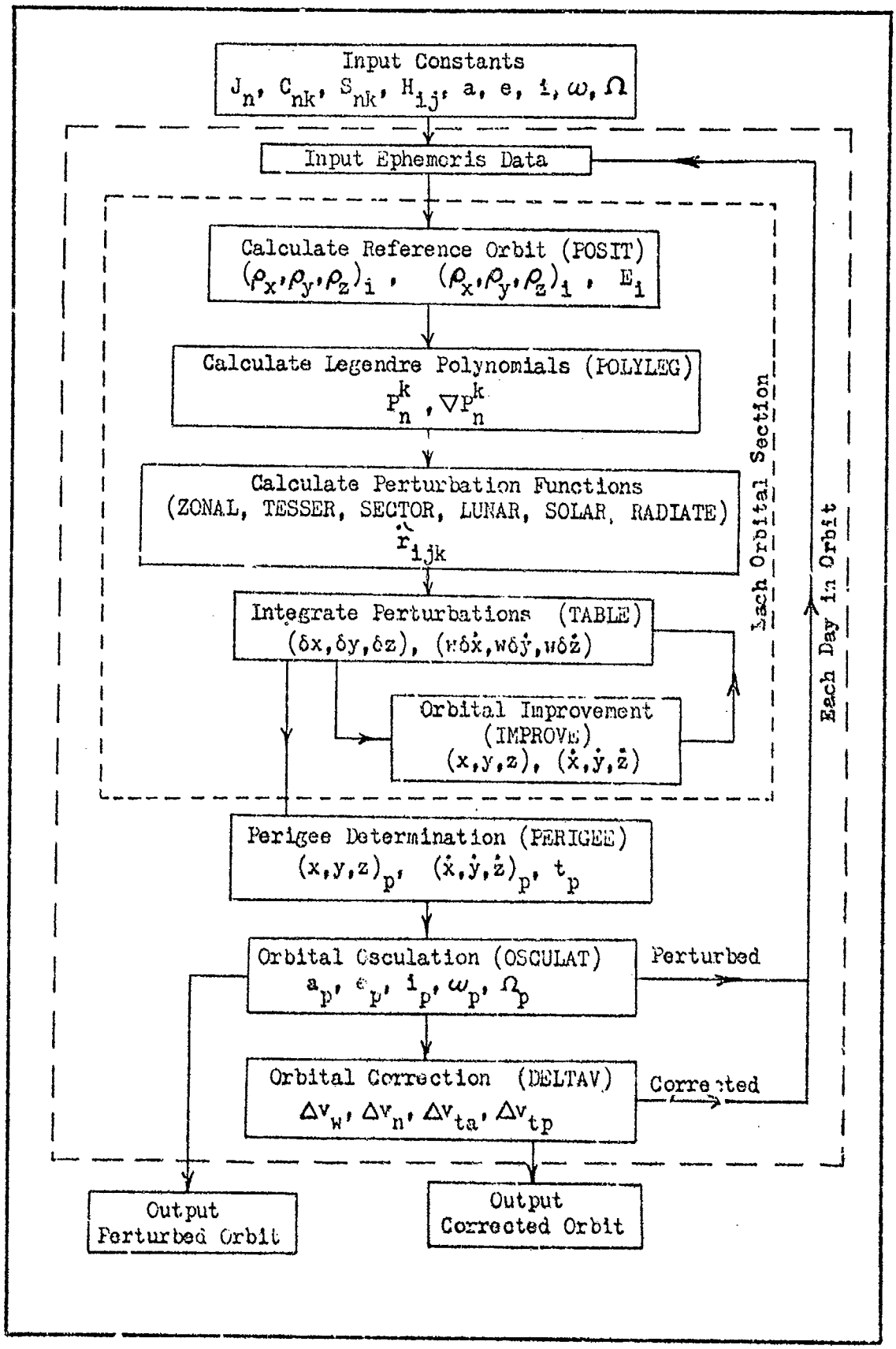

Figure 32. Flow Diagram of Computer Model

oblate earth perturbative acceleration.

6) SUBROUTINE SECTOR provides the sectorial harmonic contribution of the oblate earth perturbative acceleration.

7) SUBROUTINE LUNAR computes the third-body attractive perturbation due to the lunar mass for each orbital point as called by PROGRAM ENCKE.

8) SUBROUTINE SOLAR computes the third-body attractive perturbation due to the solar mass for each orbital point as called.

9) SUBROUTINE RADIATE calculates the perturbation due to solar radiation pressure for each orbital point as called by PROGRAM ENCKE.

10) SUBROUTINE TABLE calculates the components of δr and $w\delta\dot{r}$, given the component values of the acceleration functions $w^2\delta\ddot{r}$. The integration technique is the $\sum^2$ - method discussed in Section 2 of Appendix C. The x, y, and z components are computed separately in successive calls from PROGRAM ENCKE.

11) SUBROUTINE IMPROVE applies Encke's technique to improve the orbital integration initially provided by TABLE. The orbit will be improved using the number of iterations given by the integer NN. TABLE is successively called to integrate the components of the improved perturbative acceleration functions.

12) SUBROUTINE OSCULAT calculates the orbital elements of the perturbed orbit given the position and velocity components at the point of interest defined by the integer NOSC. The basic equations used are discussed in Section 2 of Appendix B.

13) SUBROUTINE PERIGEE calculates the position and velocity components and the time of arrival at perigee (or apogee) by interpolation between equally spaced data points surrounding the approximate orbital point defined by the integers NPER or NAPO. The actual time of arrival

is calculated by using the fourth-order technique described in Sections 3 and 4 of Appendix C.

14) SUBROUTINE DELT V calculates the values of the instantaneous impulses required to correct the perturbed orbital parameters, according to Section 3 of Appendix B.

Computer Program and Subroutine Listings. The following section provides a listing of the executive program compiled to provide daily correction of the orbital parameters. The general subroutines discussed in the previous section are also listed. A glossary of the major variables used in the programs is provided in Section 3 of this appendix.

```
      PROGRAM ENCKE (INPUT,OUTPUT)
      COMMON/BLKA/RHO(3,60),ELEM(10),PARA(10),E(60)
      COMMON/BLKB/P(8,5),DP(8,5),DQ(8,5),DR(8,5),RR(6)
      COMMON/BLKC/BJ(5),C(7,5),S(7,5),FAC(7,5)
      COMMON/BLKD/PERT(7,3,60)
      COMMON/BLKE/DIFF(10,60),TAB(4,60),H(3,5),TABS(2,7,3)
      COMMON/BLKF/RRS(3,60),RRM(3,60)
      COMMON/BLKG/REF(8,60),EREF(60),ELREF(10)
      DIMENSION RM(3,5),RS(3,5)
81    FORMAT (1X,5E18.10,2F12.8,F12.6)
94    FORMAT (F15.0)
95    FORMAT (5I4,2F15.0)
97    FORMAT (6F12.0)
102   FORMAT(3X,10E12.5)
      READ 94, (BJ(I),I=1,5)
      READ 94, ((C(I,J),J=1,5),I=1,7)
      READ 94, ((S(I,J),J=1,5),I=1,7)
      READ 94, ((H(I,J),J=1,5),I=1,2)
      READ 94, (PARA(I),I=1,10)
      READ 94, (ELEM(I), I=1,10)
      READ 95, MDAY,NDAY,NN,N,NOSC,W,THETA0
      READ 97,(((RM(I,J),I=1,3),(RS(I,J),I=1,3)),J=2,5)
      DO 14 I=1,8
      DO 14 J=1,5
14    P(I,J)=0.
      ALPHA1=0.
      ALPHA2=0.
      U=0.
      USAVE=0.
      RHO(1,1)=2.64429
      RHO(5,1)=3.470844
      DO 48 I=1,10
      EREF(I)=0.
48    ELREF(I)=ELEM(I)
      ELREF(3)=ELREF(3)/PARA(3)
      ELREF(4)=ELREF(4)/PARA(3)
      ELREF(5)=ELREF(5)/PARA(3)
      DO 400 ITOSC=MDAY,NDAY
      ALOMAX=-360.
      DO 50 J=1,4
      DO 50 I=1,3
      RM(I,J)=RM(I,J+1)
50    RS(I,J)=RS(I,J+1)
      READ 97, (RM(I,5),I=1,3),(RS(I,5),I=1,3)
      IF (RM(1,5).GT.RM(1,4)) GO TO 51
      RM(1,4)=RM(1,4)-24.
      RM(1,3)=RM(1,3)-24.
      RM(1,2)=RM(1,2)-24.
      RM(1,1)=RM(1,1)-24.
51    NPER=-1
      NAPO=-1
      MAPO=-1
      E(1)=-.32
      E(6)=0.
      PARA(8)=0.
```

```
      U=(ITOSC-1)-U
      DO 390 I SECT=1,5
      DATE= SAVE+(I ECT-1)*0.2
      IF (ISECT.GT.1) GO TO 53
      PRINT 8  (ELEM(I) ,I=1,5),RHO(1,1),RHO(5,1),DATE
53    ELEM(3)= ELEM(3)/PARA(3)
      ELEM(4)=ELEM(4)/PARA(3)
      ELEM(5)=ELEM(5)/PARA(3)
      CALL POSIT (ITOSC,ISECT,N,W,NOSC)
      IF (ITOSC.EQ.1.AND.ISECT.EQ.1) EREF(1)=RHO(1,6)
      DO 200 I=1,N
      RR(1)=RHO(1,I)
      DO 54 K=2,6
54    RR(K)=RR(K-1)*RR(1)
      CALL POLYLEG (I)
      T=(I-6.)*W+(ISECT-1)*4.8-U*24.
      IF (T.EQ.0.) GO TO 120
      IF (T.EQ.24.) GO TO 125
      TT=T/24.
      AAA=TT*(TT*TT-1.)*(TT*TT-4.)/24.
      AA=AAA/(TT+2.)
      BB=-(AAA*4.)/(TT+1.)
      CC=AAA*6./TT
      DD=-(AAA*4.)/(TT-1.)
      EE=AAA/(TT-2.)
      GO TO 130
120   DD=0.
      CC=1.
      GO TO 127
125   CC=0.
      DD=1.
127   AA=0.
      BB=0.
      EE=0.
130   DO 160 J=1,3
      RRM(J,I)=AA*RM(J,1)+BB*RM(J,2)+CC*RM(J,3)+DD*RM(J,4)
     1    +EE*RM(J,5)
      RRS(J,I)=AA*RS(J,1)+BB*RS(J,2)+CC*RS(J,3)+DD*RS(J,4)
     1    +EE*RS(J,5)
      RRS(J,I)=RRS(J,I)*PARA(6)
160   CONTINUE
      RRM(1,I)=15.*RRM(1,I)/PARA(3)
      RRM(2,I)=RRM(2,I)/PARA(3)
      RRM(3,I)=RRM(3,I)*PARA(5)
      XM=RRM(3,I)*COS(RRM(1,I))
      YM=RRM(3,I)*SIN(RRM(1,I))
      RRM(3,I)=RRM(3,I)*SIN(RRM(2,I))
      RRM(1,I)=XM
      RRM(2,I)=YM
      T=T+(USAVE+U)*24.
      AT=ATAN2(RHO(3,I),RHO(2,I))
      ALPHA=AT+ALPHA1
      AL=ALPHA-66.*0.00+3752695*T-THETA0
      ALO=AL*PARA(3)
      IF (ALO.LT.-180.) ALPHA1=ALPHA1+2*PARA(2)
```

```
      IF (ALO.LT.-180.)  ALO=ALO+360.
      PERT(7,1,I)=T
      CALL ZONAL (I)
      CALL TESSER (AL,I)
      CALL SECTOR (AL,I)
      CALL LUNAR (I)
      CALL SOLAR (I)
      CALL RADIAT (I)
  200 CONTINUE
      DO 242 K=1,N
      DO 241 J=1,3
      DO 240 I=2,6
  240 PERT(1,J,K)=PERT(1,J,K)+PERT(I,J,K)
  241 PERT(1,J,K)=PERT(1,J,K)*W*W
  242 CONTINUE
      DO 245 K=1,N
      DO 245 J=1,8
  245 REF(J,K)=RHO(J,K)
      DO 350 I=1,1
      DO 320 K=1,N
      DO 320 JJ=1,3
  320 PERT(7,JJ,K)=PERT(I,JJ,K)
      DO 300 J=1,3
      TABS(1,I,J)=0.
      TABS(2,I,J)=0.
      CALL TABLE (I,J,N)
      DO 310 K=1,N
  310 PERT(I,J,K)=TAB(1,K)
  300 CONTINUE
      CALL IMPROVE (I,N,W,NN)
  350 CONTINUE
      DO 349 I=1,N
      T=(I-6.)*W+(ISECT-1)*4.8-U*24.
      T=T+(USAVE+U)*24.
  349 PERT(7,1,I)=T
      DO 360 I=1,1
      DO 360 J=1,3
      II=J+5
      TABS(1,I,J)=0.
      TABS(2,I,J)=0.
      CALL TABLE (I,J,N)
      DO 370 K=1,N
      RHO(J+1,K)=RHO(J+1,K)+TAB(1,K)
      RHO(II,K)=RHO(II,K)+TAB(2,K)/W
  370 CONTINUE
  360 CONTINUE
      DO 380 K=1,N
      RHO(1,K)=SQRT(RHO(2,K)*RHO(2,K)+RHO(3,K)*RHO(3,K) +
     1     RHO(4,K)*RHO(4,K))
      RHO(5,K)=SQRT(RHO(6,K)*RHO(6,K)+RHO(7,K)*RHO(7,K)+
     1     RHO(8,K)*RHO(8,K))
      IF (NAPO.GT.0.OR.K.LT.6.OR.K.GT.54) GO TO 371
      IF (RHO(1,K).GE.RHO(1,K-1).AND.RHO(1,K).GT.RHO(1,K+1))
     1     GO TO 369
      GO TO 371
```

```
369   NAPO=K
371   IF (NPER.GT.0.OR.K.LT.20.OR.K.GT.57) GO TO 380
      IF (RHO(1,K).LE.RHO(1,K-1).AND.RHO(1,K).LT.RHO(1,K+1))
     1     GO TO 372
      GO TO 380
372   NPER=K
380   CONTINUE
      IF (NAPO.GT.0.OR.NAPO.LT.0) GO TO 383
      CALL PERIGEE(NAPO,DU1)
      DU1=(PERT(7,1,NAPO)+DU1*W)/24.-USAVE
      CALL OSCULAT(1)
      PRINT 81, (ELEM(I),I=1,5),RHO(1,1),RHO(5,1),DU1
      EREF(21)=ELEM(1)
      EREF(22)=ELEM(2)
      EREF(23)=ELEM(3)/PARA(3)
      EREF(24)=ELEM(4)/PARA(3)
      EREF(25)=ELEM(5)/PARA(3)
      EREF(19)=RHO(1,1)
      EREF(20)=RHO(5,1)
      NAPO=1
383   IF (NPER.LT.0) GO TO 385
      CALL PERIGEE (NPER,U)
      U=(PERT(7,1,NPER)+U*W)/24.
      CALL OSCULAT (1)
      PRINT 81, (ELEM(I),I=1,5),RHO(1,1),RHO(5,1),U
      NPER=-1
      ELEM(3)=ELEM(3)/PARA(3)
      ELEM(4)=ELEM(4)/PARA(3)
      ELEM(5)=ELEM(5)/PARA(3)
      CALL DELTAV
      PRINT 102, (EREF(I),I=1,10)
      DU2=(U-USAVE)-DU1
      DU2=1./(1./DU2+EREF(11)/PARA(2))
      U=USAVE+DU1+DU2
      USAVE=U
      IF (ISECT.EQ.5) GO TO 390
385   CALL OSCULAT (NOSC)
      IF (ISECT.NE.1) GO TO 390
      EREF(31)=ELEM(1)
      EREF(32)=ELEM(2)
      EREF(33)=ELEM(3)/PARA(3)
390   CONTINUE
400   CONTINUE
      STOP
      END
```

```
      SUBROUTINE POSIT (ITOSC,ISECT,N,W,NOSC)
      COMMON/BLKA/RHO(8,60),ELEM(10),PARA(10),E(60)
      IF (ITOSC.GT.1) GO TO 5
      IF (ISECT.GT.1) GO TO 5
      E(1)=-.32
      E(6)=0.
      GO TO 10
    5 E(6)=E(NOSC)
      E(1)=E(NOSC-5)
   10 DO 20 I=1,N
      T=PARA(8)+(I-6.)*W
      M=0
      IF (I.EQ.6.AND.ISECT.EQ.1.AND.ITOSC.EQ.1) GO TO 18
   16 F=E(I)-T*PARA(4)-ELEM(2)*SIN(E(I))
      FF=1.-ELEM(2)*COS(E(I))
      M=M+1
      E(I)=E(I)-F/FF
      IF (M.GE.100) GO TO 18
      IF (ABS(F).LE.0.000000000001) GO TO 18
      GO TO 16
   18 IF (I.EQ.N) GO TO 20
      IF(I.EQ.5.AND.ISECT.EQ.1.AND.ITOSC.EQ.1) GO TO 20
      E(I+1)=E(I)
   20 CONTINUE
   21 A=COS(ELEM(5))
      AA=SIN(ELEM(5))
      B=COS(ELEM(3))
      BB=SIN(ELEM(3))
      V3=SQRT(PARA(1)/ELEM(6))
      DO 30 I=1,N
      D=(COS(E(I))-ELEM(2))/(1.-ELEM(2)*COS(E(I)))
      RHO(1,I)=ELEM(6)/(1.+ELEM(2)*D)
      DD=(ELEM(1)*SQRT(1.-ELEM(2)*ELEM(2))*SIN(E(I)))/RHO(1,I)
      CCC=ATAN2(DD,D)+ELEM(4)
      C=COS(CCC)
      CC=SIN(CCC)
      RHO(2,I)=(A*C-AA*CC*B)*RHO(1,I)
      RHO(3,I)=(AA*C+A*CC*B)*RHO(1,I)
      RHO(4,I)=(CC*BB)*RHO(1,I)
      V1=-V3*DD
      V2=(ELEM(2)+D)*V3
      C=COS(ELEM(4))
      CC=SIN(ELEM(4))
      RHO(5,I)=SQRT(PARA(1)*((2./RHO(1,I))-(1./ELEM(1))))
      RHO(6,I)=V1*(C*A-CC*AA*B)+V2*(-A*CC-AA*C*B)
      RHO(7,I)=V1*(C*AA+CC*A*B)+V2*(-AA*CC+A*C*B)
   30 RHO(8,I)=V1*CC*BB+V2*C*BB
      RETURN
      END
```

```
      SUBROUTINE POLYLEG (II)
      COMMON/BLKA/RHO(8,60),ELEM(10),PARA(10),G(60)
      COMMON/BLKB/P(8,5),DP(8,5),DQ(8,5),DR(8,5),RR(6)
      A=RHO(4,II)/RHO(1,II)
      B=A*A
      C=A*B
      D=A*C
      E=A*D
      F=A*E
      AA=SQRT(1.-B)
      BB=1.-B
      CC=AA*BB
      DD=BB*BB
      EE=BB*CC
      FF=BB*DD
      AAA=-RHO(4,II)*RHO(2,II)/RR(3)
      BBB=-RHO(4,II)*RHO(3,II)/RR(3)
      CCC=(RR(2)-RHO(4,II)*RHO(4,II))/RR(3)
      P(1,1)= 1.5*E-0.5
      P(1,2)=2.5*C-1.5*A
      P(1,3)=0.125*(35.*D-30.*B+3.)
      P(1,4)=0.125*(63.*E-70.*C+15.*A)
      P(1,5)=0.0625*(231.*F-315.*D+105.*B-5.)
      P(2,1)=AA*3.*A
      P(2,2)=AA*(7.5*B-1.5)
      P(2,3)=AA*(17.5*C-7.5*A)
      P(2,4)=AA*0.125*(315.*D-210.*B+15.)
      P(2,5)=AA*0.125*(693.*E-630.*C+105.*A)
      P(3,1)=BB*3.
      P(3,2)=BB*15.*A
      P(3,3)=BB*(52.5*B-7.5)
      P(3,4)=BB*(157.5*C-52.5*A)
      P(3,5)=BB*0.125*(3465.*D-1890.*B+105.)
      P(4,2)=CC*15.
      P(4,3)=CC*105.*A
      P(4,4)=CC*(472.5*B-52.5)
      P(4,5)=CC*(1732.5*C-472.5*A)
      P(5,3)=DD*105.
      P(5,4)=DD*945.*A
      P(5,5)=DD*(5697.5*B-472.5)
      P(6,4)=EE*945.
      P(6,5)=EE*10395.*A
      P(7,5)=FF*10395.
      DO 20 I=1,7
      DO 20 J=1,5
      K=I-1
      L=I+1
      DR(I,J)=CCC*((P(L,J)/AA)-(K*A*P(I,J)/BB))
      DP(I,J)=DR(I,J)*AAA/CCC
      DQ(I,J)=DR(I,J)*BBB/CCC
   20 CONTINUE
      RETURN
      END
```

```
      SUBROUTINE ZONAL (II)
      COMMON/BLKA/RHO(8,60),ELEM(10),PARA(10),E(60)
      COMMON/BLKB/P(8,5),DP(8,5),DQ(8,5),DR(8,5),RR(6)
      COMMON/BLKC/BJ(5),C(7,5),S(7,5),FAC(7,5)
      COMMON/BLKC/PERT(7,3,60)
      PX=PARA(1)/RR(3)
      DDPX=0.
      DDPY=0.
      DDPZ=0.
      DO 20 I=1,5
      BB=BJ(I)/RR(I+1)
      CC=(I+2)*P(1,I)
      DD=DP(1,I)*RR(2)
      EE=DQ(1,I)*RR(2)
      FF=DR(1,I)*RR(2)
      DDPX=BB*(CC*RHO(2,II)-DD)+DDPX
      DDPY=BB*(CC*RHO(3,II)-EE)+DDPY
      DDPZ=BB*(CC*RHO(4,II)-FF)+DDPZ
20    CONTINUE
      PERT(1,1,II)=PX*DDPX
      PERT(1,2,II)=PX*DDPY
      PERT(1,3,II)=PX*DDPZ
      RETURN
      END
```

```
      SUBROUTINE TESSER (AL,II)
      COMMON/BLKA/RHO(8,60),ELEM(10),PARA(10),E(60)
      COMMON/BLKB/P(8,5),DP(8,5),DQ(8,5),DR(8,5),RR(6)
      COMMON/BLKC/BJ(5),C(7,5),S(7,5),FAC(7,5)
      COMMON/BLKD/PERT(7,3,60)
      PX=PARA(1)/RR(3)
      RRR=RR(1)*(RHO(2,II)*RHO(2,II)+RHO(3,II)*RHO(3,II))
      PXX=-PARA(1)*RHO(3,II)/RRR
      PYY=PARA(1)*RHO(2,II)/RRR
      DDPX1=0.
      DDPX2=0.
      DDPY1=0.
      DDPY2=0.
      DDPZ=0.
      DO 20 I=1,5
      K=I+1
      DO 20 J=2,K
      M=J-1
      CO1=COS(M*AL)
      SI1=SIN(M*AL)
      COSI1=CO1*C(J,I)+SI1*S(J,I)
      COSI2=CO1*S(J,I)-SI1*C(J,I)
      AA=-(K+1)*P(J,I)/RR(I+1)
      BB=DP(J,I)/RR(I+1)
      CC=DQ(J,I)/RR(I+1)
      DD=DR(J,I)/RR(I+1)
      EE=M*P(J,I)/RR(I+1)
      DDPX1=(AA*RHO(2,II)+BB*RR(2))*COSI1+DDPX1
      DDPY1=(AA*RHO(3,II)+CC*RR(2))*COSI1+DDPY1
      DDPZ=(AA*RHO(4,II)+DD*RR(2))*COSI1+DDPZ
      DDPX2=EE*COSI2+DDPX2
   20 CONTINUE
      DDPX1=PX*DDPX1
      DDPY2=PYY*DDPX2
      DDPX2=PXX*DDPX2
      DDPY1=PX*DDPY1
      PERT(2,1,II)=DDPX1+DDPX2
      PERT(2,2,II)=DDPY1+DDPY2
      PERT(2,3,II)=PX*DDPZ
      RETURN
      END
```

```
      SUBROUTINE SECTOR (AL,II)
      COMMON/BLKA/RHO(3,60),ELEM(10),PARA(10),E(60)
      COMMON/BLKB/P(8,5),DP(8,5),DQ(8,5),DR(8,5),RR(6)
      COMMON/BLKC/EJ(5),C(7,5),S(7,5),FAC(7,5)
      COMMON/BLKD/PERT(7,3,60)
      PX=PARA(1)/RR(3)
      RRR=RR(1)*(RHO(2,II)*RHO(2,II)+RHO(3,II)*RHO(3,II))
      PXX=-PARA(1)*RHO(3,II)/RRR
      PYY=PARA(1)*RHO(2,II)/RRR
      DDPX1=0.
      DDPX2=0.
      DDPY1=0.
      DDPZ1=0.
      KKK=1
      DO 20 I=1,5
      K=I+1
      J=I+2
      KKK=(2*K-1)*KKK
      CO1=COS(K*AL)
      SI1=SIN(K*AL)
      COSI1=CO1*C(J,I)+SI1*S(J,I)
      COSI2=CO1*S(J,I)-SI1*C(J,I)
      AA=-KKK*(K+1)*COSI1/RR(K)
      DDPX1=AA*RHO(2,II)+DDPX1
      DDPY1=AA*RHO(3,II)+DDPY1
      DDPZ1=AA*RHO(4,II)+DDPZ1
      DDPX2=KKK*K*COSI2/RR(K)+DDPX2
20    CONTINUE
      PERT(3,1,II)=PX*DDPX1+PXX*DDPX2
      PERT(3,2,II)=PX*DDPY1+PYY*DDPX2
      PERT(3,3,II)=PX*DDPZ1
      RETURN
      END


      SUBROUTINE LUNAR (I)
      COMMON/BLKA/RHO(3,60),ELEM(10),PARA(10),E(60)
      COMMON/BLKD/PERT(7,3,60)
      COMMON/BLKF/RRS(3,60),RRM(3,60)
      PARL=0.01226*PARA(1)
      A=RHO(2,I)-RRM(1,I)
      B=RHO(3,I)-RRM(2,I)
      C=RHO(4,I)-RRM(3,I)
      D=SQRT(A*A+B*B+C*C)
      D=D*D*D
      DD=SQRT(RRM(1,I)*RRM(1,I)+RRM(2,I)*RRM(2,I)
     1        +RRM(3,I)*RRM(3,I))
      EE=DD*DD*DD
      PERT(4,1,I)=-PARL*(A/D+RRM(1,I)/EE)
      PERT(4,2,I)=-PARL*(B/D+RRM(2,I)/EE)
      PERT(4,3,I)=-PARL*(C/D+RRM(3,I)/EE)
      RETURN
      END
```

```
      SUBROUTINE SCLAR (I)
      COMMON/BLKA/RHO(3,60),ELEM(10),PARA(10),E(60)
      COMMON/BLKD/PERT(7,3,60)
      COMMON/BLKF/RRS(3,60),RRM(3,60)
      PARS=332952.*PARA(1)
      A=RHO(2,I)-RRS(1,I)
      B=RHO(3,I)-RRS(2,I)
      C=RHO(4,I)-RRS(3,I)
      D=SQRT(A*A+B*B+C*C)
      D=D*D*D
      DD=SQRT(RRS(1,I)*RRS(1,I)+RRS(2,I)*RRS(2,I)
     1      +RRS(3,I)*RRS(3,I))
      EE=DD*DD*DD
      PERT(5,1,I)=-PARS*(A/D+RRS(1,I)/EE)
      PERT(5,2,I)=-PARS*(B/D+RRS(2,I)/EE)
      PERT(5,3,I)=-PARS*(C/D+RRS(3,I)/EE)
      RETURN
      END
```

```
      SUBROUTINE RADIAT (I)
      COMMON/BLKA/RHO(3,60),ELEM(10),PARA(10),E(60)
      COMMON/BLKD/PERT(7,3,60)
      COMMON/BLKF/RRS(3,60),RRM(3,60)
      A=RHO(2,I)-RRS(1,I)
      B=RHO(3,I)-RRS(2,I)
      C=RHO(4,I)-RRS(3,I)
      RSD=SQRT(A*A+B*B+C*C)
      GAM=ASIN(1./RHO(1,I))
      EPS=ACOS((A*RHO(2,I)+B*RHO(3,I)+C*RHO(4,I))
     1      /(RSD*RHO(1,I)))
      AEPS=ABS(EPS)
      PAR=(PARA(10)*PARA(9))/(RSD*RSD*RSD)
      IF (AEPS.GE.GAM) GO TO 50
      GO TO 60
50    PERT(6,1,I)=PAR*A
      PERT(6,2,I)=PAR*B
      PERT(6,3,I)=PAR*C
      RETURN
60    PERT(6,1,I)=0.
      PERT(6,2,I)=0.
      PERT(6,3,I)=0.
      RETURN
      END
```

```
      SUBROUTINE TABLE(II,JJ,N,NOSC)
      COMMON/BLK0/PERT(7,3,60)
      COMMON/BLKE/DIFF(10,60),TAB(4,60),H(3,5),TABS(2,7,3)
      M=N-1
      DO 10 I=1,10
      DO 10 J=1,5
      DIFF(I,J)=0.
      K=N+1-J
10    DIFF(I,K)=0.
      DO 20 I=1,5
      I2=2*I
      I1=I2-1
      DO 18 J=1,M
      IF (I.GT.1) GO TO 17
      DIFF(1,J)=PERT(II,JJ,J+1)-PERT(II,JJ,J)
      GO TO 18
17    DIFF (I1,J)=DIFF(I1-1,J+1)-DIFF(I1-1,J)
18    CONTINUE
      DO 19 K=2,N
19    DIFF(I2,K)=DIFF(I1,K)-DIFF(I1,K-1)
20    CONTINUE
      TAB(4,6)=TABS(2,II,JJ)+PERT(II,JJ,6) *0.5
      TAB(3,6)=TABS(1,II,JJ)-PERT(II,JJ,6)/12.
      DO 30 I=1,5
      I2=2*I
      I1=I2-1
      TAB(3,6)=TAB(3,6)-DIFF(I2,6)*H(2,I)
30    TAB(4,6)=TAB(4,6)-(DIFF(I1,5)+DIFF(I1,6))*0.5*H(1,I)
      DO 40 I=7,N
      TAB(4,I)=TAB(4,I-1)+PERT(II,JJ,I)
40    TAB(3,I)=TAB(3,I-1)+TAB(4,I-1)
      DO 50 I=1,5
      J=6-I
      TAB(4,J)=TAB(4,J+1)-PERT(II,JJ,J+1)
50    TAB(3,J)=TAB(3,J+1)-TAB(4,J)
      A=DIFF(10,7)-DIFF(10,6)
      B=DIFF(10,N-5)-DIFF(10,N-6)
      DO 60 I=1,5
      J=6-I
      DIFF(10,J)=DIFF(10,J+1)-A
      J=N-5+I
60    DIFF(10,J)=DIFF(10,J-1)+B
      DO 70 I=1,9
      J=10-I
      L=J/2
      LL=N-(J-1)/2
      LLL=(J+1)/2
      DO 71 I1=LL,N
71    DIFF(J,I1)=DIFF(J,I1-1)+DIFF(J+1,I1-L/LLL)
      IF (I.EQ.9) GO TO 70
      DO 72 I1=1,L
      I2=L+1-I1
72    DIFF(J,I2)=DIFF(J,I2+1)-DIFF(J+1,I2+1-L/LLL)
70    CONTINUE
      DO 80 I=1,N
```

```
      TAB(1,I)=TAB(3,I)+PERT(II,JJ,I)/12.
      TAB(2,I)=TAB(4,I)-PERT(II,JJ,I)*0.5
      DO 80 J=1,5
      TAB(1,I)=TAB(1,I)+DIFF(2*J,I)*H(2,J)
      IF (I.EQ.1) GO TO 80
      TAB(2,I)=TAB(2,I)+(DIFF(2*J-1,I)+DIFF(2*J-1,I-1))
     1      *0.5*H(1,J)
   80 CONTINUE
      TABS(1,II,JJ)=TAB(1,6)
      TABS(2,II,JJ)=TAB(2,6)
      RETURN
      END



      SUBROUTINE IMPROVE (I,N,W,NN,NOSC)
      COMMON/BLKA/REF(3,60),ELEM(10),PARA(10),E(60)
      COMMON/BLKD/PERT(7,3,60)
      COMMON/BLKE/DIFF(10,50),TAB(4,60),H(3,5),TABS(2,7,3)
      COMMON/BLKG/REF(3,50),EREF(60),ELREF(10)
      DO 50 ITER=1,NN
      DO 20 K=1,N
      X=REF(2,K)+PERT(I,1,K)
      Y=REF(3,K)+PERT(I,2,K)
      Z=REF(4,K)+PERT(I,3,K)
      XX=PERT(I,1,K)*(REF(2,K)+0.5*PERT(I,1,K))
      YY=PERT(I,2,K)*(REF(3,K)+0.5*PERT(I,2,K))
      ZZ=PERT(I,3,K)*(REF(4,K)+0.5*PERT(I,3,K))
      Q=(XX+YY+ZZ)/(REF(1,K)*REF(1,K))
      F=3.-7.5*Q+17.5*Q*Q-39.375*Q*Q*Q+86.625*Q*Q*Q*Q
     1  -187.6875*Q*Q*Q*Q*Q +402.1875*Q*Q*Q*Q*Q*Q
     2  -854.64844 *Q*Q*Q*Q*Q*Q*Q
      PAR=PARA(1)/(REF(1,K)*REF(1,K)*REF(1,K))
      CORR1=PAR*(F*Q*X-PERT(I,1,K))
      CORR2=PAR*(F*Q*Y-PERT(I,2,K))
      CORR3=PAR*(F*Q*Z-PERT(I,3,K))
      PERT(1,1,K)=PERT(7,1,K)+CORR1*W*W
      PERT(1,2,K)=PERT(7,2,K)+CORR2*W*W
      PERT(1,3,K)=PERT(7,3,K)+CORR3*W*W
      REF(2,K)=X
      REF(3,K)=Y
      REF(4,K)=Z
   20 CONTINUE
      IF (ITER.EQ.NN) GO TO 50
      DO 40 J=1,3
      TABS(1,I,J)=0.
      TABS(2,I,J)=0.
      CALL TABLE (I,J,N,NOSC)
      DO 30 K=1,N
   30 PERT(I,J,K)=TAB(1,K)
   40 CONTINUE
   50 CONTINUE
      RETURN
      END
```

```
      SUBROUTINE OSCULAT (NOSC)
      COMMON/BLKA/RHO(8,60),ELEM(10),PARA(10),E(60)
      COMMON/BLKC/PERT(7,3,60)
      VX=RHO(6,NOSC)
      VY=RHO(7,NOSC)
      VZ=RHO(8,NOSC)
      V2=VX*VX+VY*VY+VZ*VZ
      X=RHO(2,NOSC)
      Y=RHO(3,NOSC)
      Z=RHO(4,NOSC)
      R=SQRT(X*X+Y*Y+Z*Z)
      ELEM(1)=1./(2./R-V2/PARA(1))
      HX=Y*VZ-Z*VY
      HY=Z*VX-X*VZ
      HZ=X*VY-Y*VX
      H2=HX*HX+HY*HY+HZ*HZ
      ELEM(6)=H2/PARA(1)
      ELEM(2)=SQRT(1.-ELEM(6)/ELEM(1))
      A=V2-PARA(1)/R
      B=X*VX+Y*VY+Z*VZ
      EX=(A*X-B*VX)/PARA(1)
      EY=(A*Y-B*VY)/PARA(1)
      EZ=(A*Z-B*VZ)/PARA(1)
      AA=SQRT(H2)
      ELEM(3)=ACOS(HZ/AA)
      AN=SQRT(HX*HX+HY*HY)
      ELEM(5)=ACOS(-HY/AN)
      IF (HX.LT.0.) ELEM(5)=2.*PARA(2)-ELEM(5)
      ELEM(4)=ACOS((-HY*EX+HX*EY)/(AN*ELEM(2)))
      IF (EZ.LT.0.) ELEM(4)=2.*PARA(2)-ELEM(4)
      ELEM(4)=ELEM(4)*PARA(3)
      ELEM(5)=ELEM(5)*PARA(3)
      ELEM(3)=ELEM(3)*PARA(3)
      PARA(4)=SQRT(PARA(1)/(ELEM(1)*ELEM(1)*ELEM(1)))
      ECOS=(EX*X+EY*Y+EZ*Z)/(ELEM(2)*R)
      IF (ABS(ECOS).LE.1.) GO TO 10
      PRINT 100, ECOS
  100 FORMAT (/,5X,E15.6,/)
      IF (ECOS.GT.0.) ECOS=1.
      IF (ECOS.LT.0.) ECOS=-1.
   10 E(1)=ACOS(ECOS)
      IF (B.LT.0.) E(1)=2.*PARA(2)-E(1)
      E(NOSC)=ACOS((ELEM(2)+ECOS)/(1.+ELEM(2)*ECOS))
      IF (B.LT.0.) E(NOSC)=2.*PARA(2)-E(NOSC)
      PARA(8)=(1./PARA(4))*(E(NOSC)-ELEM(2)*SIN(E(NOSC)))
      RETURN
      END
```

```
      SUBROUTINE PERIGEE (NPER,U)
      COMMON/BLKA/RHO(8,60),ELEM(10),PARA(10),G(60)
      U=0.
      A=RHO(1,NPER-2)
      B=RHO(1,NPER-1)
      C=RHO(1,NPER)
      D=RHO(1,NPER+1)
      E=RHO(1,NPER+2)
      A4=(A-4.*B+6.*C-4.*D+E)/(24.)
      A3=(-A+2.*B-2.*D+E)/(12.)
      A2=(-A+16.*B-30.*C+16.*D-E)/(24.)
      A1=(A-8.*B+8.*D-E)/(12.)
      M=0
10    F=4.*A4*U*U*U+3.*A3*U*U+2.*A2*U+A1
      FF=12.*A4*U*U+6.*A3*U+2.*A2
      M=M+1
      U=U-F/FF
      IF (M.GE.10) GO TO 20
      IF (ABS(F).LE..0000001) GO TO 20
      GO TO 10
20    CONTINUE
      IF (ABS(U).LT..001) GO TO 23
      IF (U.GT..999.AND.U.LT.1.001) GO TO 24
      IF (U.GT.-1.001.AND.U.LT.-.999) GO TO 25
      AAA=U*(U*U-1.)*(U*U-4.)/24.
      AA=AAA/(U+2.)
      BB=-(AAA*4.)/(U+1.)
      CC=AAA*6./U
      DD=-(AAA*4.)/(U-1.)
      EE=AAA/(U-2.)
      GO TO 27
23    DD=0.
      BB=0.
      CC=1.
      GO TO 26
24    CC=0.
      DD=1.
      BB=0.
      GO TO 26
25    BB=1.
      CC=0.
      DD=0.
26    AA=0.
      EE=0.
27    CONTINUE
      DO 30 J=1,8
      RHO(J,1)=AA*RHO(J,NPER-2)+BB*RHO(J,NPER-1)+
     1 CC*RHO(J,NPER)+DD*RHO(J,NPER+1)+EE*RHO(J,NPER+2)
30    CONTINUE
      RETURN
      END
```

```
      SUBROUTINE DELTAV
      COMMON/BLKA/RHO(6,60),ELEM(10),PARA(10),E(60)
      COMMON/BLKG/REF(6,60),EREF(60),ELREF(10)
      RA=EREF(19)
      VA=EREF(20)
      D3=ELEM(3)-ELREF(3)
      D4=2.*PARA(2)-ELEM(4)
      D5=(ELREF(5)-ELEM(5))*SIN(EREF(33))
      DNU=-ATAN2(D5,D3)
      ENU=COS(D4+DNU)
      VAZ=SQRT((PARA(1)*RA)/(EREF(31)*RHO(1,1)))*
     1     (1.+EREF(32)*ENU)/(1.+EREF(32))
      DVW=D5*VAZ/SIN(DNU)
      D6=ELREF(4)-ELEM(4)
      DVN=D6*VA*EREF(21)*EREF(22)
      DVN=DVN/(2.*EREF(21)*EREF(22)-RA)
      D7=(2.*ELEM(1)-RHO(1,1)+EREF(41))/2.-ELEM(1)
      DVT1=PARA(1)*D7/(2.*EREF(21)*EREF(21)*VA)
      D8=2.*(EREF(22)-1.)*DVT1/VA
      D9=ELREF(2)-ELEM(2)-D8
      RHO(5,1)=SQRT(PARA(1)*((2./RHO(1,1))-(1./(ELEM(1)+D7))))
      DVT2=RHO(5,1)*D9/(2.*(1.+ELEM(2)+D8))
      D1=(2.*(ELEM(1)+D7)*(ELEM(1)+D7)*RHO(5,1)*DVT2)/PARA(1)
      ELEM(1)=ELEM(1)+D1+D7
      ELEM(2)=ELEM(2)+D8+D9
      ELEM(3)=(ELEM(3)-D3)*PARA(3)
      ELEM(4)=(ELEM(4)+D6)*PARA(3)
      ELEM(5)=(ELEM(5)+D5)*PARA(3)
      ELEM(6)=ELEM(1)*(1.-ELEM(2)*ELEM(2))
      PARA(4)=SQRT(PARA(1)/(ELEM(1)*ELEM(1)*ELEM(1)))
      CON=6378165./3600.
      EREF(1)=DVW*CON
      EREF(3)=DVN*CON
      EREF(5)=DVT1*CON
      EREF(7)=DVT2*CON
      EREF(9)=0.
      EREF(2)=ABS(EREF(1))+EREF(2)
      EREF(4)=ABS(EREF(3))+EREF(4)
      EREF(6)=ABS(EREF(5))+EREF(6)
      EREF(8)=ABS(EREF(7))+EREF(8)
      DO 10 I=1,4
10    EREF(9)=ABS(EREF(2*I-1))+EREF(9)
      EREF(10)=EREF(9)   +EREF(10)
      EREF(11)=-72.*VA*DVT1/SQRT(PARA(1)*EREF(21))
      RHO(1,1)=ELEM(6)/(1.+ELEM(2))
      RHO(5,1)=SQRT(PARA(1)*((2./RHO(1,1))-(1./ELEM(1))))
      RETURN
      END
```

Glossary of Major Variables. The following glossary is a list of major variables used in the computer model listed in the previous section. Intermediate variables are not defined since they are functions of the major variables.

ALO	Geographic longitude of the vehicle, λ_E
ALPHA	Cumulative right ascension of the vehicle
AT	Right ascension of the vehicle, α
BJ(I)	Zonal harmonic coefficients, J_n $(n = I+1)$
C(I,J)	Earth geopotential harmonic coefficients, C_{nk} $\begin{bmatrix} n = J+1 \\ k = I-1 \end{bmatrix}$
DATE	Time from launch (days)
DIFF(I,J)	Tabular differences, δ^n_j $\left[n = I, \quad j = \begin{cases} J-6 \text{ for n-even} \\ J-\frac{11}{2} \text{ for n-odd} \end{cases} \right]$
DP(I,J)	$\nabla_x P(I,J)$
DQ(I,J)	$\nabla_y P(I,J)$
DR(I,J)	$\nabla_z P(I,J)$
DU1	Time from perigee to apogee (hrs)
DU2	Time from apogee to perigee (hrs)
DVN	Normal impulse, Δv_n
DVT1	Tangential impulse at apogee, Δv_{ta}
DVT2	Tangential impulse at perigee, Δv_{tp}
DVW	Orthogonal impulse, Δv_w
E(I)	Eccentric anomaly, E
ELEM(I)	Semi-major axis, a (I=1)
	Eccentricity, e (I=2)
	Inclination, i (I=3)
	Argument of perigee, ω (I=4)
	Longitude of Ascending Node, Ω (I=5)
	Semi-latus rectum, p (I=6)
REFF(I)	Utility array (Eccentric anomaly of reference orbit, orbital elements, etc)

ELREF(I)	Nominal orbital parameters (Initial values of ELEM(I))
F	Series expansion of parameter q in Enckes' method, f
H(1,J)	Coefficients of central difference integration formulas given by Eqs (143) and (144) $H(1,J) * (\delta_1^{2J-1})$, $H(2,J) * \delta_1^{2J}$
ISECT	Integer representing the section of the orbit
ITOSC	Integer representing the day of orbital life from launch
N	Number of data points considered in each integration section
NAIO	Integer representing data point nearest to the apogee point
NDAY	Total number of days of orbit life to be analysed
NN	Number of iterations in Encke improvement
NOSC	Integer representing point of orbit osculation
NPER	Integer representing data point nearest to the perigee point
P(I,J)	Legendre polynomials, P_n^k $\left[\begin{matrix} n = J+1 \\ k = I-1 \end{matrix}\right]$
PARA(I)	(I=1) Earth gravitational parameter, K_e (I=2) Arithmetic constant, (3.14[illegible]26535897) (I=3) Arithmetic constant, (57.295779513 deg/rad) (I=4) $(K_e a^3)^{\frac{1}{2}}$ (I=5) Reference radius distance (3.6775087 R_e/arc-min) (I=6) Constant (2/3=0.667 R_e/n.m.) (I=7) Unused (I=8) Time at osculation point, from the previous perigee point (I=9) Area-mass ratio of vehicle, A/m (I=10) Radiation pressure factor (33.444239 R_e^2/n.m.^{2} per unit A/m)
PERT(I,J,K)	Perturbative accelerations or distances (I=1) Zonal/Total (I=2) Tesseral — (J=1) x-component (I=3) Sectorial — (J=2) y-component (I=4) Lunar — (J=3) z-component (I=5) Solar (I=6) Radiation — (K=1→N) orbital point (I=7) Drilling only
Q	Parameter q in Encke method

REF(I,J) Utility array for temporary storage of data from RHO(I,J) and for storage of nominal orbit position/velocity components

MR(K) Integral powers of radial distance, r^n (n=K)

RHO(I,J) Reference orbit position and velocity components

(I=2)	ρ_x	(I=6)	$\dot{\rho}_x$	(I=1)	ρ
(I=3)	ρ_y	(I=7)	$\dot{\rho}_y$	(I=5)	$\dot{\rho}$
(I=4)	ρ_z	(I=8)	$\dot{\rho}_z$	J = orbital point	

RM(I,J) Daily 0^h values of lunar ephemeris, (J=day)

(I=1) Right ascension, α
(I=2) Declination, δ_m
(I=3) Semi-diameter, s

RRM(I,J) Position components of the Moon for the orbital point J

( )	x_m	(I=2)	y_m	(I=3)	z_m

RRS(I,J) Position components of the Sun for the orbital point J

(I=1)	x_s	(I=2)	y_s	(I=3)	z_s

RS(I,J) Daily 0^h values of solar ephemeris, (J=day)

(I=1)	x_s	(I=2)	y_s	(I=3)	z_s

S(I,J) Earth geopotential harmonic coefficients, S_{nk} $\begin{bmatrix} n = J+1 \\ k = I-1 \end{bmatrix}$

T Time (hr)

TAB(J,I) Tabular differences and sums in integration table

(J=1)	δx_i (i = I-6)	(J=3)	$\sum_1^2$ (i = I-6)
(J=2)	$w\,\delta\dot{x}_i$ (i = I-6)	(J=4)	$\sum_1^1$ (i = I-11/2)

TABS(1,I,J) Initial values for δr_o [(J = 1,2,3 for x,y,z-components)]

TABS(2,I,J) Initial values for $\delta \dot{r}_o$ [(I = 1 → 7 as in PERT(I,J,K))]

THETAO Greenwich sidereal time at vehicle launch, θ_{go}

TT Time (days)

U Total time spent in orbit or normalized time, τ

USAVE Total time spent in orbit prior to orbit being analysed, (hrs)

W Time interval between data points (hrs)

GA/NC/73-7

Vita

Allen LeRoy Thede was born on 31 December 1935 in Muscatine, Iowa. He graduated from high school in Durant, Iowa in 1953 and entered the U. S. Air Force in June 1954. He served as a technical instructor and an analyst in the USAF Security Service until he was accepted into the Airman Education and Commissioning Program in June 1962. He attended the University of Wyoming from which he received the Bachelor of Science degree in Mechanical Engineering with a Nuclear Option and was elected to Sigma Tau. He received a regular commission in the U. S. Air Force upon graduation from Officer Training School in December 1964. He served in the Air Force Systems Command at the Air Force Weapons Laboratory as a space radiation research project officer until January 1969, and at the Foreign Technology Division as a technical intelligence officer until June 1971. In June 1971, he entered the Graduate Astronautics program at the Air Force Institute of Technology School of Engineering.

Permanent Address: 1203 10th Street
Durant, Iowa 52747

This thesis was typed by the author.